FEEDBACK CONTROL ALGORITHMS THROUGH LYAPUNOV OPTIMIZING CONTROL AND TRAJECTORY FOLLOWING OPTIMIZATION

By

DALE BRIAN MCDONALD

A dissertation submitted in partial fulfillment of
the requirements for the degree of

DOCTOR OF PHILOSOPHY

WASHINGTON STATE UNIVERSITY
School of Mechanical and Materials Engineering

May 2006

©Copyright by DALE BRIAN MCDONALD, 2006

All Rights Reserved

©Copyright by DALE BRIAN MCDONALD, 2006

All Rights Reserved

To the Faculty of Washington State University:

The members of the Committee appointed to examine the dissertation of DALE BRIAN MCDONALD find it satisfactory and recommend that it be accepted.

Walter J. Grantham
Chair

ACKNOWLEDGMENTS

I have greatly enjoyed my time at Washington State University and have many individuals who I wish to acknowledge. First and foremost I would like to thank my advisor, Professor Walter J. Grantham. It was in an undergraduate dynamic systems course he instructed that I was first exposed to control systems theory; this experience ultimately led to my decision to attend graduate school. He has not only provided countless hours of guidance and expertise pertaining to this research, but also great encouragement as I begin an academic career. I feel extremely fortunate to have had Professor Grantham as an advisor and mentor; he has made my graduate school experience truly rewarding and I am forever grateful for this. I would also like to thank Professor Charles Pezeshki for his support and guidance throughout my graduate school career. I very much enjoyed working closely with Professor Pezeshki during the development of the laboratory portion of the mechatronics course and on several consulting projects. I feel that these experiences will serve me well as I transition into a faculty career and I am exceedingly grateful for this. I wish to thank Professor Robert H. Dillon for his guidance and efforts during this research. Early in my Ph. D. program, Professor Dillon taught a numerical analysis course that I enjoyed greatly; that experience has given me the tools and inspiration to extend the current research by discretizing the developed algorithms.

I would also like to thank Professor Hussein M. Zbib; the School of Mechanical and Materials Engineering has allowed me to gain extensive teaching experience and I am grateful for this. I wish to thank Annette Cavalieri, Jan Danforth, Mary Simonsen, Gayle

Landeen, and Sophia Tseng for all of their assistance over the last several years; it has been an absolute pleasure to work with them. I would like to thank my friend and office mate Steve Edburg who has provided much moral support throughout graduate school.

I wish to thank my parents, Larry and Cheryl M^{c}Donald for their great support throughout my life. I could not imagine more caring, supportive parents. I am particularly grateful that they encouraged me to follow a technical career and for their financial and emotional support through the years. I am also thankful for the help and guidance of my brother Matt M^{c}Donald. I wish to thank my children, Rosalia, Cole, and Hayley. They are able to relieve the stress of the most difficult day with a smile and a hug and I am truly lucky to be their Father. Finally, I would like to thank my wife Elizabeth. She has always supported me and has sacrificed so much during my academic career. I am so thankful that I am married to such a wonderful wife and mother; I am excited to travel down life's road with her at my side.

FEEDBACK CONTROL ALGORITHMS THROUGH LYAPUNOV

OPTIMIZING CONTROL AND TRAJECTORY

FOLLOWING OPTIMIZATION

Abstract

by Dale Brian M^{c}Donald, Ph.D.
Washington State University
May 2006

Chair: Walter J. Grantham

This research is concerned with the development of feedback control laws specified through the combination of Lyapunov optimizing control techniques with trajectory following optimization algorithms. Initially, this research extends the application of Lyapunov optimizing control to explicitly consider periods of singular control when a state-space switching surface is encountered. A detailed investigation of minimum-time optimal control problems, where the state equations are linear and decoupled from the bounded, scalar control, is presented. A primary outcome is the specification of control design steps for the selection of an appropriate descent function. This analysis explicitly considers how a quadratic approximation to the optimal return function affects stability, chatter, and the existence of singular control. An additional concern is the presence of two time scales; whether part of the original state-space system or induced by control gains. Such time scales complicate the analysis make efficient numerical implementation of any algorithm more difficult. These time scales, or, singular perturbations are examined and interesting results are obtained. The second major focus of this research is the combination of trajectory following optimization techniques with Lyapunov

optimizing control methods to produce new control algorithms for generating feedback controls “on-line”. During this analysis we are concerned with the presence of time scales that appear in the augmented set of differential equations. The resulting Lyapunov optimizing control algorithms via trajectory following optimization allow the analyst to specify efficient feedback control algorithms that are especially well suited for on-line applications.

TABLE OF CONTENTS

LIST OF FIGURES

To Elizabeth, Rosalia, Cole, and Hayley

CHAPTER I

INTRODUCTION

1.1 Research Objectives

This research considers the problem of determining a closed-loop or "feedback" control $\mathbf{u}(\mathbf{x})$ for a system of the form

$$\dot{\mathbf{x}} = \mathbf{f}(\mathbf{x}, \mathbf{u}) \tag{1}$$

where $\mathbf{x} \in R^n$, and $\mathbf{u} \in R^m$, where $(\dot{}) = d()/dt$ and t denotes time. Of particular interest is the specification of sub-optimal controls associated with the optimal control problem of minimizing an integral "cost"

$$J[\mathbf{u}(\cdot)] = \int_0^{t_f} f_0(\mathbf{x}, \mathbf{u})\, dt. \tag{2}$$

The concept of feedback control is fundamental to the interaction between many dynamical systems of interest and desired behavior of that system. Once specified, an admissible feedback control allows the analyst to dictate an acceptable, or perhaps an optimal response. Modern optimal control theory provides the analyst the means to accomplish this task; typically two methodologies are followed which ultimately produce an optimal feedback control law. Pontryagin's minimum principle provides necessary conditions that an optimal, open-loop control law must satisfy. Certain classes of optimal control problem allow for a feedback control to be synthesized from the open-loop solution, often relying upon geometrical considerations. An optimal feedback control may be obtained directly through

the solution of the well-known Hamilton-Jacobi-Bellman partial differential equation; this approach is referred to as dynamic programming.

For the general optimal control problem, specification of the feedback control is quite difficult. Synthesis of a feedback control law from the open-loop control obtained through the application of the minimum principle is most often tractable only for systems that exhibit a favorable geometrical structure or a simple analytical structure. For complex or higher-dimensional systems this task may be quite tedious. The dynamic programming approach is appealing since the feedback control is specified directly; however analytical solutions are quite rare. Numerical solutions may be obtained but these may be cumbersome or impractical, especially when an automatic or "on-line" control is desired.

Due to the mathematical and logistical difficulties associated with generation and implementation of truly optimal feedback controls, sub-optimal methodologies have become increasingly important. A great number of such methodologies exist which is a reflection of the theoretical complexity and widespread applicability of the field of optimal control to many problems throughout engineering and the sciences. For example, Lyapunov optimizing control combines Lyapunov stability theory with that of function minimization to yield feedback controls. Two Lyapunov optimizing control techniques studied in this research are steepest descent control and quickest descent control. These control strategies have proven quite effective for both linear and nonlinear problems; they are also quite well suited to on-line implementation. Another important example is that of variable structure control. Under variable structure control the control may switch to any member of a set of allowable continuous functions of the state. Often, variable structure control algorithms are designed to drive the state to a lower-dimensional, stable manifold which contains the target (usually taken as the origin). The lower-dimensional manifold and its boundary of attraction define

the domain of attraction of the origin under the control law.

The focus of this research is to extend the theory of Lyapunov optimizing control in the following areas. Considered first are minimum-time optimal control problems where the system is linear in the state and decoupled from the scalar, bounded control. The resulting sub-optimal controllers exhibit optimal structure; that is they are able to produce periods of bang-bang or bang-intermediate control. In doing so, significant results regarding stability, chatter, and other performance characteristics are established. The second major research thrust concerns the implementation of these new algorithms using the techniques of trajectory-following optimization. Use of this optimization technique produces algorithms that are fairly straightforward to implement and especially well suited to on-line applications. During this portion of the analysis singular perturbations, which produce systems of differential equations that exist on disparate time scales will be investigated. Finally, the general optimal control problem, where the state equations are nonlinear in the state and control, is considered. Two algorithms are developed; the analysis is concerned with local stability, time scale considerations, and the underlying optimization problem.

1.2 Significance and Justification

The impetus for this research is provided by the need for easily implementable, feedback control laws. As previously mentioned, analytic optimal controls may be difficult or impossible to find; numerical solutions present their own difficulties. This research develops sub-optimal control laws by addressing theoretical and practical issues, including stability, intermediate control, chatter, stiffness, and others. Of particular interest are the relationships that exist between these system characteristics and the notion of an approximation to the optimal return function.

Existing sub-optimal methodologies such as sliding mode control generally focus upon

driving the state to some lower-dimensional stable manifold of the state space. Descent toward this manifold is generally emphasized over reaching the origin (target). As such, system stability, chatter considerations, etc. are somewhat disconnected from the notion of an optimal return function. The control strategies developed in this research explicitly investigate these issues with consideration of an approximate optimal return function. Current Lyapunov optimizing controls take advantage of an optimal problem structure, but typically do not address the form of any intermediate control and the associated system behavior. As a major focus, this research considers this situation in great detail. Of further significance is the incorporation of trajectory-following optimization methods into the control scheme. This provides the analyst with a particularly effective tool for on-line control applications. Derivation of suitable trajectory-following algorithms is a further significant outcome of this research. Control laws derived through the combination of Lyapunov optimizing control techniques with trajectory-following optimization eliminate chatter and address numerical stiffness by addressing the presence of disparate time scales within systems of relevant differential equations.

1.3 Technical Background

1.3.1 Optimization Necessary Conditions

Specification of an optimal control is accomplished by solving an underlying optimization problem. Necessary conditions that a local minimum must satisfy are given first. An extension of this research to two-player, min-max differential games is presented; therefore, local min-max necessary conditions are presented.

1.3.1.1 Minimization Necessary Conditions

Consider the minimization of a scalar-valued function $G(\mathbf{u})$; the variable $\mathbf{u} \in R^m$ is constrained to be an element of the constraint set

$$\mathcal{U} = \{\mathbf{u} \in R^m : \mathbf{h}(\mathbf{u}) \geq \mathbf{0}\} \tag{3}$$

where

$$\mathbf{h}(\mathbf{u}) = [h_1(\mathbf{u}) \cdots h_k(\mathbf{u})]^\intercal, \tag{4}$$

and $()^\intercal$ denotes transpose. The necessary conditions for a local minimum can be summarized as follows [1, pp. 521–522]. Let $\mathbf{u}^*$ be a regular points of $\mathcal{U}$; if $G(\mathbf{u})$ takes on a minimum at $\mathbf{u} = \mathbf{u}^*$ then there exists a vector

$$\boldsymbol{\gamma} = [\gamma_1 \cdots \gamma_k]^\intercal \tag{5}$$

such that

$$\begin{aligned} \frac{\partial L}{\partial \mathbf{u}} &= \mathbf{0}^\intercal \\ \mathbf{h}(\mathbf{u}^*) &\geq \mathbf{0} \\ \boldsymbol{\gamma}^\intercal \mathbf{h}(\mathbf{u}^*) &= 0 \\ \boldsymbol{\gamma} &\geq \mathbf{0}, \end{aligned} \tag{6}$$

where $\boldsymbol{\gamma}$ is called a Lagrange multiplier vector and the Lagrangian function L is defined as

$$L(\mathbf{u}, \boldsymbol{\gamma}) = G(\mathbf{u}) - \boldsymbol{\gamma}^\intercal \mathbf{h}(\mathbf{u}). \tag{7}$$

1.3.1.2 Min-Max Necessary Conditions

Consider the min-max of a scalar valued function $G(\mathbf{u}, \mathbf{v})$; the variables $\mathbf{u}$ and $\mathbf{v}$ are constrained to be elements of the constraint sets

$$\begin{aligned} \mathcal{U} &= \{\mathbf{u} \in R^m : \mathbf{h}(\mathbf{u}) \geq \mathbf{0}\} \\ \mathcal{V} &= \left\{\mathbf{v} \in R^p : \bar{\mathbf{h}}(\mathbf{v}) \geq \mathbf{0}\right\} \end{aligned} \tag{8}$$

where

$$\begin{aligned} \mathbf{h}(\mathbf{u}) &= [h_1(\mathbf{u}) \cdots h_k(\mathbf{u})]^\intercal \\ \bar{\mathbf{h}}(\mathbf{v}) &= \left[\bar{h}_1(\mathbf{v}) \cdots \bar{h}_l(\mathbf{v})\right]^\intercal . \end{aligned} \tag{9}$$

The necessary conditions for a game theoretic saddle point solution can be summarized as follows [1, pp. 521–522]. Let $\mathbf{u}^*$ and $\mathbf{v}^*$ be regular points of $\mathcal{U}$ and $\mathcal{V}$ respectively. If $G(\mathbf{u}, \mathbf{v})$ takes on a min-max at $\mathbf{u} = \mathbf{u}^*$ and $\mathbf{v} = \mathbf{v}^*$, then Lagrange multipliers

$$\begin{aligned} \boldsymbol{\gamma} &= [\gamma_1 \cdots \gamma_k]^\intercal \\ \bar{\boldsymbol{\gamma}} &= [\bar{\gamma}_1 \cdots \bar{\gamma}_l]^\intercal \end{aligned} \tag{10}$$

exist such that

$$\begin{aligned} \frac{\partial L}{\partial \mathbf{u}} &= \mathbf{0}^\intercal \\ \frac{\partial L}{\partial \mathbf{v}} &= \mathbf{0}^\intercal \end{aligned} \tag{11}$$

$$\begin{aligned} \mathbf{h}(\mathbf{u}^*) &\geq \mathbf{0} \\ \bar{\mathbf{h}}(\mathbf{v}^*) &\geq \mathbf{0} \end{aligned} \tag{12}$$

$$\begin{aligned} \boldsymbol{\gamma}^\intercal \mathbf{h}(\mathbf{u}^*) &= 0 \\ \bar{\boldsymbol{\gamma}}^\intercal \bar{\mathbf{h}}(\mathbf{v}^*) &= 0 \end{aligned} \tag{13}$$

$$\begin{aligned} \boldsymbol{\gamma} &\geq \mathbf{0} \\ \bar{\boldsymbol{\gamma}} &\leq \mathbf{0}, \end{aligned} \tag{14}$$

where

$$L(\mathbf{u}, \mathbf{v}, \boldsymbol{\gamma}, \bar{\boldsymbol{\gamma}}) = G(\mathbf{u}, \mathbf{v}) - \boldsymbol{\gamma}^\intercal \mathbf{h}(\mathbf{u}) - \bar{\boldsymbol{\gamma}}^\intercal \bar{\mathbf{h}}(\mathbf{v}) \tag{15}$$

and the partial derivatives are evaluated at $\mathbf{u} = \mathbf{u}^*$ and $\mathbf{v} = \mathbf{v}^*$.

1.3.2 Trajectory Following Optimization

Trajectory following optimization algorithms provide solutions by solving special sets of continuous differential equations. These differential equations are defined so that their equilibrium solutions satisfy local necessary conditions for the optimization at hand; minimization, maximization, or min-max. It is well known that trajectory-following algorithms are quite robust; unencumbered by the need to calculate an appropriate step size, many problems that are difficult to solve by other methods can be solved by trajectory-following methods. These algorithms are also user-friendly; any programming required is straightforward and does not require a large time investment.

1.3.2.1 Unconstrained Trajectory Following Optimization

A few of the most popular unconstrained trajectory-following optimization algorithms are presented here. Algorithms developed as a portion of this research make use of these.

Steepest Descent Consider the minimization of the scalar valued function $G(\mathbf{u})$; necessary conditions are presented in Section 1.3.1.1. Consider setting

$$\dot{\mathbf{u}} = -\left[\frac{\partial G}{\partial \mathbf{u}}\right]^{\intercal} \tag{16}$$

and suppose that $G(\cdot)$ has a proper local minimum at $\mathbf{u} = \mathbf{u}^*$ [1, pp. 143-145]. In some neighborhood of $\mathbf{u}^*$, we then have

$$\frac{dG}{dt} = \frac{\partial G}{\partial \mathbf{u}}\dot{\mathbf{u}} \tag{17}$$

which from (16) yields

$$\frac{dG}{dt} = -\frac{\partial G}{\partial \mathbf{u}}\left[\frac{\partial G}{\partial \mathbf{u}}\right]^{\intercal} < 0, \tag{18}$$

for $\partial G/\partial \mathbf{u} \neq \mathbf{0}^{\intercal}$. Asymptotic stability occurs after selection of an appropriate initial condition; the integration process is stopped when an accuracy criterion, such as $\|\partial G/\partial \mathbf{u}\|$ is sufficiently small, where $\|\cdot\|$ denotes the Euclidean norm.

Newton's Method A continuous-time trajectory-following algorithm analogous to Newton's method may be implemented, as in [20] and [21]. In Newton's method we have

$$\frac{\partial^2 G}{\partial \mathbf{u}^2}\dot{\mathbf{u}} = -\left[\frac{\partial G}{\partial \mathbf{u}}\right]^{\intercal} \tag{19}$$

which implies

$$\dot{\mathbf{u}} = -\left(\frac{\partial^2 G}{\partial \mathbf{u}^2}\right)^{-1}\left[\frac{\partial G}{\partial \mathbf{u}}\right]^{\intercal}. \tag{20}$$

provided

$$\left|\frac{\partial^2 G}{\partial \mathbf{u}^2}\right| \neq 0. \tag{21}$$

multiple equilibria exist.

Gradient Enhanced Newton Implementing the Gradient Enhanced Newton algorithm dictates that

$$\dot{\mathbf{u}} = -\left[\Theta\left\|\frac{\partial G}{\partial \mathbf{u}}\right\|\mathbf{I} + \frac{\partial^2 G}{\partial \mathbf{u}^2}\right]^{-1}\left[\frac{\partial G}{\partial \mathbf{u}}\right]^{\intercal} \tag{22}$$

where Θ is a constant. In [7] it is proven that the Gradient Enhanced Newton method is globally asymptotically stable for functions that satisfy a Lyapunov growth condition and have a single proper stationary minimum point. The Gradient Enhanced Newton algorithm has been shown to be nonstiff; this is reflected in the speed at which the minimizer is approached.

1.3.2.2 Trajectory Following Optimization with Simple Constraints

Based on the minimization necessary conditions, the following trajectory-following algorithm was developed in [1, pp. 145-149] for problems that have simple constraints

$$\mathbf{u}_{\min} \leq \mathbf{u} \leq \mathbf{u}_{\max}$$

on $\mathbf{u} \in R^m$:

$$\dot{u}_i = \begin{cases} 0 & \text{if} \quad u_i = u_{i\max} \text{ and } \dfrac{\partial G}{\partial u_i} \leq 0 \\ -\dfrac{\partial G}{\partial u_i} & \text{otherwise} \\ 0 & \text{if} \quad u_i = u_{i\min} \text{ and } \dfrac{\partial G}{\partial u_i} \geq 0 \end{cases}$$

where $i = 1, \ldots, m$.

1.3.3 Time Scales in Systems of Differential Equations

We consider time scales that enter the analysis in two ways. Induced time scales due to the presence of a control gain or time scales that exist due to small system parameters.

1.3.3.1 Induced Time scales

During the incorporation of trajectory-following optimization into the control strategy, it may occur that a gain, or equivalently, a singular perturbation introduced into a system of differential equations creates a more robust strategy update $\dot{\mathbf{u}}$. Defining a small, positive, singular perturbation parameter ϵ consider the augmented system

$$\begin{aligned} \dot{\mathbf{x}} &= \mathbf{f}(\mathbf{x},\mathbf{u},\epsilon) \\ \epsilon\dot{\mathbf{u}} &= \hat{\mathbf{f}}(\mathbf{x},\mathbf{u},\epsilon). \end{aligned} \tag{23}$$

The system (23) possesses a two-time-scale property with n primarily slow modes and m primarily fast modes [2, p. 531]. Equations (23) represent a stiff system of differential equations, which can make numerical integration difficult. Singular perturbation solution methodology will be used to relieve the numerical stiffness and produce a fast, efficient trajectory-following algorithm. Stiff differential equation solvers can handle (23), but we will address this issue up front and give the analyst low-level control over the process. Singular perturbation theory provides a means by which the system (23) may be converted into slow

and fast subsystems [2, p. 531]. Each subsystem may be examined on a single time scale to determine information about the original system. In this research we will extract such information from the slow and fast subsystems to develop a trajectory-following update $\dot{\mathbf{u}}$ that can be efficiently handled with a nonstiff numerical integrator for differential equations.

1.3.3.2 Existing Time Scales

A small singular perturbation parameter, multiplying the highest derivative of the state equations also creates a two time scale system. Consider systems of the form

$$\begin{aligned} \dot{\mathbf{x}}_r &= \tilde{\mathbf{A}}\hat{\mathbf{x}} \\ \epsilon \dot{x}_n &= \mathbf{a}^\intercal \mathbf{x} + u \end{aligned} \tag{24}$$

where

$$\mathbf{x} = \begin{bmatrix} \mathbf{x}_r \\ x_n \end{bmatrix}$$

$$\tilde{\mathbf{A}} = \begin{bmatrix} 1 & 0 & \cdots & 0 \\ 0 & 1 & \cdots & 0 \\ \vdots & & \ddots & \vdots \\ 0 & 0 & \cdots & 1 \end{bmatrix} \tag{25}$$

$$\hat{\mathbf{x}} = \begin{bmatrix} x_2 \\ x_3 \\ \vdots \\ x_n \end{bmatrix} \tag{26}$$

$$\mathbf{x}_r = \begin{bmatrix} x_1 \\ x_2 \\ \vdots \\ x_{n-1} \end{bmatrix}$$

$$\mathbf{a} = [a_1, \ldots, a_n], \tag{27}$$

with ϵ a positive parameter multiplying the time derivative of x_n. As $\epsilon \to 0$, equations (24) become a stiff set of differential equations [3, p. 531]. In the next section, we present a brief discussion of the issues encountered when dealing with a singularly perturbed system of differential equations.

1.3.3.3 Singular Perturbation Analysis

Exact solutions to many problems of interest in engineering and the sciences are difficult, if not impossible to find. Typically, some approximate solution methodology must be invoked. This may include numerical solution methods, iterative solution methods (such as fixed point iteration), or perturbation methods [4]. Numerical integrators for stiff differential equations, while extremely useful, may disguise underlying system phenomena. In this research we are interested in the interplay between control law design and stiff differential equations. The control algorithms developed in the following sections explicitly consider the presence of disparate time scales. To facilitate the development of these control laws and to also serve as a take of point for future research, we present a brief discussion of existing singular perturbation analysis techniques and their application to certain example problems. As mentioned in [6, pp. 1-2], among others, the singular perturbation strategy varies from problem class to problem class (and often problem to problem). Results presented here are

not exhaustive, but reflect techniques that have been used on frequently studied problems.

Background and Definitions Consider the system

$$\begin{aligned} \dot{\mathbf{x}} &= \mathbf{f}(\mathbf{x},\mathbf{u},\epsilon) \\ \dot{\mathbf{u}} &= \hat{\mathbf{f}}(\mathbf{x},\mathbf{u},\epsilon), \end{aligned} \tag{28}$$

and think of $\mathbf{u}$ strictly as a state variable. That is, for the present analysis, we are simply interested in a system of differential equations (28) without distinguishing a control vector from a state vector. In a regular perturbation problem, denoted $P_{r\epsilon}$, the solution $\mathbf{x}(t,\epsilon)$, $\mathbf{u}(t,\epsilon)$ of (28) depends on the singular perturbation parameter ϵ in such a manner that as $\epsilon \to 0$ these solutions converge to the "limiting outer" solution found by setting $\epsilon = 0$ in (28) and solving the resulting differential equation for $\mathbf{x}(t,0)$, $\mathbf{u}(t,0)$. That is, as $\epsilon \to 0$, $\mathbf{x}(t,\epsilon)$, $\mathbf{u}(t,\epsilon)$ converge uniformly with respect to t to the solution $\mathbf{x}(t,0)$, $\mathbf{u}(t,0)$. In a singular perturbation problem, denoted $P_{s\epsilon}$, this uniform convergence breaks down. At $t = 0$ the solution $\mathbf{x}(t,\epsilon)$, $\mathbf{u}(t,\epsilon)$ has a discontinuous limit as $\epsilon \to 0$ [5, pp.5-6].

As a simple example to illustrate this nonuniform convergence consider

$$\epsilon\dot{x} + x = 1$$

$$x(0) = x_0$$

for $t \geq 0$; the full solution is $\mathbf{x}(t,\epsilon) = 1 + [x_0 - 1]\, e^{-t/\epsilon}$, with the limiting outer solution $x(t,0) = 1$. For $t > 0$ as $\epsilon \to 0$, $\mathbf{x}(t,\epsilon) \to 1$; for $t = 0$ as $\epsilon \to 0$, $\mathbf{x}(t,\epsilon) \to x_0$. Unless it happens that $x_0 = 1$, the discontinuous limit at $t = 0$ is observed.

The discontinuous limit poses several difficulties that complicate the analysis of singularly perturbed problems. The parameter ϵ creates a stiff set of differential equations that

make numerical integrations difficult and inefficient. As another alternative, a change of variables can, in a few special cases, transform a singularly perturbed problem to a regularly perturbed problem. Traditional ordinary differential equation solution methods are then much easier to apply [4, p. 20]. In terms of approximate, closed form solutions for problems that are more complex than the simple example just considered, the perturbation parameter creates difficulties as well. An approximate solution technique that has been quite successful in accurately displaying the system behavior for regularly and singularly perturbed problems is asymptotic expansion [4, pp.12-21], [5, pp. 17-55]. The basic idea is to specify an approximate solution in the form of a Poincare power series in ϵ [5, p. 2]. For a regularly perturbed system, one is often able to specify an approximation in terms of a single expansion. For a singularly perturbed system, a single expansion cannot satisfy the boundary conditions while accurately reflecting long-term or steady state behavior. Therefore, a second (if not a third ...) expansion is needed.

Solution Form For the singularly perturbed problem

$$\begin{aligned} \dot{\mathbf{x}} &= \mathbf{f}(\mathbf{x},\mathbf{u},\epsilon) \\ \epsilon\dot{\mathbf{u}} &= \hat{\mathbf{f}}(\mathbf{x},\mathbf{u},\epsilon)\,. \end{aligned} \tag{29}$$

the fundamental work of Tikhonov and Levinson [5, pp. 46-56] suggests that an approximate solution should consist of two sets of terms. One set, that evolves on a fast or "stretched" time scale τ (such as $\tau = t/\epsilon$), should allow for satisfaction of the initial conditions on an "inner" boundary layer. As $\tau \to \infty$, this set should decay to zero and yield to a set of terms that evolve on the slow time scale t, creating an "outer" boundary layer. This second set of terms dictates the long-term or steady-state behavior of the solution. Success of the method

then, depends upon two critical factors. The first is the ability to match these inner and outer boundary layer solutions in a satisfactory manner, creating a uniform approximation. The second factor is that this approximation then provides valid solution, to some order (first, second, etc.), for all t in the domain of interest.

Reduced Problems To construct such an approximate solution, reduced inner and outer forms of (29) must be defined. Consider the reduced outer problem

$$\begin{aligned} \dot{\mathbf{X}}_0 &= \mathbf{f}\left(\mathbf{X}_0, \mathbf{U}_0, t, 0\right) && (30) \\ 0 &= \hat{\mathbf{f}}\left(\mathbf{X}_0, \mathbf{U}_0, t, 0\right) && (31) \end{aligned}$$

with initial condition $\mathbf{X}_0(0) = \mathbf{x}\left(0\right)$ and where the subscript "0" corresponds to the fact that we have obtained this reduced problem by letting $\epsilon \to 0$. Similarly, consider a change of variable $\tau = t/\epsilon$ that allows us to focus on the inner or fast reduced problem. With $d\tau/dt = 1/\epsilon$ and the initial condition $\mathbf{z}_0\left(0\right) = \mathbf{u}(0)$, (29) becomes

$$\begin{aligned} \frac{d\mathbf{x}}{d\tau}\frac{d\tau}{dt} &= \mathbf{f}\left(\mathbf{x}, \mathbf{z}_0, t, \epsilon\right) && (32) \\ \epsilon\frac{d\mathbf{u}}{d\tau}\frac{d\tau}{dt} &= \hat{\mathbf{f}}\left(\mathbf{x}, \mathbf{z}_0, t, \epsilon\right) \end{aligned}$$

and letting $\epsilon \to 0$ yields

$$\begin{aligned} \frac{d\mathbf{x}}{d\tau} &= \epsilon\mathbf{f}\left(\mathbf{x}\left(0\right), \mathbf{z}_0\left(0\right), 0, 0\right) = 0 && (33) \\ \frac{d\mathbf{z}_0}{d\tau} &= \hat{\mathbf{f}}\left(\mathbf{x}\left(0\right), \mathbf{z}_0, 0, 0\right). && (34) \end{aligned}$$

Note that we have introduced the variable $\mathbf{z}_0(\tau)$ to describe the evolution of the primarily fast variable $\mathbf{u}$ in the inner boundary layer. The ultimate goal from a stability point of view is to satisfy $\mathbf{z}_0(\tau \to \infty) = \mathbf{U}_0(t=0)$, creating a uniform solution over $t \geq 0$ interval of interest.

Construction of Approximate Solutions In this section, we present a discussion on how a uniform, approximate solution may be constructed from the reduced problems (30) and (33). This discussion is meant to provide insight on the process and is not exhaustive. For a more detailed discussion see [5, pp. 46-56], [6, pp.22-27] and [4, pp.1-30]. We begin by attempting to solve (31) for $\mathbf{U}_0 = \mathbf{\Omega}(\mathbf{X}_0, t)$. If successful, $\mathbf{\Omega}(\mathbf{X}_0, t)$ may be substituted into (30) yielding

$$\dot{\mathbf{X}}_0 = \mathbf{f}(\mathbf{X}_0, \mathbf{\Omega}(\mathbf{X}_0, t), t, 0). \tag{35}$$

With $\mathbf{X}_0(0) = \mathbf{x}(0)$, (35) is integrated yielding $\mathbf{X}_0(t)$ and then $\mathbf{U}_0(t)$. As another approach, (31) could be differentiated yielding

$$0 = \frac{\partial \hat{\mathbf{f}}(\mathbf{X}_0, \mathbf{U}_0, t, 0)}{\partial \mathbf{x}} \mathbf{f}(\mathbf{X}_0, \mathbf{U}_0, t, 0) + \frac{\partial \hat{\mathbf{f}}(\mathbf{X}_0, \mathbf{U}_0, t, 0)}{\partial \mathbf{u}} \dot{\mathbf{U}}_0 + \frac{\partial \hat{\mathbf{f}}(\mathbf{X}_0, \mathbf{U}_0, t, 0)}{\partial t} \tag{36}$$

yielding

$$\dot{\mathbf{U}}_0 = -\left[\frac{\partial \hat{\mathbf{f}}(\mathbf{X}_0, \mathbf{U}_0, t, 0)}{\partial \mathbf{u}}\right]^{-1} \left[\frac{\partial \hat{\mathbf{f}}(\mathbf{X}_0, \mathbf{U}_0, t, 0)}{\partial \mathbf{x}} \mathbf{f}(\mathbf{X}_0, \mathbf{U}_0, t, 0) + \frac{\partial \hat{\mathbf{f}}(\mathbf{X}_0, \mathbf{U}_0, t, 0)}{\partial t}\right]. \tag{37}$$

Equations (30) and (37) may be integrated to yield $\mathbf{X}_0(t)$ and $\mathbf{U}_0(t)$. The above process, whether the root $\mathbf{\Omega}(\mathbf{X}_0, t)$ is found exactly or numerically, is nontrivial; for conditions regarding the existence of such solutions see [5, pp. 46-49]. Now, the inner problem (34) is integrated. Assuming $\mathbf{z}_0(\tau)$ has a limit as $\tau \to \infty$, with $\mathbf{U}_0(0) = \mathbf{z}_0(\infty)$ we may assemble

a solution of the form

$$\begin{aligned} \hat{\mathbf{x}}(t,\epsilon) &= \hat{\mathbf{X}}(t,\epsilon) + \epsilon\boldsymbol{\xi}(\tau,\epsilon) \\ \hat{\mathbf{u}}(t,\epsilon) &= \hat{\mathbf{X}}(t,\epsilon) + \epsilon\boldsymbol{\xi}(\tau,\epsilon) \end{aligned} \tag{38}$$

where the terms $\hat{\mathbf{X}}$ and $\hat{\mathbf{U}}$ are approximations derived from the outer problem, with $\boldsymbol{\xi}$ and $\boldsymbol{\eta}$ derived from the inner problem.

To see one way in which this may be accomplished, we will expand (28) in a power series of the form

$$\begin{bmatrix} \hat{\mathbf{X}}(t,\epsilon) \\ \hat{\mathbf{U}}(t,\epsilon) \end{bmatrix} \sim \sum_{j=0}^{\infty} \begin{bmatrix} \hat{\mathbf{X}}_j(t) \\ \hat{\mathbf{U}}_j(t) \end{bmatrix} \epsilon^j. \tag{39}$$

Substituting (39) into (28) and equating coefficients of powers of ϵ, illustrates that to zeroth order the approximation requires that the coefficients $\hat{\mathbf{X}}_0$ and $\hat{\mathbf{U}}_0$ satisfy

$$\frac{d}{dt}\hat{\mathbf{X}}_0 = \mathbf{f}\left(\hat{\mathbf{X}}_0, \hat{\mathbf{U}}_0, t, 0\right) \tag{40}$$

and

$$\epsilon\hat{\mathbf{U}}_0 = \hat{\mathbf{f}}\left(\hat{\mathbf{X}}_0, \hat{\mathbf{U}}_0, t, 0\right) \tag{41}$$

which implies

$$\begin{aligned} \frac{d}{dt}\hat{\mathbf{X}}_0 &= \mathbf{f}\left(\hat{\mathbf{X}}_0, \hat{\mathbf{U}}_0, t, 0\right) \\ 0 &= \hat{\mathbf{f}}\left(\hat{\mathbf{X}}_0, \hat{\mathbf{U}}_0, t, 0\right). \end{aligned}$$

That, of course, is the exact form of the reduced solution (30) and (31). Higher order

approximations are found recursively in terms of t and preceding coefficients $\hat{\mathbf{X}}_j$ and $\hat{\mathbf{U}}_j$.

The assumed solution (38) satisfies

$$\begin{aligned} \frac{d\hat{\mathbf{x}}}{dt} &= \frac{d}{dt}\hat{\mathbf{X}} + \frac{d\boldsymbol{\xi}}{d\tau} = \mathbf{f} \\ \frac{\epsilon d\hat{\mathbf{u}}}{dt} &= \frac{\epsilon d}{dt}\hat{\mathbf{U}} + \frac{d\boldsymbol{\eta}}{d\tau} = \hat{\mathbf{f}}. \end{aligned}$$

The inner boundary terms $\boldsymbol{\xi}$ and $\boldsymbol{\eta}$ must then obey the equations

$$\begin{aligned} \frac{d\boldsymbol{\xi}}{d\tau} &= \mathbf{f}(\hat{\mathbf{X}} + \epsilon\boldsymbol{\xi}, \hat{\mathbf{U}} + \epsilon\boldsymbol{\eta}, \epsilon\tau, \epsilon) - \mathbf{f}(\hat{\mathbf{X}}, \hat{\mathbf{U}}, \epsilon\tau, \epsilon) \\ \frac{d\boldsymbol{\eta}}{d\tau} &= \hat{\mathbf{f}}(\hat{\mathbf{X}} + \epsilon\boldsymbol{\xi}, \hat{\mathbf{U}} + \epsilon\boldsymbol{\eta}, \epsilon\tau, \epsilon) - \hat{\mathbf{f}}(\hat{\mathbf{X}}, \hat{\mathbf{U}}, \epsilon\tau, \epsilon). \end{aligned} \tag{42}$$

Since $(\hat{\mathbf{x}}, \hat{\mathbf{y}})$ and, from (40) and (41), that $(\hat{\mathbf{X}}, \hat{\mathbf{U}})$ satisfy the differential equation, the terms (42) decay to zero as $\tau \to \infty$.

The methods outlined above allow for the analysis of some very complex problems. A very interesting system is that of the singularly perturbed Van der Pol oscillator; one form of which

$$\begin{aligned} \dot{x} &= u \\ \epsilon\dot{u} &= u - \frac{1}{3}u^3 - x \end{aligned} \tag{43}$$

is studied in [5, pp. 62-69]. It is shown that the slow and fast motions of the system (43) produce an asymptotically closed trajectory. This leads to a relaxation oscillation [5, pp. 63]; the resulting periodic solution developed using the above methodology. The matching process for the complex system (43) is quite interesting and is well worth the reading.

1.3.4 Discontinuous Ordinary Differential Equations

Closed-loop control laws may result in discontinuous state equations across a switching surface $S = \{\mathbf{x} : \sigma(\mathbf{x}) = 0\}$ in state space. This discontinuity may produce a phenomenon known as chatter [1, p. 14]. Let $\dot{\mathbf{x}}(t-) = \dot{\mathbf{x}}^{-}(t)$ and $\dot{\mathbf{x}}(t+) = \dot{\mathbf{x}}^{+}(t)$ denote the velocity vector just before and just after t. Assuming that neither $\dot{\mathbf{x}}(t-)$ nor $\dot{\mathbf{x}}(t+)$ are tangent to S at a point where it meets $\mathbf{x}(t)$, necessary conditions for chatter are that

$$\frac{\partial \sigma}{\partial \mathbf{x}} \dot{\mathbf{x}}(t-) \tag{44}$$

and

$$\frac{\partial \sigma}{\partial \mathbf{x}} \dot{\mathbf{x}}(t+) \tag{45}$$

have opposite signs.

A function $\mathbf{x}(t)$ is a solution to

$$\dot{\mathbf{x}}(t) = \mathbf{f}(\mathbf{x})$$

in the sense of Fillipov [1, p. 16-17] if $\dot{\mathbf{x}}(t)$ is a convex combination of $\dot{\mathbf{x}}(t-)$ and $\dot{\mathbf{x}}(t+)$. That is, there exists an $\alpha \in [0, 1]$ such that

$$\dot{\mathbf{x}}(t) = \alpha \dot{\mathbf{x}}(t-) + (1 - \alpha)\dot{\mathbf{x}}(t+). \tag{46}$$

1.3.5 Lyapunov Exponents

This research explicitly considers the presence of distinct time scales in systems of differential equations. For linear systems, eigenvalues provide a relevant measure of this phenomenon. For nonlinear systems, Lyapunov exponents will illustrate widely separated time scales [7].

Lyapunov exponents provide information about the average rates at which neighboring trajectories converge or diverge in a nonlinear dynamical system. A detailed discussion of Lyapunov exponents is given in [1, p. 205-208]. One class of problems that is considered here contains discontinuous differential equations; this discontinuity must be accounted for while calculating the Lyapunov exponents. In [8] a state perturbation jump condition is presented that allows the state perturbation equations [1, p. 328-329] to accurately represent neighboring trajectories. These state perturbation equations are the primary feature of any algorithm that calculates Lyapunov exponents; this jump condition must be considered when calculating Lyapunov exponents for systems with discontinuous controls.

1.3.6 State of the Art Control Methodologies

Portions of the sub-optimal control algorithms developed in this research have certain similarities to existing classes of control algorithms. To explore relevant similarities and differences, a brief account of some of these classes is given here.

1.3.6.1 Variable Structure Control

Under variable structure control the admissible control set consists of a number of continuous subsystems. At any instant the control may switch discontinuously from one member of the set to another [9]. A particular type of variable structure control, know as sliding mode control, attempts to drive the state to a lower-dimensional manifold. If this manifold is attractive and the reduced state equations are stable on this manifold, then their exists a nonempty domain of attraction to the origin [10]. In general, effort is first concentrated on the region of attraction to the lower-dimensional manifold. Once on this manifold, control effort is focused upon origin stability. Such control methodology is applicable to a wide array of dynamic systems. In [11] a variable structure control is developed for asymptotic

stabilization of a class of disturbances. In [12] variable structure control algorithms were specified for systems subject to nonlinear friction. In [13] chatter avoidance through sliding mode control is considered. An excellent reference for optimal control problems subject to discontinuous switches in the control is [14].

1.3.6.2 Model Predictive Control

Model predictive control, also known as receding horizon control, develops a feedback control strategy by solving finite open-loop optimal control problems at each point along the state trajectory. Based upon measurements of the state and control, the open-loop optimal control problem attempts to predict the future behavior of the dynamical system. From this knowledge, a feedback control is implemented and the state evolves accordingly. In [15] this methodology is applied in a min-max setting where feedback control is introduced into the receding horizon. In [16] suboptimal model predictive control algorithms are developed and their stabilizing characteristics for nonlinear systems are discussed.

CHAPTER II

LYAPUNOV OPTIMIZING CONTROL

Lyapunov optimizing control has many of the characteristics of truly optimal controls. Before discussing Lyapunov optimizing control a summary of modern optimal control theory is presented. In this section we present the formal optimal control and differential game formulations considered in this research. State of the art Lyapunov optimizing control methodologies are discussed before presenting our research.

2.1 Open-Loop Optimal Control Theory

In general, this research considers the following optimal control problem [1, pp. 365-366] of minimizing a "cost" integral

$$J[\mathbf{u}(\cdot)] = \int_0^{t_f} f_0(\mathbf{x}, \mathbf{u})\, dt \tag{47}$$

which is associated with transporting the state $\mathbf{x}$

$$\dot{\mathbf{x}} = \mathbf{f}(\mathbf{x}, \mathbf{u}) \tag{48}$$

from some initial point

$$\mathbf{x}(0) = \mathbf{x}_i \tag{49}$$

to any final state $\mathbf{x}(t_f)$ in a specified terminal set $\mathcal{X} \subset R^n$,

$$\mathbf{x}(t_f) \in \mathcal{X} = \{\mathbf{x} \in R^n | \mathbf{g}(\mathbf{x}) = 0\}, \tag{50}$$

where $\mathbf{g}(\mathbf{x}) = [g_1(\mathbf{x}), \ldots, g_z(\mathbf{x})]$. The target set is typically given in terms of equality constraints on the state. The final time t_f is generally left unspecified and is defined as the first time that the state reaches the target. The player strategy variables are constrained to be elements of the constraint set

$$\mathcal{U} = \{\mathbf{u} \in R^m : \mathbf{h}(\mathbf{u}) \geq \mathbf{0}\}. \tag{51}$$

The analyst chooses the strategy $\mathbf{u}(\mathbf{x})$ and desires to minimize (47). We assume that $f_0(\mathbf{x}, \mathbf{u})$ and each component of the vector functions $\mathbf{f}(\mathbf{x}, \mathbf{u})$, $\mathbf{g}(\mathbf{x})$, and $\mathbf{h}(\mathbf{u})$ are continuous and continuously differentiable with respect to their arguments. Furthermore, we assume that the gradient vectors $\partial g_i(\mathbf{x})/\partial \mathbf{x}$, $i = 1, \ldots, z$ are linearly independent at each point in $\mathcal{X}$. The gradient vectors $\partial h_j(\mathbf{u})/\partial \mathbf{u}$, $j = 1, \ldots, k$ are also assumed to be linearly independent at any active constraint.

Solution of the optimal control problem requires that we confront an underlying, possibly nonlinear, minimization problem at each point $\mathbf{x}$ along the state trajectory. In general terms we must

$$\min_{\mathbf{u} \in \mathcal{U}} H(\mathbf{x}, \mathbf{u}, \boldsymbol{\lambda}) \tag{52}$$

subject to

$$\mathbf{u} \in \mathcal{U} = \{\mathbf{h}(\mathbf{u}) \geq \mathbf{0}\}. \tag{53}$$

The optimal control H function is given by

$$H(\mathbf{x},\mathbf{u},\boldsymbol{\lambda}) \triangleq f_0(\mathbf{x}, \mathbf{u}) + \boldsymbol{\lambda}^{\intercal}\mathbf{f}(\mathbf{x}, \mathbf{u})$$

where f_0 is the rate of change of accumulated cost, $\mathbf{f}$ contains the system dynamics, and $\boldsymbol{\lambda}$

is the adjoint vector. We assume that $H(\mathbf{x}, \mathbf{u}, \boldsymbol{\lambda})$ is continuous and continuously differentiable in $\mathbf{u}$. First-order necessary conditions for the underlying minimization problem can be summarized as follows [1, p. 374].

Let $\mathbf{u}^*$ *be a regular point of* $\mathcal{U}$*. If* H *takes on a minimum with respect to* $\mathbf{u}$ *at* $\mathbf{u}^*$*, then Lagrange multipliers*

$$\boldsymbol{\gamma} = [\gamma_1 \cdots \gamma_k]^\intercal \tag{54}$$

exist such that

$$\frac{\partial \mathbf{L}^\intercal}{\partial \mathbf{u}} = \mathbf{0} \tag{55}$$

$$\mathbf{h}(\mathbf{u}^*) \geq \mathbf{0} \tag{56}$$

$$\boldsymbol{\gamma}^\intercal \mathbf{h}(\mathbf{u}^*) = 0 \tag{57}$$

$$\boldsymbol{\gamma} \geq \mathbf{0} \tag{58}$$

where the Lagrangian function is

$$\mathbf{L}(\mathbf{x}, \mathbf{u}, \boldsymbol{\lambda}, \boldsymbol{\gamma}) \triangleq H(\mathbf{x}, \mathbf{u}, \boldsymbol{\lambda}) - \boldsymbol{\gamma}^\intercal \mathbf{h}(\mathbf{u}) \tag{59}$$

and the partial derivatives are evaluated at $\mathbf{u} = \mathbf{u}^*$. For state-independent control constraints the above results can be re-stated in terms of an optimal control minimum principle [1, pp. 375-376].

Given the constraint set $\mathcal{U}$, if $\mathbf{u}^*(\mathbf{x}) \in \mathcal{U}$ is an optimal control for the integral cost

optimal control problem (47)–(51), then there must exist a continuous and piecewise differentiable vector function

$$\boldsymbol{\lambda}(t) = [\lambda_1 \cdots \lambda_n]^\intercal, \tag{60}$$

and a constant multiplier vector

$$\boldsymbol{\rho} = [\rho_1 \cdots \rho_z]^\intercal \tag{61}$$

such that $\boldsymbol{\lambda}(t)$ satisfies the adjoint equations

$$\dot{\boldsymbol{\lambda}}^\intercal = -\frac{\partial H}{\partial \mathbf{x}}, \tag{62}$$

where at the terminal set $\mathcal{X}$, $\boldsymbol{\lambda}(t_f)$ satisfies the transversality conditions

$$\boldsymbol{\lambda}^\intercal(t_f) = \boldsymbol{\rho}^\intercal \frac{\partial \mathbf{g}[\mathbf{x}(t_f)]}{\partial \mathbf{x}} \tag{63}$$

and such that H takes on a global minimum value with respect to $\mathbf{u}$ at each point $\mathbf{x}$ along the trajectory generated by $\mathbf{u}^*(\mathbf{x})$. The minimum value of H at every such point is zero.

2.2 Closed-Loop Optimal Control Theory

For the optimal control problem, the optimal return function [1, pp. 420-422] is defined as

$$V^*(\mathbf{x}) = \int_t^{t_f} f_0[\mathbf{x}, \mathbf{u}^*(\mathbf{x})]\, dt, \tag{64}$$

where $\mathbf{u}^*(\mathbf{x})$ is the optimal feedback control law. Assuming $V^*(\mathbf{x})$, the optimal return function, is C^2 then Bellman's Principle of Optimality allows for the derivation of the

Hamilton-Jacobi-Bellman partial differential equation

$$0 = \min_{\mathbf{u} \in \mathcal{U}} \left\{ H \left(\mathbf{x}, \mathbf{u}, \frac{\partial V^*}{\partial \mathbf{x}} \right) \right\}, \tag{65}$$

where

$$H = f_0 \left(\mathbf{x}, \mathbf{u} \right) + \frac{\partial V^*}{\partial \mathbf{x}} \mathbf{f} \left(\mathbf{x}, u \right), \tag{66}$$

with the boundary condition

$$V^* \left(\mathbf{x} \right) = 0 \text{ on } \mathbf{g} \left(\mathbf{x} \right) = \mathbf{0}. \tag{67}$$

2.3 Min-Max Differential Game Theory

In general, for systems with two control entities, we consider a min-max differential game [1, pp. 513–514] having a cost functional

$$J[\mathbf{u}(\cdot), \mathbf{v}(\cdot)] = \int_0^{t_f} f_0 \left(\mathbf{x}, \mathbf{u}, \mathbf{v} \right) dt \tag{68}$$

which is associated with transporting the state $\mathbf{x}(t) \in R^n$ of a system

$$\dot{\mathbf{x}} = \mathbf{f} \left(\mathbf{x}, \mathbf{u}, \mathbf{v} \right) \tag{69}$$

from some initial point

$$\mathbf{x} \left(0 \right) = \mathbf{x}_i \tag{70}$$

to any final state $\mathbf{x}(t_f)$ in a specified terminal set $\mathcal{X} \subset R^n$,

$$\mathbf{x} \left(t_f \right) \in \mathcal{X} = \left\{ \mathbf{x} \in R^n : \mathbf{g} \left(\mathbf{x} \right) = \mathbf{0} \right\}, \tag{71}$$

where $\mathbf{g}(\mathbf{x}) = [g_1(\mathbf{x}) \cdots g_z(\mathbf{x})]^\intercal$. The final time t_f is generally left unspecified and is defined as the first time that the state reaches the target. The player strategy variables $\mathbf{u} \in R^m$ and $\mathbf{v} \in R^p$, respectively, are constrained to be elements of the constraint sets

$$\mathcal{U} = \{\mathbf{u} \in R^m : \mathbf{h}(\mathbf{u}) \geq \mathbf{0}\} \tag{72}$$

and

$$\mathcal{V} = \left\{\mathbf{v} \in R^p : \bar{\mathbf{h}}(\mathbf{v}) \geq \mathbf{0}\right\}, \tag{73}$$

where

$$\mathbf{h}(\mathbf{u}) = [h_1(\mathbf{u}) \cdots h_k(\mathbf{u})]^\intercal \tag{74}$$

and

$$\bar{\mathbf{h}}(\mathbf{v}) = \left[\bar{h}_1(\mathbf{v}) \cdots \bar{h}_l(\mathbf{v})\right]^\intercal. \tag{75}$$

Player 1 chooses the strategy $\mathbf{u}(\mathbf{x})$ and desires to minimize (68). Player 2 chooses the strategy $\mathbf{v}(\mathbf{x})$ and desires to maximize (68). We assume that $f_0(\mathbf{x}, \mathbf{u}, \mathbf{v})$ and each component of the vector functions $\mathbf{f}(\mathbf{x}, \mathbf{u}, \mathbf{v})$, $\mathbf{g}(\mathbf{x})$, $\mathbf{h}(\mathbf{u})$, and $\bar{\mathbf{h}}(\mathbf{v})$ are continuous and continuously differentiable with respect to their arguments. Furthermore, we assume that all points in $\mathcal{X}, \mathcal{U}$, and $\mathcal{V}$ are regular points [1, pp. 513–514]. In particular, we assume that the gradient vectors $\partial g_i(\mathbf{x})/\partial \mathbf{x}$, $i = 1, \ldots, z$ are linearly independent at each point in $\mathcal{X}$. The gradient vectors $\partial h_j(\mathbf{u})/\partial \mathbf{u}$, $j = 1, \ldots, k$ are also assumed to be linearly independent at any active $\mathcal{U}$ constraint $h_j(\mathbf{u}) = 0$. Similarly, the gradient vectors $\partial \bar{h}_{\hat{j}}(\mathbf{v})/\partial \mathbf{v}$, $\hat{j} = 1, \ldots, l$ are assumed to be linearly independent at any active $\mathcal{V}$ constraint $\bar{h}_{\hat{j}}(\mathbf{v}) = 0$ [1, pp. 513–514]. Solution of a min-max differential game requires that we confront an underlying, possibly nonlinear, min-max optimization problem at each point $\mathbf{x}$ along a state trajectory $\mathbf{x}(t)$. In general

terms we must

$$\min_{\mathbf{u}\in\mathcal{U}} \max_{\mathbf{v}\in\mathcal{V}} H(\mathbf{x},\mathbf{u},\mathbf{v},\boldsymbol{\lambda}) \tag{76}$$

subject to

$$\begin{aligned} \mathbf{h}(\mathbf{u}) &\geq \mathbf{0} \\ \bar{\mathbf{h}}(\mathbf{v}) &\geq \mathbf{0}. \end{aligned} \tag{77}$$

The differential game H function is given by

$$H(\mathbf{x},\mathbf{u},\mathbf{v},\boldsymbol{\lambda}) = f_0(\mathbf{x},\mathbf{u},\mathbf{v}) + \boldsymbol{\lambda}^{\intercal}\mathbf{f}(\mathbf{x},\mathbf{u},\mathbf{v}), \tag{78}$$

where f_0 is the rate of change of accumulated cost, $\mathbf{f}$ contains the system dynamics, and $\boldsymbol{\lambda}$ is the adjoint vector. The vector $\mathbf{x}$ is the state, $\mathbf{u}$ and $\mathbf{v}$ are control vectors with $\mathcal{U} \subseteq R^m$ and $\mathcal{V} \subseteq R^p$ specified constraint sets consisting of k-dimensional and l-dimensional vectors of inequality constraint functions $\mathbf{h}(\mathbf{u}) \geq \mathbf{0}$ and $\bar{\mathbf{h}}(\mathbf{v}) \geq \mathbf{0}$, respectively. Our assumptions on $f_0(\cdot)$ and $\mathbf{f}(\cdot)$ imply that $H(\mathbf{x},\mathbf{u},\mathbf{v},\boldsymbol{\lambda})$ is continuous and continuously differentiable in $\mathbf{u}$ and $\mathbf{v}$.

2.4 State of the Art in Lyapunov Optimizing Control

Existing Lyapunov optimizing control algorithms are capable of producing robust controllers for a variety of linear and nonlinear systems. Construction of a Lyapunov optimizing control begins by selecting an appropriate "Lyapunov-like" function that provides some measure of descent or convergence to the target set. For example, distance to the target is often a useful Lyapunov-like function; if the analyst selects $\mathbf{u}(\mathbf{x})$ such that this distance always decreases, the target is asymptotically stable. Fundamental to the development of such control laws is Lyapunov stability.

A reference solution $\bar{\mathbf{x}}(t)$ to the differential equation (48) is said to be Lyapunov stable if

solutions with initial conditions near $\bar{\mathbf{x}}(0)$ stay in a neighborhood of the reference trajectory $\bar{\mathbf{x}}(t)$ for all $t > 0$. Of interest in this research is the regulator problem, where the reference trajectory $\bar{\mathbf{x}}(t)$ is an equilibrium point in state space. The constant reference solution $\bar{\mathbf{x}}(t) = \bar{\mathbf{x}}$ is Lyapunov stable if for any $\varepsilon > 0$ there exists an $\xi = \xi(\varepsilon)$ such that for any $\mathbf{x}(0)$ where

$$\|\mathbf{x}(0) - \bar{\mathbf{x}}\| < \xi \tag{79}$$

then

$$\|\mathbf{x}(t) - \bar{\mathbf{x}}\| < \varepsilon \tag{80}$$

for all $t > 0$. The solution $\bar{\mathbf{x}}(t) = \bar{\mathbf{x}}$ is locally asymptotically stable if, in addition,

$$\|\mathbf{x}(t) - \bar{\mathbf{x}}\| \to 0 \quad \text{as} \quad t \to 0, \tag{81}$$

and globally asymptotically stable if (79)-(81) hold for all solutions to (48) [1, pp. 513–514].

The selection of an appropriate descent function to the target is critical to the success of the resulting control. Let $\Psi(\mathbf{x})$ denote such a descent function; then $\Psi(\mathbf{x})$ satisfies the following at all points that are controllable to the target [1, pp. 513–514]:

1) $\Psi(\mathbf{x})$ is continuous and continuously differentiable outside the target set as well as on the boundary of the target set.

2) The regions $\Psi(\mathbf{x}) \leq c$ are nested.

3) The target is contained in a region $\Psi(\mathbf{x}) \leq c$.

4) If the target set $\mathcal{X}$ is bounded then the regions $\Psi(\mathbf{x}) \leq c$ are also bounded.

Of particular interest are three types of Lyapunov optimizing control; steepest descent

control, quickest descent control, and minimum cost descent control. A thorough derivation of each control methodology is presented in [1, pp. 513–514]; the results are stated here.

2.4.1 Steepest Descent Control

Implementation of steepest descent control requires that once a descent function to the target $\Psi(\mathbf{x})$ is selected, a control $\mathbf{u}(\mathbf{x})$ is selected (if admissible) such that the velocity $\dot{\mathbf{x}}(t)$ points as closely as possible to the direction opposite to the gradient $\partial\Psi(\mathbf{x})/\partial\mathbf{x}$. For the dynamical system (48) this is accomplished [1, pp. 513–514] by

$$\min_{\mathbf{u}\in\mathcal{U}}\left[\Psi'(\mathbf{x},\mathbf{u})\right]$$

where

$$\Psi'(\mathbf{x},\mathbf{u}) = \frac{\partial\Psi(\mathbf{x})}{\partial\mathbf{x}}\frac{\mathbf{f}(\mathbf{x},\mathbf{u})}{\|\mathbf{f}(\mathbf{x},\mathbf{u})\|}. \tag{82}$$

2.4.2 Quickest Descent Control

Implementation of quickest descent control requires that once a descent function to the target $\Psi(\mathbf{x})$ is selected, an admissible control $\mathbf{u}(\mathbf{x})$ is selected such that the velocity $\dot{\mathbf{x}}(t)$ tries to penetrate contours $\Psi(\mathbf{x})$ as quickly as possible. For the dynamical system (48) this is accomplished by [1, pp. 513–514]

$$\min_{\mathbf{u}\in\mathcal{U}}\left[\dot{\Psi}(\mathbf{x},\mathbf{u})\right]$$

where

$$\dot{\Psi}(\mathbf{x},\mathbf{u}) = \frac{\partial\Psi(\mathbf{x})}{\partial\mathbf{x}}\mathbf{f}(\mathbf{x},\mathbf{u}). \tag{83}$$

2.4.3 Minimum Cost Descent Control

Implementation of minimum cost descent control incorporates a term into the descent function that reflects the rate, f_0, at which cost accumulates. With

$$x_0 = \int_0^{t_f} f_0 \left(\mathbf{x}, \mathbf{u} \right) dt, \tag{84}$$

the optimal control problem (47) yields an approximation

$$W_0 = x_0 + \Psi \left(\mathbf{x} \right)$$

to the optimal return function (64), with rate of change

$$\dot{W}_0 = f_0 \left(\mathbf{x}, \mathbf{u} \right) + \frac{\partial \Psi \left(\mathbf{x} \right)}{\partial \mathbf{x}} \mathbf{f} \left(\mathbf{x}, \mathbf{u} \right) \tag{85}$$

where the control is chosen by $\min_{\mathbf{u} \in \mathcal{U}} \left[\dot{W}_0 \left(\mathbf{x}, \mathbf{u} \right) \right]$. Comparison of equations (83) and (85) reveal that quickest descent control is a special case of minimum cost descent control.

CHAPTER III

LYAPUNOV OPTIMIZING CONTROL RESEARCH

We first develop an algorithm applicable to minimum-time optimal control problems where the state is linear and decoupled from a scalar control u.

3.1 Minimum Time Optimal Control – Linear Systems

This section is concerned with the determination of closed-loop, sub-optimal controllers applicable to linear, minimum-time optimal control problems subject to a bounded scalar control. This class of problems is often studied, due to its wide ranging applicability. Of great interest are algorithms that address the difficulties imposed by the control limits, i.e., actuator saturation. The class of algorithms we derive extends existing Lyapunov Optimizing Control (LOC) theory by merging aspects of optimal control theory with traditional linear feedback control. That is, we design algorithms that exhibit "optimal" characteristics; this includes optimal control solution structure, explicit consideration of control bounds, and finite convergence time to a small neighborhood of the target, which is taken as the origin. Additionally, these algorithms utilize linear control theory to guarantee asymptotic stability of the origin. What results are feedback control strategies that are easy to implement, especially in automatic or "on-line" applications. We term the extension of LOC methods to the minimum-time optimal control setting Lyapunov Optimizing Switching Control (LOSC).

The motivation for developing such controllers arises from the nontrivial nature of the solution methodology provided by modern optimal control theory. Exact or approximate closed-loop controls may be synthesized from the open-loop solution found through the

application of Pontryagin's minimum principle. Alternatively, the dynamic programming approach yields the closed-loop solution directly, through the solution of the Hamilton-Jacobi-Bellman partial differential equation. Specification of such controls may be extremely difficult even for seemingly simple systems, due to the complicated synthesis problem or the need to solve the HJB partial differential equation. In either case, this task grows more difficult as the dimension of the system increases.

The primary difficulty associated with extending the LOC method to the optimal control setting is selection of an appropriate "Lyapunov-like" descent function that is critical to the success of the method. A fundamental outcome of this work is the specification of conditions on the form of this descent function. We assume a positive definite quadratic form; the exact form of this function is specified through a detailed analysis of possible system behaviors.

We develop conditions on the descent function that guarantee local stability of the origin for the general linear system. During this portion of the analysis we maintain optimal problem structure and control sequences throughout state space by requiring maximum or minimum control effort off the switching surface, with intermediate control (if desired) on the switching surface. Near the origin, on the switching surface, we establish stability by implementing a feedback intermediate control. This terminating strategy also eliminates limit cycles that may occur due to bang-bang control. Secondly, we address chatter; an undesirable behavior that is frequently encountered during the design of feedback optimal controls. We show that chatter is dependent upon the specified descent function and additional system quantities. Chatter is influenced in two ways; through the placement of a switching surface, which depends on the form of the descent function, or through the implementation of an intermediate control, which also depends upon the form of the descent function. Reduction of chatter through either of these means generates additional

conditions on the form of the descent function. Finally, we examine the issue of global stability of the origin. Depending upon the eigenvalue structure of the linear system we specify conditions on the descent function that provide a domain of attraction that is the entire controllable set. We illustrate trade-offs between local and global stability that arise due to our assumption and desired system behavior.

The minimum-time optimal control problem is, of course, a special case of the general integral cost problem of (47). The problem formulation is now to minimize the cost

$$J[u(\cdot)] = x_0 = \int_0^{t_f} f_0(\mathbf{x}, u)\, dt = \int_0^{t_f} dt \tag{86}$$

associated with transporting the state $\mathbf{x}(t) \in R^n$ of a system

$$\begin{aligned} \dot{\mathbf{x}} &= \mathbf{f}(\mathbf{x}, u) \\ &= \mathbf{A}\mathbf{x} + \mathbf{b}u \end{aligned} \tag{87}$$

from some initial point

$$\mathbf{x}(0) = \mathbf{x}_i \tag{88}$$

to any final state $\mathbf{x}(t_f)$ in the specified terminal set $\mathcal{X} \subset R^n$. For our purposes

$$\mathbf{g}(\mathbf{x}) = \mathbf{x}(t_f) = \mathbf{0} \tag{89}$$

and the final time t_f is defined as the first time that the state reaches the origin. The player

strategy variables are constrained to be elements of the constraint set

$$\mathcal{U} = \left\{ u \in R^1 : u_{\min} \leq u(\mathbf{x}) \leq u_{\max} \right\}, \tag{90}$$

where $u_{\min} < 0 < u_{\max}$. The analyst chooses the strategy $u(\mathbf{x})$ and desires to minimize (86). We assume that each component of the vector functions $\mathbf{f}(\mathbf{x}, u)$ and $\mathbf{g}(\mathbf{x})$ are continuous and continuously differentiable with respect to their arguments.

The class of optimal control problems where the control vector appears linearly in the H function (66) results in control laws of the general form

$$u = \begin{cases} u_{\max} & \text{if} \quad \sigma(\mathbf{x}) < 0 \\ \in [u_{\min}, u_{\max}] & \text{if} \quad \sigma(\mathbf{x}) = 0 \\ u_{\min} & \text{if} \quad \sigma(\mathbf{x}) > 0 \end{cases}, \tag{91}$$

where the control switches discontinuously across the switching surface $\sigma(\mathbf{x}) = 0$. The switching function for the control, derived from (66), is

$$\sigma(\mathbf{x}) \triangleq \frac{\partial H}{\partial u} \tag{92}$$

and singular control over a nonzero time interval requires that $\sigma(\mathbf{x}) = \dot{\sigma}(\mathbf{x}, u) \equiv 0$ [1, pp. 406-408]. The switching surface will be given by

$$S \triangleq \{ \mathbf{x} : \sigma(\mathbf{x}) = 0 \}. \tag{93}$$

3.1.1 Lyapunov Optimizing Switching Control

The LOSC method generates feedback controls through the solution of approximate problems with optimal structure. For the minimum-time optimal control problem where switching control is possible, our aim is to develop a suitable approximation W_0 to the optimal return function $V^*(\mathbf{x})$ [1, p. 421] by specifying the descent function

$$\Psi(\mathbf{x}) = \frac{1}{2}\mathbf{x}^\intercal \frac{\partial^2 \Psi}{\partial \mathbf{x}^2}\mathbf{x}, \tag{94}$$

where $\partial^2\Psi/\partial\mathbf{x}^2$ is constant, symmetric, and positive definite. Note from (85) and (94) that

$$\dot{W}_0 = \dot{x}_0 + \dot{\Psi} \tag{95}$$

$$= f_0 + \dot{\Psi} = 1 + \dot{\Psi}. \tag{96}$$

With (95) similar to the optimal control H function [1, p. 421], the control is found by the minimization $\min_{u\in\mathcal{U}} \dot{W}_0(\mathbf{x}, u)$. Resulting control laws take the form

$$u(\mathbf{x}) = \begin{cases} u_{\max} & \text{if} \quad \sigma(\mathbf{x}) < 0 \\ u_s(\mathbf{x}) & \text{if} \quad \sigma(\mathbf{x}) = 0 \\ u_{\min} & \text{if} \quad \sigma(\mathbf{x}) > 0 \end{cases} \tag{97}$$

where we may specify a feedback control $u_s(\mathbf{x})$ to stabilize the origin, to keep $\sigma(\mathbf{x}) \equiv 0$, or both. A control $u(\mathbf{x}) = u_s(\mathbf{x})$ that results in $\sigma[\mathbf{x}(t)] \equiv 0$ for a nonzero time interval is called "singular control". Otherwise, the control switches between $u(\mathbf{x}) = u_{\max}$ and $u(\mathbf{x}) = u_{\min}$ and is called "bang-bang" (or switching) control.

Conditions on the form of $\dot{W}_0(\mathbf{x}, u)$ are established such that local stability of the origin is provided by control laws of the form (97). This implies that the switching surface S is placed such that $\Psi(\mathbf{x})$ is a Lyapunov function establishing at least local asymptotic stability of the origin, subject to the state (87) and the control law (97). Conditions on $\Psi(\mathbf{x})$, that allow for the reduction or elimination of chatter in the solution are established next. Finally, conditions which allow for global stability of the origin are discussed.

3.1.1.1 Stability of the Origin

We investigate the manner in which the assumed structure of the descent function $\Psi(\mathbf{x})$ effects system stability. It is proven that the control law (97) provides local, asymptotic stability in a neighborhood of the origin, provided certain requirements are satisfied. Conditions on the specific form of $\Psi(\mathbf{x})$ are obtained as we choose it such that these requirements are realized. We obtain local and global results; these will be distinguished accordingly as we proceed.

From (95) we see that the portion of $\dot{W}_0$ which is the time rate of change of $\Psi(\mathbf{x})$, is crucial to determining if the origin is stable. For the linear system (87), considering (94),

$$\begin{aligned}\dot{\Psi}(\mathbf{x},u) &= \frac{1}{2}\mathbf{x}^{\intercal}\frac{\partial^2\Psi}{\partial\mathbf{x}^2}\dot{\mathbf{x}} + \frac{1}{2}\dot{\mathbf{x}}^{\intercal}\frac{\partial^2\Psi}{\partial\mathbf{x}^2}\mathbf{x} \\ &= \frac{1}{2}\mathbf{x}^{\intercal}\left[\frac{\partial^2\Psi}{\partial\mathbf{x}^2}\mathbf{A} + \mathbf{A}^{\intercal}\frac{\partial^2\Psi}{\partial\mathbf{x}^2}\right]\mathbf{x} + \mathbf{x}^{\intercal}\frac{\partial^2\Psi}{\partial\mathbf{x}^2}\mathbf{b}u \end{aligned} \tag{98}$$

and the switching surface entities

$$\sigma(\mathbf{x}) = \frac{\partial\dot{W}_0}{\partial u} = \frac{\partial f_0}{\partial u} + \mathbf{x}^{\intercal}\frac{\partial^2\Psi}{\partial\mathbf{x}^2}\mathbf{b} = \mathbf{x}^{\intercal}\frac{\partial^2\Psi}{\partial\mathbf{x}^2}\mathbf{b}, \tag{99}$$

$$\frac{\partial \sigma}{\partial \mathbf{x}} = \mathbf{b}^{\intercal} \frac{\partial^2 \Psi}{\partial \mathbf{x}^2}, \tag{100}$$

and

$$\dot{\sigma}\left(\mathbf{x}, u\right) = \mathbf{b}^{\intercal} \frac{\partial^2 \Psi}{\partial \mathbf{x}^2} \left[\mathbf{A}\mathbf{x} + \mathbf{b}u\right]. \tag{101}$$

Trajectories that travel along the singular manifold for a finite time period are generated by singular control $u_s\left(\mathbf{x}\right)$; this requires $\sigma\left(\mathbf{x}\right) = \dot{\sigma}\left(\mathbf{x}, u\right) = 0$. For the linear system (87), via (99), (100), and (101)

$$\begin{aligned} u_s\left(\mathbf{x}\right) &= -\frac{\mathbf{b}^{\intercal} \dfrac{\partial^2 \Psi}{\partial \mathbf{x}^2} \mathbf{A}}{\mathbf{b}^{\intercal} \dfrac{\partial^2 \Psi}{\partial \mathbf{x}^2} \mathbf{b}} \mathbf{x} \\ &= -\frac{\left(\partial \sigma / \partial \mathbf{x}\right) \mathbf{A}}{\left(\partial \sigma / \partial \mathbf{x}\right) \mathbf{b}} \mathbf{x}. \end{aligned} \tag{102}$$

Now, let $\hat{S}$ denote all states on the switching surface S for which the singular control $u_s\left(\mathbf{x}\right)$ is admissible. That is,

$$\hat{S} = \left\{\mathbf{x} \in S \ : \ u_{\min} \leq u_s\left(\mathbf{x}\right) \leq u_{\max}\right\}. \tag{103}$$

For notational simplicity let

$$\mathbf{P} = \left[\frac{\partial^2 \Psi}{\partial \mathbf{x}^2} \mathbf{A} + \mathbf{A}^{\intercal} \frac{\partial^2 \Psi}{\partial \mathbf{x}^2}\right]. \tag{104}$$

From (98) we have

$$\dot{\Psi}\left(\mathbf{x}, u\right) = \frac{1}{2} \mathbf{x}^{\intercal} \mathbf{P} \mathbf{x} + u \frac{\partial \sigma}{\partial \mathbf{x}} \mathbf{x}. \tag{105}$$

The assumption that $\partial^2 \Psi / \partial \mathbf{x}^2 > 0$ and (100) require

$$\frac{\partial \sigma}{\partial \mathbf{x}} \mathbf{b} = \mathbf{b}^{\intercal} \frac{\partial^2 \Psi}{\partial \mathbf{x}^2} \mathbf{b} > \mathbf{0} \tag{106}$$

for $\mathbf{b} \neq \mathbf{0}$. Note that for a system satisfying the Kalman controllability condition [17, p. 54] we have $\mathbf{b} \neq \mathbf{0}$ and hence (52) requires

$$\frac{\partial \sigma}{\partial \mathbf{x}}\mathbf{b} = \mathbf{b}^{\intercal}\frac{\partial^2 \Psi}{\partial \mathbf{x}^2}\mathbf{b} > \mathbf{0}. \tag{107}$$

We may now formally state the first condition that must be satisfied by $\Psi(\mathbf{x})$.

Condition 1 *For a controllable system* (87)*, the assumed structure* (94) *of* $\Psi(\mathbf{x})$*, requires that we choose* $\partial\sigma/\partial\mathbf{x}$ *such that*

$$\frac{\partial \sigma}{\partial \mathbf{x}}\mathbf{b} > \mathbf{0}.$$

For a given descent function $\Psi(\mathbf{x})$, we show that the control law (97) is capable of providing asymptotic stability in some neighborhood of the origin. In large part, this requires that $\Psi(\mathbf{x})$ must be specified, or equivalently $\partial\sigma/\partial\mathbf{x}$ must be placed such that $\dot{\Psi}(\mathbf{x}) < 0$ for all nonzero $\mathbf{x}$ in a neighborhood of the origin. As one would expect, the eigenvalue structure of $\mathbf{A}$ plays a major role in this process. Throughout this analysis, it will be convenient to analyze stability phenomena specific to states located on or off S. Let $\mathbf{x}_\sigma$ satisfy

$$\sigma(\mathbf{x}_\sigma) = 0, \tag{108}$$

that is, $\mathbf{x}_\sigma$ denotes a state on S. Let $\delta\mathbf{x}$ denote a displacement from S; this results in

$$\mathbf{x} = \mathbf{x}_\sigma + \delta\mathbf{x}. \tag{109}$$

It is well known that Pontryagin's minimum principle does not allow singular optimal control for controllable, minimum-time, linear systems [1, p. 452]. However, imposing the requirement that trajectories terminate with singular control, implemented in some small

neighborhood of the origin, is appealing for several reasons. It is unlikely that $\Psi(\mathbf{x})$ will yield a switching surface S that correctly produces the final switch for the trajectory to reach the origin. Singular control preserves optimal structure and eliminates limit cycles about the origin induced by bang-bang control. We may also wish to apply this methodology to systems where the Kalman controllability criterion is not satisfied. Finally, the minimum-time optimal control problem formulation does not guarantee asymptotic stability of the origin. Certain similarities exist, but specification of a control law in the form (97) using the LOSC approach, which includes singular control, is fundamentally different than in the LOC or traditional linear feedback control approaches.

We wish to specify conditions on $\Psi(\mathbf{x})$ that establish stability of the origin under singular control; this is accomplished in a two stage process. First we prove that the control effort effecting $\dot{\Psi}$ goes to zero as $\|\delta\mathbf{x}\| \to 0$. We then prove that the switching surface S is reached in finite time. Later we show that trajectories on S asymptotically approach the origin.

Theorem 1 *As $\|\delta\mathbf{x}\| \to 0$, the LOSC control effect $u(\mathbf{x})$ on $\dot{\Psi}(\mathbf{x},u)$ approaches zero.*

Proof. From equations (104) and (105)

$$\dot{\Psi}(\mathbf{x},u) = \frac{1}{2}\mathbf{x}^{\mathsf{T}}\left[\frac{\partial^2\Psi}{\partial\mathbf{x}^2}\mathbf{A} + \mathbf{A}^{\mathsf{T}}\frac{\partial^2\Psi}{\partial\mathbf{x}^2}\right]\mathbf{x} + \mathbf{x}^{\mathsf{T}}\frac{\partial^2\Psi}{\partial\mathbf{x}^2}\mathbf{b}u. \tag{110}$$

Substituting (109) into (110) results in

$$\dot{\Psi}(\mathbf{x},u) = \frac{1}{2}[\mathbf{x}_\sigma + \delta\mathbf{x}]^{\mathsf{T}}\left[\frac{\partial^2\Psi}{\partial\mathbf{x}^2}\mathbf{A} + \mathbf{A}^{\mathsf{T}}\frac{\partial^2\Psi}{\partial\mathbf{x}^2}\right][\mathbf{x}_\sigma + \delta\mathbf{x}] + [\mathbf{x}_\sigma + \delta\mathbf{x}]^{\mathsf{T}}\frac{\partial^2\Psi}{\partial\mathbf{x}^2}\mathbf{b}u. \tag{111}$$

which, with $(\partial\sigma/\partial\mathbf{x})\,\mathbf{x}_\sigma \equiv 0$ from (99) and (100), yields

$$\begin{aligned}\dot{\Psi}\,(\mathbf{x},u) &= \frac{1}{2}\,[\mathbf{x}_\sigma+\delta\mathbf{x}]^\intercal\left[\frac{\partial^2\Psi}{\partial\mathbf{x}^2}\mathbf{A}+\mathbf{A}^\intercal\frac{\partial^2\Psi}{\partial\mathbf{x}^2}\right][\mathbf{x}_\sigma+\delta\mathbf{x}]+\delta\mathbf{x}^\intercal\frac{\partial^2\Psi}{\partial\mathbf{x}^2}\mathbf{b}u \\ &= \frac{1}{2}\,[\mathbf{x}_\sigma+\delta\mathbf{x}]^\intercal\left[\frac{\partial^2\Psi}{\partial\mathbf{x}^2}\mathbf{A}+\mathbf{A}^\intercal\frac{\partial^2\Psi}{\partial\mathbf{x}^2}\right][\mathbf{x}_\sigma+\delta\mathbf{x}]+u\frac{\partial\sigma}{\partial\mathbf{x}}\delta\mathbf{x}. \qquad (112)\end{aligned}$$

From (112) we observe that as $\|\delta\mathbf{x}\| \to 0$, the control effect term $u\,[\partial\sigma/\partial\mathbf{x}]\,\delta\mathbf{x}$ approaches zero. ■

Since the control effect term $u\,[\partial\sigma/\partial\mathbf{x}]\,\delta\mathbf{x}$ in (112) approaches zero as $\|\delta\mathbf{x}\| \to 0$, we cannot guarantee that $\dot{\Psi}\,(\mathbf{x},u) < 0$ for all $\mathbf{x}$. To prove stability we must, in part, show that trajectories reach S in finite time.

Theorem 2 *If the system* (87) *is controllable and* $u = 0$ *is interior to the control constraint set* $\mathcal{U}$*, then for* $\|\mathbf{x}\|$ *sufficiently small, trajectories reach the switching surface* S *in finite time.*

Proof. Consider the region $\sigma\,(\mathbf{x}) < 0$, where $u\,(\mathbf{x}) = u_{\max}$ from (97). The time rate of change of σ is

$$\begin{aligned}\dot{\sigma} &= \frac{\partial\sigma}{\partial\mathbf{x}}\dot{\mathbf{x}} \\ &= \frac{\partial\sigma}{\partial\mathbf{x}}\,[\mathbf{A}\mathbf{x}+\mathbf{b}u]\,. \qquad (113)\end{aligned}$$

From Condition 1 $(\partial\sigma/\partial\mathbf{x})\,\mathbf{b} > \mathbf{0}$; with $\sigma\,(\mathbf{x}) < 0$ and $u = 0$ interior to $\mathcal{U}$, we have the constant term

$$\frac{\partial\sigma}{\partial\mathbf{x}}\mathbf{b}u > 0. \qquad (114)$$

For $\|\mathbf{x}\|$ sufficiently small the term (114) dominates $[\partial\sigma/\partial\mathbf{x}]\,\mathbf{A}\mathbf{x}$. This implies that $\dot{\sigma} > 0$ with $\sigma(\mathbf{x}) < 0$. Analogous results hold for the region $\sigma(\mathbf{x}) > 0$, which proves trajectories reach S in finite time. ■

To simplify several expressions consider the following. From (102) we have

$$u_s(\mathbf{x}) = -\frac{(\partial\sigma/\partial\mathbf{x})\,\mathbf{A}}{(\partial\sigma/\partial\mathbf{x})\,\mathbf{b}}\mathbf{x}. \tag{115}$$

Substitution of this expression into (87) yields

$$\begin{aligned}
\dot{\mathbf{x}} &= \mathbf{A}\mathbf{x} + \mathbf{b}u_s \\
&= \mathbf{A}\mathbf{x} - \mathbf{b}\left[\frac{(\partial\sigma/\partial\mathbf{x})\,\mathbf{A}}{(\partial\sigma/\partial\mathbf{x})\,\mathbf{b}}\right]\mathbf{x} \\
&= \left[\mathbf{A} - \mathbf{b}\left(\frac{(\partial\sigma/\partial\mathbf{x})\,\mathbf{A}}{(\partial\sigma/\partial\mathbf{x})\,\mathbf{b}}\right)\right]\mathbf{x}.
\end{aligned} \tag{116}$$

Two additional, constant, system matrices play a major role in the derivation of the LOSC intermediate control $u_s(\mathbf{x})$. Define

$$\mathbf{\Phi} = \mathbf{b}\frac{(\partial\sigma/\partial\mathbf{x})\,\mathbf{A}}{(\partial\sigma/\partial\mathbf{x})\,\mathbf{b}} \tag{117}$$

and

$$\mathbf{\Gamma} = \mathbf{A} - \mathbf{\Phi} \tag{118}$$

so that equation (116) may now be expressed as

$$\dot{\mathbf{x}} = \mathbf{\Gamma}\mathbf{x}. \tag{119}$$

Note that $\mathbf{\Gamma}$ is only defined on the surface S, where the intermediate control (115) has been implemented. Consider the time rate of change $\dot{\Psi}$ for states restricted to S; (118) substituted into the first of the equivalent equations (98), yields

$$\begin{aligned} \dot{\Psi}(\mathbf{x},u) &= \frac{1}{2}\mathbf{x}^{\intercal}\frac{\partial^2\Psi}{\partial\mathbf{x}^2}\mathbf{\Gamma}\mathbf{x}+\frac{1}{2}\left[\mathbf{\Gamma}\mathbf{x}\right]^{\intercal}\frac{\partial^2\Psi}{\partial\mathbf{x}^2}\mathbf{x} \\ &= \frac{1}{2}\mathbf{x}^{\intercal}\left[\frac{\partial^2\Psi}{\partial\mathbf{x}^2}\mathbf{\Gamma}+\mathbf{\Gamma}^{\intercal}\frac{\partial^2\Psi}{\partial\mathbf{x}^2}\right]\mathbf{x}. \end{aligned} \tag{120}$$

Let

$$\hat{\mathbf{P}} = \left[\frac{\partial^2\Psi}{\partial\mathbf{x}^2}\mathbf{\Gamma}+\mathbf{\Gamma}^{\intercal}\frac{\partial^2\Psi}{\partial\mathbf{x}^2}\right] \tag{121}$$

which yields

$$\dot{\Psi}(\mathbf{x},u) = \frac{1}{2}\mathbf{x}^{\intercal}\hat{\mathbf{P}}\mathbf{x}. \tag{122}$$

Selection of $\Psi(\mathbf{x})$ such that the eigenvalues of $\hat{\mathbf{P}}$ have negative real parts would guarantee asymptotic stability of the origin. Equation (120) reveals the fundamental difference in how this selection is accomplished in traditional linear feedback control approach in comparison to the LOSC methodology. Traditional methods specify the control as a product of a matrix of gains, $\mathbf{K}$, and the state variables. These gains, and therefore the form of the control, are free to be chosen such that a positive definite matrix $\mathbf{P}_{FB}$ (analogous to $\partial^2\Psi/\partial\mathbf{x}^2$) exists, with corresponding function $V(\mathbf{x}) = (1/2)\,\mathbf{x}^{\intercal}\mathbf{P}_{FB}\mathbf{x}$ which dictates that $\dot{V}(\mathbf{x},u) < 0$ (a function similar to $\dot{\Psi}(\mathbf{x},u)$). This may be accomplished by solving a matrix Lyapunov

equation

$$\mathbf{P}_{FB}\mathbf{A} + \mathbf{A}^{\intercal}\mathbf{P}_{FB} = -\mathbf{Q} \tag{123}$$

where $\mathbf{Q}$ is positive definite [1, pp. 222-223]. Equation (123) is linear in the elements of $\mathbf{P}_{FB}$; the elements of the $\mathbf{K}$ are free to be chosen. The LOSC methodology is fundamentally different; the "feedback" control $u_s(\mathbf{x})$ has been dictated in terms of $\partial^2\Psi/\partial\mathbf{x}^2$. Therefore, as in (121), $\hat{\mathbf{P}}$ is in general, nonlinear in the elements of $\partial^2\Psi/\partial\mathbf{x}^2$. Due to this nonlinearity we will choose $\Psi(\mathbf{x})$ to directly effect $\mathbf{\Gamma}$; $\hat{\mathbf{P}}$ will be effected indirectly.

3.1.1.2 Stability Through Manipulation of the Descent Function

To this point we have analyzed stability given some approximation $W_0(\mathbf{x}) = x_0 + \Psi(\mathbf{x})$ to the optimal return function $V^*(\mathbf{x})$. To guarantee stability, restrictive assumptions on system structure are required. Specification of $\Psi(\mathbf{x})$ is completely at our disposal; in the following sections we will show how careful manipulation of $\Psi(\mathbf{x})$ allows us to establish stability of the origin under less restrictive assumptions. Whether a feedback optimal control has been synthesized from an open-loop solution or obtained through solution of the HJB partial differential equation, satisfaction of relevant necessary conditions assures the analyst that a truly optimal control has been found. Sub-optimal methods, such as LOSC, may satisfy some of these conditions, but to achieve desirable results and relax these assumptions we must consider practical behavior in a more explicit manner. Specification of $\Psi(\mathbf{x})$ will be guided by the structure of the state equations. Considerations include nonzero equilibrium manifolds (points), elimination of chatter, elimination of limit cycles, and controllability properties.

Nonzero Equilibria in Regions of Constant Control We now address the existence of nonzero equilibrium manifolds in regions of constant control effort.

Theorem 3 *If* $\mathbf{A}$ *is nonsingular, with* $u = 0$ *interior to the control constraint set* $\mathcal{U}$*, choosing* $\Psi(\mathbf{x})$ *such that*

$$\frac{\partial \sigma}{\partial \mathbf{x}} \mathbf{A}^{-1} \mathbf{b} \leq 0 \tag{124}$$

guarantees that trajectories generated by the control law (97) *do not converge to nonzero equilibrium points in regions of constant control.*

Proof. A nonzero equilibrium point requires

$$\mathbf{0} = \mathbf{A}\mathbf{x} + \mathbf{b}u \tag{125}$$

which, since $\mathbf{A}$ is invertible yields

$$\mathbf{x}_{eq} = -\mathbf{A}^{-1}\mathbf{b}u. \tag{126}$$

Let $\delta \mathbf{x}_{eq}$ locate an equilibrium point $\mathbf{x}_{eq}$ relative to S, with

$$\mathbf{x}_{eq} = \mathbf{x}_{\sigma} + \delta \mathbf{x}_{eq} \tag{127}$$

where, as before, $\mathbf{x}_{\sigma}$ is on S. Consider the region $\sigma(\mathbf{x}) > 0$; let $\mathbf{x}_{eq}^{+}$ denote equilibrium in this region of state space and let $\delta \mathbf{x}_{eq}^{+}$ locate this point relative to S. Now

$$\mathbf{x}_{eq}^{+} = \mathbf{x}_{\sigma} + \delta \mathbf{x}_{eq}^{+} \tag{128}$$

and so we have

$$\mathbf{x}_{\sigma} + \delta \mathbf{x}_{eq}^{+} = -\mathbf{A}^{-1}\mathbf{b}u_{\min}. \tag{129}$$

Now,

$$\frac{\partial \sigma}{\partial \mathbf{x}}\left[\mathbf{x}_\sigma + \delta \mathbf{x}_{eq}^{+}\right] = \frac{\partial \sigma}{\partial \mathbf{x}}\left[-\mathbf{A}^{-1}\mathbf{b}u_{\min}\right] \tag{130}$$

which implies that

$$\frac{\partial \sigma}{\partial \mathbf{x}}\delta \mathbf{x}_{eq}^{+} = \frac{\partial \sigma}{\partial \mathbf{x}}\left[-\mathbf{A}^{-1}\mathbf{b}u_{\min}\right] \tag{131}$$

since $(\partial\sigma/\partial\mathbf{x})\,\mathbf{x}_\sigma \equiv 0$. With $\sigma(\mathbf{x})$ a linear function

$$\sigma\left(\mathbf{x}_{eq}^{+}\right) = \frac{\partial \sigma}{\partial \mathbf{x}}\delta \mathbf{x}_{eq}^{+}. \tag{132}$$

Since $\sigma\left(\mathbf{x}_{eq}^{+}\right) > 0$, $(\partial\sigma/\partial\mathbf{x})\,\delta\mathbf{x}_{eq}^{+} > 0$; this suggests that for a nonzero equilibrium point to exist in this region the right side of (131) must be greater than zero. With $u_{\min} < 0$ this requires

$$\frac{\partial \sigma}{\partial \mathbf{x}}\left[\mathbf{A}^{-1}\mathbf{b}\right] > 0. \tag{133}$$

Similarity, consider the region $\sigma(\mathbf{x}) < 0$; let $\mathbf{x}_{eq}^{-}$ denote equilibrium in this region of state space and let $\delta\mathbf{x}_{eq}^{-}$ locate this point relative to S, with

$$\mathbf{x}_{eq}^{-} = \mathbf{x}_\sigma + \delta \mathbf{x}_{eq}^{-}. \tag{134}$$

Then we have

$$\mathbf{x}_\sigma + \delta \mathbf{x}_{eq}^{-} = -\mathbf{A}^{-1}\mathbf{b}u_{\max}, \tag{135}$$

which implies that

$$\frac{\partial \sigma}{\partial \mathbf{x}}\delta \mathbf{x}_{eq}^{-} = \frac{\partial \sigma}{\partial \mathbf{x}}\left[-\mathbf{A}^{-1}\mathbf{b}u_{\max}\right]. \tag{136}$$

Since $\sigma\left(\mathbf{x}_{eq}^{-}\right) < 0$, $\left(\partial\sigma/\partial\mathbf{x}\right)\delta\mathbf{x}_{eq}^{-} < 0$; this suggests that for a nonzero equilibrium point to exist in this region the right side of (136) must be less than zero; with $u_{\max} > 0$ this also requires

$$\frac{\partial\sigma}{\partial\mathbf{x}}\left[\mathbf{A}^{-1}\mathbf{b}\right] > 0. \tag{137}$$

A nonzero equilibrium point requires that $\Psi\left(\mathbf{x}\right)$ is chosen such that (137) is satisfied. However, we have specified

$$\frac{\partial\sigma}{\partial\mathbf{x}}\left[\mathbf{A}^{-1}\mathbf{b}\right] \leq 0 \tag{138}$$

and therefore conclude that trajectories generated by the control law (97) do not converge to nonzero equilibrium points in regions of constant control. ■

Condition 2 *From the results of Theorem 4, if* $\mathbf{A}^{-1}$ *exists select* $\Psi(\mathbf{x})$ *such that*

$$\frac{\partial\sigma}{\partial\mathbf{x}}\mathbf{A}^{-1}\mathbf{b} \leq 0. \tag{139}$$

We must also consider equilibrium manifolds, in regions of constant control, for the case where $\mathbf{A}$ is singular. Due to this singularity, the equation $\mathbf{A}\mathbf{x} + \mathbf{b}u = 0$ may have an infinite number of solutions [18, p. 8]. These results are established assuming the Kalman controllability criterion is satisfied and are remarkably similar to (139).

For the remainder of the paper, the companion form representation of (87) will be quite convenient. We will work, without loss of generality, under the assumption that the system (87) is in companion form.

Theorem 4 *If the system* (87) *is controllable and* $u = 0$ *is interior to the control constraint set* $\mathcal{U}$*, then singularity of the system matrix* $\mathbf{A}$ *does not produce equilibrium manifolds in regions of bang-bang control.*

Proof. With

$$\mathbf{A} = \begin{bmatrix} 0 & 1 & 0 & & 0 \\ 0 & 0 & 1 & & 0 \\ \vdots & & & \ddots & \vdots \\ 0 & 0 & 0 & \cdots & 1 \\ a_{n1} & a_{n2} & a_{n3} & \cdots & a_{nn} \end{bmatrix},$$

the assumption that $\mathbf{A}$ is singular implies that its rows are linearly dependent; therefore $a_{n1} = 0$. A nonzero equilibrium point requires that $\dot{\mathbf{x}} = \mathbf{0}$; from (87)

$$\begin{bmatrix} 0 \\ 0 \\ \vdots \\ 0 \\ 0 \end{bmatrix} = \begin{bmatrix} 0 & 1 & 0 & & 0 \\ 0 & 0 & 1 & & 0 \\ \vdots & & & \ddots & \vdots \\ 0 & 0 & 0 & \cdots & 1 \\ a_{n1} & a_{n2} & a_{n3} & \cdots & a_{nn} \end{bmatrix} \begin{bmatrix} x_1 \\ x_2 \\ \vdots \\ x_{n-1} \\ x_n \end{bmatrix} + \begin{bmatrix} 0 \\ 0 \\ \vdots \\ 0 \\ 1 \end{bmatrix} u. \tag{140}$$

Since $a_{n1} = 0$, equation (140) can only be satisfied if $u(\mathbf{x}) = 0$. With $u(\mathbf{x}) = 0$ interior to the control constraint set, we conclude that the singularity of $\mathbf{A}$ will not induce equilibrium manifolds in regions of bang-bang control. ■

It is interesting to note that we could have derived Theorem 3 in a manner similar to that of Theorem 4, under the assumption that $\mathbf{A}$ is nonsingular. A nonzero equilibrium point in a region of constant control would require $0 = a_{n1}x_1 + u$, which implies $x_1 = -u/a_{n1}$. We could then continue with this expression as in (128) beginning with the region $\sigma(\mathbf{x}) > 0$. Ultimately, we would have an expression analogous to (139) which guarantees that an equilibrium point does not exist in regions of bang-bang control.

Nonzero Equilibria in Regions of Singular Control As in the bang-bang control case, we must explore the ramifications a particular choice of $\Psi(\mathbf{x})$ on system stability in the case of singular control. Of great interest is the eigenvalue structure of $\mathbf{\Gamma}$; in particular we will explore the existence of singular manifolds of $\mathbf{\Gamma}$.

Theorem 5 *If the system* (87) *is controllable, the matrix* $\mathbf{\Gamma}$ *is in companion form.*

Proof. For a controllable system (87) we may express $\mathbf{A}$ in companion form without loss of generality. With

$$\mathbf{b} = \begin{bmatrix} 0 \\ 0 \\ \vdots \\ 0 \\ 1 \end{bmatrix}, \tag{141}$$

Consider the matrix

$$\mathbf{\Phi} = \mathbf{b}\frac{(\partial\sigma/\partial\mathbf{x})\,\mathbf{A}}{(\partial\sigma/\partial\mathbf{x})\,\mathbf{b}}. \tag{142}$$

$\mathbf{\Phi}$ is an $n\times n$ matrix consisting of $n-1$ rows of zeros with the last row equal to $(\partial\sigma/\partial\mathbf{x})\,\mathbf{A}/\,(\partial\sigma/\partial\mathbf{x})\,\mathbf{b}$. Let

$$\mathbf{\Phi} = \begin{bmatrix} 0 & 0 & 0 & & 0 \\ 0 & 0 & 0 & & 0 \\ \vdots & & & \ddots & \vdots \\ 0 & 0 & 0 & \cdots & 0 \\ \phi_{n1} & \phi_{n2} & \phi_{n3} & \cdots & \phi_{nn} \end{bmatrix}.$$

From (118) we have

$$\mathbf{\Gamma} = \begin{bmatrix} 0 & 1 & 0 & & 0 \\ 0 & 0 & 1 & & 0 \\ \vdots & & & \ddots & \vdots \\ 0 & 0 & 0 & \cdots & 1 \\ a_{n1} & a_{n2} & a_{n3} & \cdots & a_{nn} \end{bmatrix} - \begin{bmatrix} 0 & 0 & 0 & & 0 \\ 0 & 0 & 0 & & 0 \\ \vdots & & & \ddots & \vdots \\ 0 & 0 & 0 & \cdots & 0 \\ \phi_{n1} & \phi_{n2} & \phi_{n3} & \cdots & \phi_{nn} \end{bmatrix}$$

$$= \begin{bmatrix} 0 & 1 & 0 & & 0 \\ 0 & 0 & 1 & & 0 \\ \vdots & & & \ddots & \vdots \\ 0 & 0 & 0 & \cdots & 1 \\ a_{n1} - \phi_{n1} & a_{n2} - \phi_{n2} & a_{n3} - \phi_{n3} & \cdots & a_{nn} - \phi_{nn} \end{bmatrix}. \tag{143}$$

The matrix $\mathbf{\Gamma}$ is in companion form. ■

Theorem 6 *If the system* (87) *is controllable, the matrix* $\mathbf{\Gamma}$ *is singular.*

Proof. Consider the matrix $\mathbf{\Phi}$, given by (142), consisting of $n-1$ rows of zeros with the last row equal to $(\partial\sigma/\partial\mathbf{x})\,\mathbf{A}/\,(\partial\sigma/\partial\mathbf{x})\,\mathbf{b}$. The first element in the row vector $(\partial\sigma/\partial\mathbf{x})\,\mathbf{A}$ is given by

$$\begin{bmatrix} \dfrac{\partial\sigma}{\partial x_1} & \dfrac{\partial\sigma}{\partial x_2} & \cdots & \dfrac{\partial\sigma}{\partial x_n} \end{bmatrix} \begin{bmatrix} 0 \\ 0 \\ \vdots \\ a_{n1} \end{bmatrix} = \begin{bmatrix} \dfrac{\partial\sigma}{\partial x_n} a_{n1} \end{bmatrix}, \tag{144}$$

where $\mathbf{A} = [a_{ij}]$. The first element in the last row of $\mathbf{\Phi}$ is given by

$$\begin{aligned} \phi_{n1} &= \frac{\dfrac{\partial \sigma}{\partial x}\mathbf{A}}{\dfrac{\partial \sigma}{\partial x}\mathbf{b}} \\ &= a_{n1}. \end{aligned} \tag{145}$$

With $\mathbf{\Gamma} = \left[\gamma_{ij}\right]$ in companion form and

$$\begin{aligned} \gamma_{n1} &= a_{n1} - \phi_{n1} \\ &= 0 \end{aligned} \tag{146}$$

we have

$$\mathbf{\Gamma} = \begin{bmatrix} 0 & 1 & 0 & & 0 \\ 0 & 0 & 1 & & 0 \\ \vdots & & & \ddots & \vdots \\ 0 & 0 & 0 & \cdots & 1 \\ 0 & a_{n2} - \phi_{n2} & a_{n3} - \phi_{n3} & \cdots & a_{nn} - \phi_{nn} \end{bmatrix} \tag{147}$$

and conclude that it is singular. ■

To illustrate the importance of considering singularity of system matrices during design of the control law, we present the following example [1, pp. 464-466]. In particular, we note that we must select $\Psi(\mathbf{x})$ carefully to avoid creating a nonzero equilibrium manifold.

Example 1 *Consider the problem of transferring the state to the origin in minimum time*

for the system governed by state equations

$$\begin{aligned}\dot{\mathbf{x}} &= \mathbf{A}\mathbf{x} + \mathbf{b}u \\ &= \begin{bmatrix} 0 & 1 \\ -1 & 1 \end{bmatrix} \mathbf{x} + \begin{bmatrix} 0 \\ 1 \end{bmatrix} u. \end{aligned} \tag{148}$$

The eigenvalues of $\mathbf{A}$ *are* $\mu_1 = 1/2 - i\sqrt{3}/2$ *and* $\mu_2 = 1/2 + i\sqrt{3}/2$*; the system is unstable. Suppose we approximate the optimal return function using distance to the target squared as a descent function. We have*

$$\begin{aligned}\Psi(\mathbf{x}) &= \frac{1}{2} \begin{bmatrix} x_1 & x_2 \end{bmatrix} \begin{bmatrix} 1 & 0 \\ 0 & 1 \end{bmatrix} \begin{bmatrix} x_1 \\ x_2 \end{bmatrix} \\ &= \frac{1}{2}x_1^2 + \frac{1}{2}x_2^2, \end{aligned} \tag{149}$$

from (99), (100), *and* (101)

$$\begin{aligned}\sigma(\mathbf{x}) &= \mathbf{x}^\intercal \frac{\partial^2 \Psi}{\partial \mathbf{x}^2} \mathbf{b} \\ &= x_2. \end{aligned} \tag{150}$$

Note that (149) *is a positive definite; Condition 1 is satisfied. Suppose we implement a singular control strategy at some point along the* x_1 *axis, near the origin. The control that will accomplish this task is found by setting* $\dot{\sigma}(\mathbf{x}, u) = 0$ *and solving for* $u_s(\mathbf{x})$*. That is, we have* $\sigma(\mathbf{x}) = x_2 = 0$ *and*

$$\dot{\sigma}(\mathbf{x}, u) = -x_1 + x_2 + u$$

which, with $x_2 = 0$ *implies that* $u_s(\mathbf{x}) = x_1$. *If we implement* $u_s(\mathbf{x})$ *at any point on* $\sigma(\mathbf{x}) = x_2 = 0$, *the state equations reduce to*

$$\begin{bmatrix} \dot{x}_1 \\ \dot{x}_2 \end{bmatrix} = \begin{bmatrix} 0 & 1 \\ -1 & 1 \end{bmatrix} \begin{bmatrix} x_1 \\ 0 \end{bmatrix} + \begin{bmatrix} 0 \\ 1 \end{bmatrix} x_1 = \begin{bmatrix} 0 \\ 0 \end{bmatrix}.$$

This result is expected; from (118), *considering* (148) *and* (149),

$$\begin{aligned} \mathbf{\Gamma} &= \begin{bmatrix} 0 & 1 \\ -1 & 1 \end{bmatrix} - \begin{bmatrix} 0 \\ 1 \end{bmatrix} \frac{\left(\begin{bmatrix} 0 & -1 \\ 1 & 1 \end{bmatrix} \begin{bmatrix} 0 \\ 1 \end{bmatrix} \right)^{\mathsf{T}}}{\begin{bmatrix} 0 & 1 \end{bmatrix} \begin{bmatrix} 0 \\ 1 \end{bmatrix}} \\ &= \begin{bmatrix} 0 & 1 \\ 0 & 0 \end{bmatrix} \end{aligned}$$

which is singular, and any point on $\sigma = x_2 = 0$, *subject to singular control, is an equilibrium point. The optimal return function approximation using (149) could be immediately improved by specifying* $\Psi(\mathbf{x}) = x_1^2 + x_1 x_2 + \frac{1}{2} x_2^2$ *yielding* $\sigma(\mathbf{x}) = x_1 + x_2$. *It is easy to verify that Conditions 1 and 2 are satisfied;* $\mathbf{\Gamma}$ *is singular. Equilibrium points occur only when* $x_2 = 0$. *However, from* $\sigma(\mathbf{x}) = x_1 + x_2 = 0$, *the only equilibrium point on the switching surface is the origin.*

With $\mathbf{\Gamma}$ singular, we expect that lower-dimensional nonzero equilibrium manifolds exist.

Theorem 7 *If the system* (87) *is controllable, the LOSC algorithm produces a one-dimensional, nonzero, equilibrium manifold.*

Proof. With

$$\mathbf{\Gamma} = \begin{bmatrix} 0 & 1 & 0 & & 0 \\ 0 & 0 & 1 & & 0 \\ \vdots & & & \ddots & \vdots \\ 0 & 0 & 0 & \cdots & 1 \\ \gamma_{n1} & \gamma_{n2} & \gamma_{n3} & \cdots & \gamma_{nn} \end{bmatrix}, \tag{151}$$

singular, we have $\gamma_{n1} = 0$. The state equations

$$\begin{aligned} \dot{\mathbf{x}} &= \mathbf{\Gamma x} \\ &= \begin{bmatrix} 0 & 1 & 0 & & 0 \\ 0 & 0 & 1 & & 0 \\ \vdots & & & \ddots & \vdots \\ 0 & 0 & 0 & \cdots & 1 \\ 0 & \gamma_{n2} & \gamma_{n3} & \cdots & \gamma_{nn} \end{bmatrix} \begin{bmatrix} x_1 \\ x_2 \\ \vdots \\ x_{n-1} \\ x_n \end{bmatrix} \end{aligned} \tag{152}$$

on the singular manifold are zero for all x_1 with $x_2 = x_3 = \cdots = x_n = 0$. The existence of the one-dimensional equilibrium manifold is proven. ■

The consequences of the existence of this manifold will be explored further; depending upon the eigenvalue structure of $\mathbf{A}$ this manifold directly impacts the specification of a control law with a domain of attraction equal to the controllable set.

Conditions 1 and 2 provide guidelines to aid in our selection of $\Psi(\mathbf{x})$. However we may have $\dot{\Psi}(\mathbf{x}) > 0$ for states near the switching surface, even in a small neighborhood of the origin. In addition, we see from (119) that $\dot{\Psi}(\mathbf{x}) > 0$ on S if $\mathbf{\Gamma}$ is unstable. We address these issues through careful selection of $\Psi(\mathbf{x})$.

3.1.1.3 Chatter

We illustrate the manner in which the chatter phenomenon may be influenced through selection of $\Psi(\mathbf{x})$ or, equivalently, the placement of $\partial\sigma/\partial\mathbf{x}$. This, in turn, effects implementation considerations of any singular or variable structure control strategy.

The singular control has been specified previously, in (115); before setting conditions let us add in Fillipov definitions. With $\sigma(\mathbf{x}^+) > 0$ let

$$\dot{\mathbf{x}}^+ = \mathbf{A}\mathbf{x}^+ + \mathbf{b}u_{\min} \tag{153}$$

and with $\sigma(\mathbf{x}^-) < 0$ let

$$\dot{\mathbf{x}}^- = \mathbf{A}\mathbf{x}^- + \mathbf{b}u_{\max}. \tag{154}$$

On the switching surface S, with $\sigma(\mathbf{x}) = 0$, the Fillipov velocity (46), is

$$\begin{aligned}
\dot{\mathbf{x}}_F &= \alpha\dot{\mathbf{x}}^+ + (1-\alpha)\dot{\mathbf{x}}^- \\
&= \alpha\left[\mathbf{A}\left(\mathbf{x}_\sigma + \delta\mathbf{x}^+\right) + \mathbf{b}u_{\min}\right] + (1-\alpha)\left[\mathbf{A}\left(\mathbf{x}_\sigma + \delta\mathbf{x}^-\right) + \mathbf{b}u_{\max}\right] \\
&= \mathbf{A}\left(\mathbf{x}_\sigma + \delta\mathbf{x}^-\right) + \alpha\mathbf{A}\left(\delta\mathbf{x}^+ - \delta\mathbf{x}^-\right) + \alpha\mathbf{b}u_{\min} + (1-\alpha)\mathbf{b}u_{\max},
\end{aligned} \tag{155}$$

where α is chosen such that (155) is tangent to S. More precisely, equation (155) is the effective velocity vector in the sense of Fillipov; we may think of a chattering trajectory as sliding along S with velocity (155). Singular control also produces velocity vectors directed along S; we expect allowable singular control and the presence of chatter to be related. In (155), α must be chosen such that $\dot{\mathbf{x}}_F$ is tangent to S. This requires $(\partial\sigma/\partial\mathbf{x})\,\dot{\mathbf{x}}_F = 0$

which is implies $\dot{\sigma} = 0$. Thus, Fillipov velocity vectors are equivalent to those produced by singular control. To investigate the chatter phenomenon in the LOSC setting, consider the following Theorems.

Theorem 8 *With $u(\mathbf{x}) = 0$ interior to the control constraint set and $\partial\sigma/\partial\mathbf{x}$ chosen such that Condition 1 is satisfied the LOSC method produces trajectories near S that satisfy necessary and sufficient conditions for chatter.*

Proof. Consider trajectories near S where $\sigma > 0$; we have

$$\begin{aligned} \frac{\partial\sigma}{\partial\mathbf{x}}\dot{\mathbf{x}}^{+} &= \frac{\partial\sigma}{\partial\mathbf{x}}\left[\mathbf{A}\mathbf{x}^{+} + \mathbf{b}u_{\min}\right] \\ &= \frac{\partial\sigma}{\partial\mathbf{x}}\left[\mathbf{A}\left(\mathbf{x}_{\sigma} + \delta\mathbf{x}^{+}\right) + \mathbf{b}u_{\min}\right]. \end{aligned} \tag{156}$$

Similarly, for trajectories near S where $\sigma < 0$ we have

$$\begin{aligned} \frac{\partial\sigma}{\partial\mathbf{x}}\dot{\mathbf{x}}^{-} &= \frac{\partial\sigma}{\partial\mathbf{x}}\left[\mathbf{A}\mathbf{x}^{-} + \mathbf{b}u_{\max}\right] \\ &= \frac{\partial\sigma}{\partial\mathbf{x}}\left[\mathbf{A}\left(\mathbf{x}_{\sigma} + \delta\mathbf{x}^{-}\right) + \mathbf{b}u_{\max}\right]. \end{aligned} \tag{157}$$

Near $\sigma = 0$, $\delta\mathbf{x} \approx \mathbf{0}$ and we have

$$\begin{aligned} \frac{\partial\sigma}{\partial\mathbf{x}}\dot{\mathbf{x}}^{+} &\approx \frac{\partial\sigma}{\partial\mathbf{x}}\left[\mathbf{A}\mathbf{x}_{\sigma} + \mathbf{b}u_{\min}\right] \\ \frac{\partial\sigma}{\partial\mathbf{x}}\dot{\mathbf{x}}^{-} &\approx \frac{\partial\sigma}{\partial\mathbf{x}}\left[\mathbf{A}\mathbf{x}_{\sigma} + \mathbf{b}u_{\max}\right]. \end{aligned} \tag{158}$$

As a trajectory approaches the target, near S, $\mathbf{x}_\sigma \to \mathbf{0}$ and (158) becomes

$$\begin{aligned} \frac{\partial \sigma}{\partial \mathbf{x}} \dot{\mathbf{x}}^+ &\approx \frac{\partial \sigma}{\partial \mathbf{x}} \mathbf{b} u_{\min} < 0 \\ \\ \frac{\partial \sigma}{\partial \mathbf{x}} \dot{\mathbf{x}}^- &\approx \frac{\partial \sigma}{\partial \mathbf{x}} \mathbf{b} u_{\max} > 0. \end{aligned} \tag{159}$$

With $\partial \sigma / \partial \mathbf{x}$ and $\mathbf{b}$ constant vectors, with $u(\mathbf{x}) = 0$ interior to the control constraint set we conclude that the quantities in (159) are of opposite sign. Furthermore, with $\sigma > 0$ we have $\dot{\sigma} < 0$ and with $\sigma < 0$ we have $\dot{\sigma} > 0$. Necessary and sufficient conditions for the existence of chatter are satisfied. ■

The proof of Theorem 8 provides us with an interesting local result as to the manner in which chatter enters the LOSC solution. We now examine chatter in a global sense, relaxing the assumption that $\mathbf{x}_\sigma$ is small. What emerges is a direct correlation between chatter and regions where the singular control $u_s(\mathbf{x})$ is admissible.

Theorem 9 *Consider a state $\mathbf{x}_\sigma$, located on S, where $\mathbf{x}_\sigma$ is not necessarily small in magnitude. If $u(\mathbf{x}) = 0$ is interior to the control constraint set and $u_{\min} < u_s(\mathbf{x}) < u_{\max}$, the LOSC method produces chatter about S at this point.*

Proof. From (156) we have

$$\frac{\partial \sigma}{\partial \mathbf{x}} \dot{\mathbf{x}}^+ = \frac{\partial \sigma}{\partial \mathbf{x}} \left[\mathbf{A} \left(\mathbf{x}_\sigma + \delta \mathbf{x}^+ \right) + \mathbf{b} u_{\min} \right] \tag{160}$$

which with $\delta \mathbf{x}^+ \approx 0$ yields

$$\frac{\partial \sigma}{\partial \mathbf{x}} \dot{\mathbf{x}}^+ \approx \frac{\partial \sigma}{\partial \mathbf{x}} \left[\mathbf{A} \mathbf{x}_\sigma + \mathbf{b} u_{\min} \right]. \tag{161}$$

Now with

$$u_s(\mathbf{x}_\sigma) = -\frac{(\partial\sigma/\partial\mathbf{x})\,\mathbf{A}}{(\partial\sigma/\partial\mathbf{x})\,\mathbf{b}}\mathbf{x}_\sigma \tag{162}$$

we have

$$\frac{\partial\sigma}{\partial\mathbf{x}}\mathbf{A}\mathbf{x}_{\boldsymbol{\sigma}} = -\frac{\partial\sigma}{\partial\mathbf{x}}\mathbf{b}u_s \tag{163}$$

which, from (161), yields

$$\begin{aligned}\frac{\partial\sigma}{\partial\mathbf{x}}\dot{\mathbf{x}}^+ &\approx -\frac{\partial\sigma}{\partial\mathbf{x}}\mathbf{b}u_s + \mathbf{b}u_{\min} \\ &= \frac{\partial\sigma}{\partial\mathbf{x}}\mathbf{b}\left[u_{\min} - u_s\right] < 0.\end{aligned} \tag{164}$$

Now from (157) we have

$$\frac{\partial\sigma}{\partial\mathbf{x}}\dot{\mathbf{x}}^- = \frac{\partial\sigma}{\partial\mathbf{x}}\left[\mathbf{A}\left(\mathbf{x}_\sigma + \delta\mathbf{x}^-\right) + \mathbf{b}u_{\max}\right] \tag{165}$$

which with $\delta\mathbf{x}^- \approx 0$ yields

$$\frac{\partial\sigma}{\partial\mathbf{x}}\dot{\mathbf{x}}^- \approx \frac{\partial\sigma}{\partial\mathbf{x}}\left[\mathbf{A}\mathbf{x}_\sigma + \mathbf{b}u_{\max}\right]. \tag{166}$$

From (163), (166) becomes

$$\frac{\partial\sigma}{\partial\mathbf{x}}\dot{\mathbf{x}}^- \approx -\frac{\partial\sigma}{\partial\mathbf{x}}\mathbf{b}u_s + \frac{\partial\sigma}{\partial\mathbf{x}}\mathbf{b}u_{\max} \tag{167}$$

which yields

$$\frac{\partial\sigma}{\partial\mathbf{x}}\dot{\mathbf{x}}^- \approx \frac{\partial\sigma}{\partial\mathbf{x}}\mathbf{b}\left[u_{\max} - u_s\right] > 0. \tag{168}$$

In comparison with (44) and (45), we see that (164) and (168) satisfy the necessary and

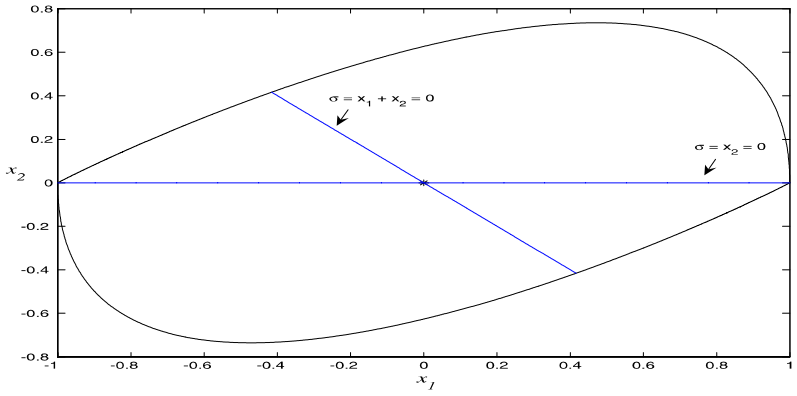

Figure 1: Controllable set for Example 2, along with two candidate switching surfaces.

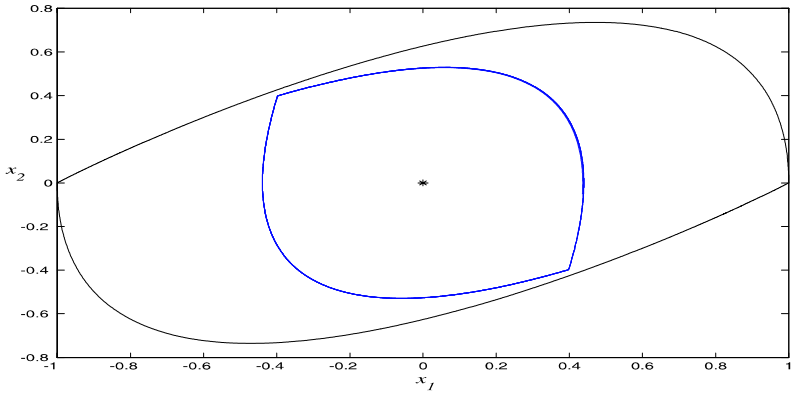

Figure 2: Region of effectiveness for Example 2 with $\sigma = x_1 + x_2$.

sufficient conditions for chatter. ■

The proof of Theorem 8 suggests that in a neighborhood of the origin, trajectories will chatter, regardless of the exact form of $\partial\sigma/\partial\mathbf{x}$. With $u_{\max}$ and $u_{\min}$ opposite in sign and Condition 1 satisfied, (159) satisfies the necessary and sufficient conditions for chatter. The proof of Theorem 9 suggests how we may effect chatter, throughout the controllable set, by altering the structure of $u_s(\mathbf{x})$.

The following example illustrates how chatter enters a solution; it also addresses singularity concerns raised in the proof of Theorem 7.

Example 2 *Consider the problem of transferring the state to the origin in minimum-time for the system governed by state equations*

$$\dot{\mathbf{x}} = \mathbf{A}\mathbf{x} + \mathbf{b}u$$

$$\begin{bmatrix} \dot{x}_1 \\ \dot{x}_2 \end{bmatrix} = \begin{bmatrix} 0 & 1 \\ -1 & 2 \end{bmatrix} \mathbf{x} + \begin{bmatrix} 0 \\ 1 \end{bmatrix} u. \tag{169}$$

The control is bounded by $|u(\mathbf{x})| \leq 1$. *The eigenvalues of* $\mathbf{A}$ *are* $\mu_1 = \mu_2 = 1$*; the system is unstable in the absence of control. The controllable set to the origin is shown in Fig. 1, along with two candidate switching surfaces. The controllable set* $\mathcal{C}$ *was generated as in* [1, pp. 458-459]. *Consider the implementation of the control law* (97) *with* $\sigma(\mathbf{x}) = x_1 + x_2 = 0$*; the region of effectiveness* $\mathcal{D}$ *under control law* (97) *is shown in Fig. 2. Typical trajectories are shown in Fig. 3; note that if the control* $u_s(\mathbf{x})$ *is admissible, trajectories chatter to the origin. Otherwise, they simply pass through the switching surface* $\sigma(\mathbf{x}) = 0$. *From* [1, pp. 98-99] *we know that the upper portion of the controllable set in Fig. 2 is generated with* $u = -1$*; the lower portion is generated with* $u = 1$. *Based upon this fact, we expect that setting* $\sigma(\mathbf{x}) = x_2$ *may allow the resulting control law* (97) *to transfer all states in the controllable set to the origin. However, the resulting matrix* $\mathbf{\Gamma}$ *is singular and the entire surface* $\sigma(\mathbf{x}) = 0$ *is an equilibrium manifold. Fig. 4 shows typical trajectories for* $\sigma(\mathbf{x}) = x_2$*; the* x_1 *axis is a one-dimensional equilibrium manifold.*

3.1.1.4 LOSC Domain of Attraction

In this section we examine the domain of attraction provided by the LOSC method. This analysis will consider stable systems (if no control were present), neutrally stable systems,

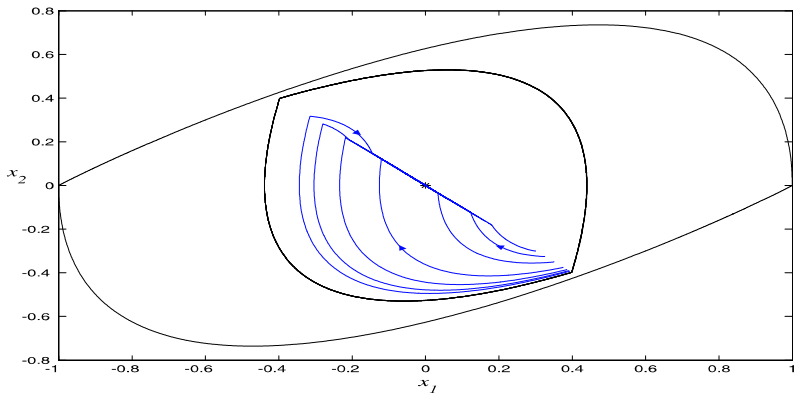

Figure 3: Typical trajectories for Example 2 with $\sigma = x_1 + x_2$.

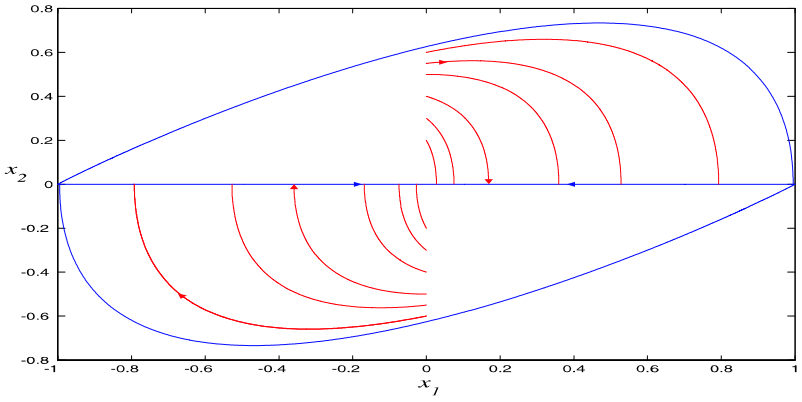

Figure 4: Typical Trajectories for Example 2 with $\sigma(\mathbf{x}) = x_2$.

and unstable systems. Asymptotic stability analysis for regions of bang-bang and singular control will be considered separately.

Stable Systems – Bang-Bang Control The underlying assumption of this section is that the eigenvalues of $\mathbf{A}$ have strictly negative real parts. For stable systems, the control law (97) produces two forced equilibrium points corresponding to $u(\mathbf{x}) = u_{\max}$ for $\sigma(\mathbf{x}) < 0$ and $u(\mathbf{x}) = u_{\min}$ for $\sigma(\mathbf{x}) > 0$. The stability properties of each forced equilibria are inherited from $\mathbf{A}$ [17, p. 133]. That is, under the control $u(\mathbf{x}) = u_{\max}$, the point $\bar{\mathbf{x}} = -\mathbf{A}^{-1}\mathbf{b}u_{\max}$ is globally asymptotically stable; similarly the point $\bar{\mathbf{x}} = -\mathbf{A}^{-1}\mathbf{b}u_{\min}$ is globally asymptotically stable for $u(\mathbf{x}) = u_{\min}$. We will formally prove global asymptotic stability of the origin after the next section, but qualitatively we may now discuss stability as it relates to bang-bang control. Consider the following result.

Theorem 10 *If $u_s(\mathbf{x}_\sigma)$ is not admissible, trajectories generated by LOSC do not chatter.*

Proof. This proof is similar to that of Theorem 9, but considered from another point of view. Consider a region near S where $\sigma(\mathbf{x}) > 0$ and $u_s(\mathbf{x}_\sigma)$ is not admissible; e.g. $u_s(\mathbf{x}_\sigma) > u_{\max}$. From (160) we have

$$\frac{\partial \sigma}{\partial \mathbf{x}}\dot{\mathbf{x}}^+ = \frac{\partial \sigma}{\partial \mathbf{x}}\left[\mathbf{A}\left(\mathbf{x}_\sigma + \delta\mathbf{x}^+\right) + \mathbf{b}u_{\min}\right] \tag{170}$$

which, considering (161), (162) and (163) yields

$$\begin{aligned}\frac{\partial \sigma}{\partial \mathbf{x}}\dot{\mathbf{x}}^+ &\approx -\frac{\partial \sigma}{\partial \mathbf{x}}\mathbf{b}u_s + \mathbf{b}u_{\min} \\ &= \frac{\partial \sigma}{\partial \mathbf{x}}\mathbf{b}\left[u_{\min} - u_s\right] < 0. \end{aligned} \tag{171}$$

For the same state $\mathbf{x}_\sigma$ in (171) consider the region $\sigma(\mathbf{x}) < 0$ and note that $u_s(\mathbf{x}_\sigma) > u_{\max}$ still holds. We have

$$\frac{\partial \sigma}{\partial \mathbf{x}} \dot{\mathbf{x}}^- = \frac{\partial \sigma}{\partial \mathbf{x}} \left[\mathbf{A} \left(\mathbf{x}_\sigma + \delta \mathbf{x}^- \right) + \mathbf{b} u_{\max} \right] \tag{172}$$

which, as before, results in

$$\begin{aligned} \frac{\partial \sigma}{\partial \mathbf{x}} \dot{\mathbf{x}}^- &\approx -\frac{\partial \sigma}{\partial \mathbf{x}} \mathbf{b} u_s + \mathbf{b} u_{\max} \\ &= \frac{\partial \sigma}{\partial \mathbf{x}} \mathbf{b} \left[u_{\max} - u_s \right] < 0. \end{aligned} \tag{173}$$

We see that with $u_s(\mathbf{x}_\sigma) > u_{\max}$, the necessary conditions for chatter are not satisfied. Analogous results hold for $u_s(\mathbf{x}_\sigma) < u_{\min}$. ■

Stable Systems – Singular Control Theorem 7 proves the existence of nonzero equilibrium manifolds in regions of intermediate control. Such manifolds certainly effect the domain of attraction for the control law (97). We now investigate relationships between the domain of attraction and the LOSC intermediate control strategy. Expanding $\mathbf{\Phi}$ from (117) yields

$$\mathbf{\Phi} = \frac{1}{(\partial \sigma / \partial \mathbf{x}) \mathbf{b}} \begin{bmatrix} 0 \\ 0 \\ \vdots \\ 0 \\ 1 \end{bmatrix} \begin{bmatrix} \frac{\partial \sigma}{\partial x_1} & \frac{\partial \sigma}{\partial x_2} & \frac{\partial \sigma}{\partial x_3} & \cdots & \frac{\partial \sigma}{\partial x_n} \end{bmatrix} \begin{bmatrix} 0 & 1 & 0 & & 0 \\ 0 & 0 & 1 & & 0 \\ \vdots & & & \ddots & \vdots \\ 0 & 0 & 0 & \cdots & 1 \\ a_{n1} & a_{n2} & a_{n3} & \cdots & a_{nn} \end{bmatrix}$$

so that

$$\mathbf{\Phi} = \frac{1}{\partial\sigma/\partial x_n}\begin{bmatrix} 0 & 0 & 0 & \cdots & 0 \\ 0 & 0 & 0 & & 0 \\ \vdots & & & \ddots & \vdots \\ 0 & 0 & 0 & \cdots & 0 \\ a_{n1}\dfrac{\partial\sigma}{\partial x_n} & \dfrac{\partial\sigma}{\partial x_1} + a_{n2}\dfrac{\partial\sigma}{\partial x_n} & \cdots & & \dfrac{\partial\sigma}{\partial x_{n-1}} + a_{nn}\dfrac{\partial\sigma}{\partial x_n} \end{bmatrix}.$$

Now from (118) $\mathbf{\Gamma} = \mathbf{A} - \mathbf{\Phi}$ yields

$$\mathbf{\Gamma} = \begin{bmatrix} 0 & 1 & 0 & & 0 \\ 0 & 0 & 1 & & 0 \\ \vdots & & & \ddots & \vdots \\ 0 & 0 & 0 & \cdots & 1 \\ a_{n1} & a_{n2} & a_{n3} & \cdots & a_{nn} \end{bmatrix}$$
$$- \frac{1}{\partial\sigma/\partial x_n}\begin{bmatrix} 0 & 0 & 0 & \cdots & 0 \\ 0 & 0 & 0 & & 0 \\ \vdots & & & \ddots & \vdots \\ 0 & 0 & 0 & \cdots & 0 \\ a_{n1}\dfrac{\partial\sigma}{\partial x_n} & \dfrac{\partial\sigma}{\partial x_1} + a_{n2}\dfrac{\partial\sigma}{\partial x_n} & \cdots & & \dfrac{\partial\sigma}{\partial x_{n-1}} + a_{nn}\dfrac{\partial\sigma}{\partial x_n} \end{bmatrix}$$

we have

$$\mathbf{\Gamma} = \begin{bmatrix} 0 & 1 & 0 & & 0 \\ 0 & 0 & 1 & & 0 \\ \vdots & & & \ddots & \vdots \\ 0 & 0 & 0 & \cdots & 1 \\ 0 & -\dfrac{\partial\sigma/\partial x_1}{\partial\sigma/\partial x_n} & -\dfrac{\partial\sigma/\partial x_2}{\partial\sigma/\partial x_n} & \cdots & -\dfrac{\partial\sigma/\partial x_{n-1}}{\partial\sigma/\partial x_n} \end{bmatrix}. \tag{174}$$

From Condition 1 we have

$$\frac{\partial\sigma}{\partial\mathbf{x}}\mathbf{b} > \mathbf{0} \tag{175}$$

which with $\mathbf{b}$ in companion form this implies that

$$\frac{\partial\sigma}{\partial x_n} > 0. \tag{176}$$

In view of (174) and (115) we may think of $\partial\sigma/\partial x_n$ as controlling the magnitude of the singular manifold eigenvalues and also the magnitude of the singular control. The remaining elements of $\partial\sigma/\partial\mathbf{x}$ may be thought of as controlling the sign of the eigenvalues of (174), which determines stability properties of trajectories on the singular manifold. We observe from equation (174) that $n-1$ eigenvalues of $\mathbf{\Gamma}$ are free to be specified; however previously established stability conditions must be considered prior to this eigenvalue selection. The following analysis illustrates this point, beginning with stable systems.

For stable systems, the controllable set is all of state space. We will show that through careful selection of $\partial\sigma/\partial\mathbf{x}$, all trajectories generated by $u_s(\mathbf{x})$ are stable. To do this, we must consider the constraints that previous stability conditions have imposed upon our

system.

Lemma 1 *If* $\mathbf{A}$ *is stable, with* $u(\mathbf{x}) = 0$ *interior to the control constraint set* $\mathcal{U}$ *then Condition 2 becomes*

$$\frac{\partial \sigma / \partial x_1}{a_{n1}} \leq 0.$$

Proof. This result follows by extending the proof of Theorem 3. With $\mathbf{A}$ in companion form

$$\mathbf{A}^{-1} = \begin{bmatrix} -\frac{a_{n2}}{a_{n1}} & -\frac{a_{n3}}{a_{n1}} & \cdots & -\frac{a_{nn}}{a_{n1}} & \frac{1}{a_{n1}} \\ 1 & 0 & \cdots & 0 & 0 \\ 0 & 1 & \ddots & 0 & 0 \\ 0 & 0 & \ddots & 0 & 0 \\ 0 & 0 & \cdots & 1 & 0 \end{bmatrix}$$

which yields

$$\mathbf{A}^{-1}\mathbf{b} = \begin{bmatrix} \frac{1}{a_{n1}} \\ \\ 0 \\ \vdots \\ 0 \\ 0 \end{bmatrix}$$

and

$$\frac{\partial \sigma}{\partial \mathbf{x}} \mathbf{A}^{-1}\mathbf{b} = \frac{\partial \sigma / \partial x_1}{a_{n1}}.$$

From Condition 2 we have

$$\frac{\partial \sigma / \partial x_1}{a_{n1}} \leq 0. \tag{177}$$

■

We are not able to freely specify $n-1$ elements of (174); this may adversely effect the domain of attraction. Fortunately for stable systems we are still able to show that the LOSC method yields a control such that the origin is globally asymptotically stable under singular control.

Theorem 11 *If*

$$\frac{\partial\sigma/\partial x_1}{a_{n1}} < 0 \tag{178}$$

then the singular surface does not contain a nonzero equilibrium manifold.

Proof. Existence of a one-dimensional equilibrium manifold for all x_1, with $x_2 = x_3 = \cdots = x_n = 0$, was proven in Theorem 7. Any plane that contains nonzero points of this equilibrium manifold would have a normal where the first entry $\partial\sigma/\partial x_1$ is zero. For stable systems, the constant a_{n1} is nonzero; the requirement (178) then implies that $\partial\sigma/\partial x_1$ is nonzero. The only point on the equilibrium manifold, contained by the switching surface with $\partial\sigma/\partial x_1 \neq 0$ is the origin. ■

We may now modify Condition 2 in light of the results of Lemma 1 and Theorem 11.

Condition 3 *Select*

$$\frac{\partial\sigma/\partial x_1}{a_{n1}} < 0. \tag{179}$$

Despite the singularity of $\mathbf{\Gamma}$, which induces a one-dimensional equilibrium manifold, Theorem 11 assures us that we do have the freedom to choose a switching surface that does not contain nonzero equilibrium points. However, as such choices are made, we must consider the resulting effects on system stability. In particular, for stable systems, can we satisfy all the conditions developed thus far and still guarantee global asymptotic stability? We first must show that there exists a neighborhood containing the origin, on the singular

manifold S, where an allowable intermediate control forces all trajectories to asymptotically approach the origin. Of particular interest is the following; can we satisfy Condition 3 and still prove asymptotic stability to the origin for trajectories on S? The major concern is that stability on S requires that we place S such that the equilibrium point corresponding to maximum control effort lies in the region $\sigma < 0$.

Theorem 12 *Assume the system* (87) *is controllable and the eigenvalues of the matrix* $\mathbf{A}$ *have strictly negative real parts. Furthermore, assume that* $\mathbf{x} \in \hat{S}$. *With* S *specified such that Conditions* 1 *and* 3 *are satisfied, the coefficients* $\gamma_{n2}, \gamma_{n3}, \ldots, \gamma_{nn}$ *can be chosen negative.*

Proof. Conditions 1 and 3 place restrictions on the signs of $\partial\sigma/\partial x_1$ and $\partial\sigma/\partial x_n$; this effects our ability to specify elements of $\mathbf{\Gamma}$. Let

$$\mathbf{\Gamma}_r = \begin{bmatrix} 0 & 1 & & 0 \\ & & \ddots & \vdots \\ 0 & 0 & \cdots & 1 \\ \gamma_{n2} & \gamma_{n3} & \cdots & \gamma_{nn} \end{bmatrix} \tag{180}$$

or, equivalently,

$$\mathbf{\Gamma}_r = \begin{bmatrix} 0 & 1 & & 0 \\ & & \ddots & \vdots \\ 0 & 0 & \cdots & 1 \\ -\dfrac{\partial\sigma/\partial x_1}{\partial\sigma/\partial x_n} & -\dfrac{\partial\sigma/\partial x_2}{\partial\sigma/\partial x_n} & \cdots & -\dfrac{\partial\sigma/\partial x_{n-1}}{\partial\sigma/\partial x_n} \end{bmatrix} \tag{181}$$

denote a reduced system matrix derived from $\mathbf{\Gamma}$, Equation (174). With $\mathbf{A}$ asymptotically

stable, $a_{n1} < 0$; through Condition 3 this implies that $\partial\sigma/\partial x_1 > 0$. With $\partial\sigma/\partial x_n > 0$ we have $\gamma_{n2} < 0$. One way to guarantee that $\gamma_{n2}, \ldots, \gamma_{nn}$ are all negative is to select

$$\gamma_{nj} = -\frac{\partial\sigma/\partial x_{j-1}}{\partial\sigma/\partial x_n} = a_{nj}, \ j = 2, ..., n. \tag{182}$$

■

Theorem 13 *Assume the system* (87) *is controllable, the eigenvalues of the matrix* $\mathbf{A}$ *have strictly negative real parts, and that* $\mathbf{x} \in \hat{S}$. *We may select* $\gamma_{n2}, \gamma_{n3}, \ldots, \gamma_{nn}$ *such that the* $n-1$ *eigenvalues of* $\mathbf{\Gamma}_r$ *have strictly negative real parts.*

Proof. From Theorem 12, using *(182),* we have $\gamma_{n2}, \gamma_{n3}, \ldots, \gamma_{nn}$ less than zero; this is a necessary condition for the eigenvalues of $\mathbf{\Gamma}_r$ to have strictly negative real parts. To demonstrate that we may always specify $\gamma_{n2}, \gamma_{n3}, \ldots, \gamma_{nn}$ such that $\mathbf{\Gamma}_r$ has eigenvalues with strictly negative real parts consider the following. Let $\mathbf{\Pi}$ be a $n \times n$ matrix of the form

$$\mathbf{\Pi} = \begin{bmatrix} 0 & 1 & 0 & & 0 \\ 0 & 0 & 1 & & 0 \\ \vdots & & & \ddots & \vdots \\ 0 & 0 & 0 & \cdots & 1 \\ -\pi_n & -\pi_{n-1} & -\pi_{n-2} & \cdots & -\pi_1 \end{bmatrix} \tag{183}$$

which satisfies the Hurwitz test for stability. That is, the coefficients $\pi_i, i = 1, \ldots, n$ of its characteristic equation

$$s^n + \pi_1 s^{n-1} + \cdots + \pi_{n-1} s + \pi_n = 0 \tag{184}$$

and the determinants $\Delta_i, i = 1, \ldots, n$, are positive, where

$$\Delta_i = \begin{vmatrix} \pi_1 & 1 & 0 & 0 & 0 & 0 & \cdots & 0 \\ \pi_3 & \pi_2 & \pi_1 & 1 & 0 & 0 & \cdots & 0 \\ \pi_5 & \pi_4 & \pi_3 & \pi_2 & \pi_1 & 1 & \cdots & 0 \\ \vdots & \vdots & \vdots & \vdots & \vdots & \vdots & \ddots & 0 \\ \pi_{2i-1} & \pi_{2i-2} & \pi_{2i-3} & \pi_{2i-4} & \pi_{2i-5} & \pi_{2i-6} & \cdots & \pi_i \end{vmatrix}. \tag{185}$$

The Hurwitz determinants are characterized by the coefficients π_i on the diagonal and increasing indices from right to left and top to bottom, see [26] for further reference. Now consider the $(n-1) \times (n-1)$ matrix $\mathbf{\Pi}_r$, found by deleting the first row and column of $\mathbf{\Pi}$.

$$\mathbf{\Pi}_r = \begin{bmatrix} 0 & 1 & & 0 \\ & & \ddots & \vdots \\ 0 & 0 & \cdots & 1 \\ -\pi_{n-1} & -\pi_{n-2} & \cdots & -\pi_1 \end{bmatrix} \tag{186}$$

with characteristic equation

$$s^{n-1} + \pi_1 s^{n-2} + \cdots + \pi_{n-2} s + \pi_{n-1} = 0. \tag{187}$$

Note that the coefficients $\pi_i, i = 1, \ldots, n-1$, of the characteristic equation (187) are positive. For $\mathbf{\Pi}_r$ to satisfy the Hurwitz test for stability and therefore have eigenvalues with strictly

negative real parts the determinants $\Delta_i^{'}, i = 1, \ldots, n-1$, must be positive. We have

$$\Delta_i^{'} = \begin{vmatrix} \pi_1 & 1 & 0 & 0 & 0 & 0 & \cdots & 0 \\ \pi_3 & \pi_2 & \pi_1 & 1 & 0 & 0 & \cdots & 0 \\ \pi_5 & \pi_4 & \pi_3 & \pi_2 & \pi_1 & 1 & \cdots & 0 \\ \vdots & \vdots & \vdots & \vdots & \vdots & \vdots & \ddots & 0 \\ \pi_{2i-1} & \pi_{2i-2} & \pi_{2i-3} & \pi_{2i-4} & \pi_{2i-5} & \pi_{2i-6} & \cdots & \pi_i \end{vmatrix}; \tag{188}$$

comparison of (185) and (188) shows that if $\Delta_i, i = 1, \ldots, n$ are positive then $\Delta_i^{'}, i = 1, \ldots, n-1$, are also positive. Hence, the $n-1$ eigenvalues of $\mathbf{\Pi}_r$ have strictly negative real parts. ■

Example 3 *Consider some matrix with characteristic equation*

$$s^4 + \pi_1 s^3 + \pi_2 s^2 + \pi_3 s + \pi_4 = 0,$$

which satisfies the Hurwitz test for stability. That is, we have $\pi_i, i = 1, ..., 4$ *greater than zero and*

$$\Delta_1 = \pi_1 > 0$$

$$\Delta_2 = \begin{vmatrix} \pi_1 & 1 \\ \pi_3 & \pi_2 \end{vmatrix} > 0$$

$$\Delta_3 = \begin{vmatrix} \pi_1 & 1 & 0 \\ \pi_3 & \pi_2 & \pi_1 \\ \pi_5 & \pi_4 & \pi_3 \end{vmatrix} > 0$$

$$\Delta_4 = \begin{vmatrix} \pi_1 & 1 & 0 & 0 \\ \pi_3 & \pi_2 & \pi_1 & 1 \\ \pi_5 & \pi_4 & \pi_3 & \pi_2 \\ \pi_7 & \pi_6 & \pi_5 & \pi_4 \end{vmatrix} > 0.$$

Now consider the characteristic polynomial of a reduced matrix

$$s^3 + \pi_1 s^2 + \pi_2 s + \pi_3 = 0.$$

For stability, we need the coefficients $\pi_i, i = 1, ..., 3$ *greater than zero; indeed this holds. We also need*

$$\Delta_1^{'} = \pi_1 > 0$$

$$\Delta_2^{'} = \begin{vmatrix} \pi_1 & 1 \\ \pi_3 & \pi_2 \end{vmatrix} > 0$$

$$\Delta_3^{'} = \begin{vmatrix} \pi_1 & 1 & 0 \\ \pi_3 & \pi_2 & \pi_1 \\ \pi_5 & \pi_4 & \pi_3 \end{vmatrix} > 0.$$

Again we verify that the determinants $\Delta_i^{'}, i = 1, \ldots, 3$ *are greater than zero.*

Theorem 14 *With the system* (4) *controllable, the real parts of the eigenvalues of the matrix* $\mathbf{A}$ *strictly negative, and Conditions 1, and 3 satisfied, the LOSC method guarantees asymptotic stability of the origin.*

Proof. The result of Theorem 12 implies that

$$\mathbf{\Gamma}_r = \begin{bmatrix} 0 & 1 & & 0 \\ & & \ddots & \vdots \\ 0 & 0 & \cdots & 1 \\ a_{n2} & a_{n3} & \cdots & a_{nn} \end{bmatrix} \tag{189}$$

which, from the proof of Theorem 13 has eigenvalues with strictly negative real parts. With Conditions 1 and 3 satisfied, trajectories will evolve under bang-bang control until a region is penetrated where $u_s(\mathbf{x})$ is admissible. With the real parts of the eigenvalues of $\mathbf{\Gamma}_r$ strictly negative, trajectories chatter about the stable surface S and asymptotically approach the origin. ■

Neutrally Stable or Unstable Systems – Local Stability For neutrally stable and unstable systems the domain of attraction is not, in general, all of state space. Therefore we wish to establish local asymptotic stability of the origin for such systems.

Theorem 15 *Assume the matrix* $\mathbf{A}$ *has at least one eigenvalue with a zero or positive real part. Also assume that* $u = 0$ *is interior to the control constraint set* $\mathcal{U}$*. The LOSC methodology provides local asymptotic convergence to the origin.*

Proof. This proof of this theorem follows from the proofs Theorems 13 and 14. We may freely specify $n-1$ elements of the matrix $\mathbf{\Gamma}_r$, producing a stable manifold S. Furthermore,

Theorem 2 assures us that there exists some region such that trajectories reach S in finite time. Therefore, the origin is locally asymptotically stable. ■

3.1.1.5 LOSC Time Scales

The preceding analysis has considered several issues that effect behavior of an implemented LOSC control. These issues include the presence of nonzero equilibrium points, equilibrium manifolds, chatter, and asymptotic convergence. Another fundamental concern, relevant to any numerical algorithm, is that of time scales in systems of differential equations. From (174) we see that the particular form of $\partial\sigma/\partial\mathbf{x}$ certainly effects the eigenvalue structure of $\mathbf{\Gamma}$, thereby dictating the time scales on S. Off of S, with $u = u_{\max}$ or $u = u_{\min}$ as required by the optimal control necessary conditions, we suppose that the placement of $\partial\sigma/\partial\mathbf{x}$ is our only tool to affect numerical stiffness. For the LOSC control methodology, applied to minimum time optimal control problems, we will investigate the time scale properties of the singularly perturbed system (24) and unperturbed system (87). In the following, we prove that the LOSC method is uniformly nonstiff on S; this allows the analyst the freedom to specify $\partial\sigma/\partial\mathbf{x}$ such that trajectories are less stiff throughout the state space.

From (174), careful selection of $\partial\sigma/\partial\mathbf{x}$ certainly allows the analyst the freedom to specify system eigenvalues on S, controlling stiffness. As in Lemma 1 and Theorem 12 one must wonder if conditions on $\partial\sigma/\partial\mathbf{x}$ may induce stiffness on S for an otherwise nonstiff system. Furthermore, the introduction of a perturbation parameter ϵ certainly introduces disparate time scales into the system (24)–(27).

$$\begin{aligned} \dot{\mathbf{x}}_r &= \tilde{\mathbf{A}}\hat{\mathbf{x}} \\ \epsilon\dot{x}_n &= \mathbf{a}^{\intercal}\mathbf{x} + u \end{aligned} \tag{190}$$

where

$$\mathbf{x} = \begin{bmatrix} \mathbf{x}_r \\ \\ x_n \end{bmatrix}. \tag{191}$$

Stiffness properties on and off S for the LOSC methodology must be investigated.

LOSC Time Scale Properties on the Switching Surface

Theorem 16 *Consider the application of the LOSC control methodology to* (190) *which contains a small, positive, perturbation parameter* ϵ*. Stiffness characteristics on* S *are independent of the magnitude of* ϵ*.*

Proof. With the state given by (190) we have

$$\begin{aligned} \dot{W}_0 &= 1 + \frac{\partial \Psi}{\partial \mathbf{x}} \dot{\mathbf{x}} \\ &= 1 + \frac{\partial \Psi}{\partial \mathbf{x}_r} \dot{\mathbf{x}}_r + \frac{\partial \Psi}{\partial x_n} \dot{x}_n \\ &= 1 + \frac{\partial \Psi}{\partial \mathbf{x}_r} \tilde{\mathbf{A}} \hat{\mathbf{x}} + \frac{1}{\epsilon} \frac{\partial \Psi}{\partial x_n} \left[\mathbf{a}^\intercal \mathbf{x} + u \right]. \end{aligned} \tag{192}$$

Now

$$\sigma = \frac{\partial \dot{W}_0}{\partial u} = \frac{1}{\epsilon} \frac{\partial \Psi}{\partial x_n} \tag{193}$$

and

$$\begin{aligned} \dot{\sigma} &= \frac{1}{\epsilon} \frac{\partial}{\partial \mathbf{x}_r} \left(\frac{\partial \Psi}{\partial x_n} \right) \dot{\mathbf{x}}_r + \frac{1}{\epsilon} \frac{\partial}{\partial x_n} \left(\frac{\partial \Psi}{\partial x_n} \right) \dot{x}_n \\ &= \frac{1}{\epsilon} \frac{\partial^2 \Psi}{\partial x_n \partial \mathbf{x}_r} \tilde{\mathbf{A}} \hat{\mathbf{x}} + \frac{1}{\epsilon^2} \frac{\partial^2 \Psi}{\partial x_n^2} \left[\mathbf{a}^\intercal \mathbf{x} + u \right] \end{aligned} \tag{194}$$

which yields

$$\epsilon^2 \dot{\sigma} = \epsilon \frac{\partial^2 \Psi}{\partial x_n \partial \mathbf{x}_r} \tilde{\mathbf{A}} \hat{\mathbf{x}} + \frac{\partial^2 \Psi}{\partial x_n^2} \left[\mathbf{a}^\intercal \mathbf{x} + u \right]. \tag{195}$$

To keep $\sigma = 0$ for a finite time period the necessary conditions require $\dot{\sigma} \equiv 0$. Therefore the intermediate or singular control u_s may be found through

$$0 = \epsilon \frac{\partial^2 \Psi}{\partial x_n \partial \mathbf{x}_r} \tilde{\mathbf{A}} \hat{\mathbf{x}} + \frac{\partial^2 \Psi}{\partial x_n^2} \left[\mathbf{a}^\intercal \mathbf{x} + u_s \right] \tag{196}$$

which implies that

$$u_s = -\epsilon \frac{\overline{\dfrac{\partial^2 \Psi}{\partial x_n \partial \mathbf{x}_r}}}{\partial^2 \Psi / \partial x_n^2} \tilde{\mathbf{A}} \hat{\mathbf{x}} - \mathbf{a}^\intercal \mathbf{x}. \tag{197}$$

Substitution of (197) into (190) results in

$$\begin{aligned} \dot{\mathbf{x}}_r &= \tilde{\mathbf{A}} \hat{\mathbf{x}} \\ \epsilon \dot{x}_n &= -\epsilon \frac{\overline{\dfrac{\partial^2 \Psi}{\partial x_n \partial \mathbf{x}_r}}}{\partial^2 \Psi / \partial x_n^2} \tilde{\mathbf{A}} \hat{\mathbf{x}} \end{aligned} \tag{198}$$

or

$$\begin{aligned} \dot{\mathbf{x}}_r &= \tilde{\mathbf{A}} \hat{\mathbf{x}} \\ \dot{x}_n &= -\frac{\overline{\dfrac{\partial^2 \Psi}{\partial x_n \partial \mathbf{x}_r}}}{\partial^2 \Psi / \partial x_n^2} \tilde{\mathbf{A}} \hat{\mathbf{x}}. \end{aligned} \tag{199}$$

The magnitude of the singular perturbation parameter ϵ does not effect time scales for the LOSC algorithm on the manifold S. ■

In addition to proving that stiffness on S is independent of ϵ, we see from (199) that system time scales on S are directly influenced by the magnitude of $\partial^2 \Psi / \partial x_n^2$. Placement of

$\partial\sigma/\partial\mathbf{x}$ plays a major role in algorithmic performance, as it did when chatter and stability were under consideration.

3.1.2 Design Summary for LOSC Applied to Linear Systems

The following design steps and general information are re-stated to aid the analyst in specification of an appropriate descent function $\Psi(\mathbf{x})$:

1) Select $(\partial\sigma/\partial\mathbf{x})\,\mathbf{b} > 0$; this follows from the assumed positive definite form of $\Psi(\mathbf{x})$.

2) Select $(\partial\sigma/\partial\mathbf{x})\,\mathbf{A}^{-1}\mathbf{b} \leq 0$; this guarantees that trajectories do not converge to nonzero equilibrium points in regions of constant control.

3) If the system is controllable, singularity of $\mathbf{A}$ does not induce equilibrium manifolds in regions of constant control.

4) Since $\mathbf{\Gamma}$ is singular, a one-dimensional equilibrium manifold exists for all x_1 with $x_2 = x_3 = \cdots x_n = 0$. To ensure that S does not contain this manifold, for a system in companion form, select

$$\frac{\partial\sigma/\partial x_1}{a_{n1}} < 0$$

5) Time scale properties on S are independent of the magnitude of the singular perturbation parameter ϵ; they are completely determined by the placement of $\partial\sigma/\partial\mathbf{x}$.

3.2 General Optimal Control Problems

In this section we consider the more general integral cost problem (47)–(51) with a scalar control and relax the assumption that the state equations are linear and decoupled. As noted throughout the literature, the selection of an appropriate Lyapunov function for a general nonlinear system is exceedingly difficult. The selection process often requires

some qualitative analysis specific to a particular problem or class of problems. In this section an approach that blends quantitative and qualitative analysis is presented for a Lyapunov sub-optimal solution of a nonlinear, integral cost, optimal control problem. The objective is to extend the application of Lyapunov optimizing control methods to nonlinear problems where a switching surface exists and singular control is possible. Selection of an appropriate descent function is achieved by satisfying optimal control necessary conditions on the switching manifold and at the target. A descent function for the general optimal control problem will be denoted by $W(\mathbf{x})$ as opposed to $\Psi(\mathbf{x})$, which, by definition, is a quadratic function.

Construction of an appropriate descent function $W(\mathbf{x})$ is accomplished in three fundamental steps.

Step One: Formally state the optimal control problem; assume that the analyst may assemble

1) $H(\mathbf{x},\mathbf{u},\boldsymbol{\lambda}) \triangleq f_0(\mathbf{x},\mathbf{u}) + \boldsymbol{\lambda}^{\intercal}\mathbf{f}(\mathbf{x},\mathbf{u})$

2) $\sigma_i \triangleq \dfrac{\partial H}{\partial u_i}$

3) $\dot{\sigma}_i \triangleq \dfrac{d}{dt}\left(\dfrac{\partial H}{\partial u_i}\right)$

4) $\dot{\boldsymbol{\lambda}}^{\intercal} = -\dfrac{\partial H}{\partial \mathbf{x}}$

5) $\boldsymbol{\lambda}_f = \left.\dfrac{\partial V^*}{\partial \mathbf{x}}\right|_{t_f}$

Step Two: Specify a descent function $W(\mathbf{x})$.

1) Determine the control law by considering the rate at which cost accumulates and descent towards the target, that is $\min_{\mathbf{u}} \dot{W}_0(\mathbf{x},\mathbf{u}) = f_0(\mathbf{x},\mathbf{u}) + [\partial W/\partial \mathbf{x}]\,\mathbf{f}(\mathbf{x},\mathbf{u})$.

2) Select a descent function to the target. For points controllable to the target, the descent function $W(\mathbf{x})$ must be continuous and continuously differentiable outside the target set and on the boundary of the target set. Contours or regions of $W(\mathbf{x}) \leq c$ are nested and the target is contained in one of these regions. If the target set is bounded, so are the regions $W(\mathbf{x}) \leq c$. That is we require $W(\mathbf{x}) > 0$ and desire $\dot{W}(\mathbf{x}) < 0$.

3) If singular control is allowed, we solve for u_{is} via

$$\sigma_i = 0 \tag{200}$$

$$\dot{\sigma}_i = 0. \tag{201}$$

Step Three: Perform analytical analysis and numerical tuning of any parameters specific to a particular problem. This will be illustrated in the following example.

We will use the Matlab constrained minimization routine **fmincon** for this numerical tuning. Parameter values chosen will minimize the cost functional over a specified reference trajectory.

The LOSC approach is illustrated through the following examples.

Example 4 ***Maximum Yield Harvest****: Consider the problem of harvesting fish from a lake over a fixed time period $T \geq 0$, such that at the end of the time period the maximum amount of fish has been harvested. With u denoting the amount of harvesting effort, we wish to minimize (maximize total harvest)*

$$J = -\int_0^T u x_1 dt, \tag{202}$$

where $x_1 \geq 0$ denotes the fish population. If we let $x_2 = t$ we may state the cost and state equations as

$$\begin{aligned} \dot{x}_0 &= -ux_1 \\ \dot{x}_1 &= x_1 (1 - x_1) - ux_1 \\ \dot{x}_2 &= 1. \end{aligned} \tag{203}$$

The harvesting effort is bounded between $u = 0$ (no harvest) and $u = u_{\max} > 0$ (maximum-effort harvest). The control set $\mathcal{U}$ is defined by

$$h_1 = u \geq 0 \tag{204}$$

$$h_2 = u_{\max} - u \geq 0, \tag{205}$$

and the terminal set is given by

$$g(\mathbf{x}) = T - x_2(t_f) = 0, \tag{206}$$

and let $T = 10$. We assemble the H function

$$H = -ux_1 + \lambda_1 [x_1 (1 - x_1) - ux_1] + \lambda_2, \tag{207}$$

the switching function $\sigma = \partial H / \partial u$

$$\sigma = -x_1 (1 + \lambda_1), \tag{208}$$

and its derivative

$$\dot{\sigma} = -\dot{x}_1 \left(1 + \dot{\lambda}_1\right), \tag{209}$$

the adjoint equations

$$\dot{\lambda}_1 = u - \lambda_1 \left(1 - 2x_1 - u\right) \tag{210}$$

$$\dot{\lambda}_2 = 0, \tag{211}$$

and the transversality conditions

$$\lambda_1 \left(T\right) = 0 \tag{212}$$

$$\lambda_2 \left(T\right) = \rho, \tag{213}$$

where ρ is a constant [1, pp. 404-409]. *From the minimum principle, singular control is allowed in this example.*

On the singular manifold S (208)-(210) imply that x_1 is constant; equation (208) implies that $\lambda_1 = -1$. From (212) we see that the problem does not terminate on a singular arc. We infer that trajectories that follow the singular manifold represent long term fishing strategies, sufficiently far from the terminal manifold. At some point in time, these trajectories must leave S and switch to maximum fishing effort as the target (terminal time) draws near. To mimic actual optimal control behavior the population x_1 should be maintained near constant levels far from the terminal manifold with bang-bang fishing effort implemented near this manifold. Intuitively we suspect that far from the terminal manifold some

intermediate control effort is needed to achieve an acceptable harvest without exhausting the fish population.

Consider the following descent function

$$W(\mathbf{x}) = \left[e^{-\alpha(T-x_2)} - 1\right] \ln(x_1 + \beta) \tag{214}$$

where α and β are positive constants. The steps taken to determine W will be presented shortly, first we need the following quantities:

$$\frac{\partial W}{\partial x_1} = \frac{e^{-\alpha(T-x_2)} - 1}{x_1 + \beta} \tag{215}$$

$$\frac{\partial W}{\partial x_2} = \alpha e^{-\alpha(T-x_2)} \ln(x_1 + \beta), \tag{216}$$

$$\begin{aligned} \dot{W}(\mathbf{x}, u) = \frac{\partial W}{\partial \mathbf{x}} \dot{\mathbf{x}} = \left[\frac{e^{-\alpha(T-x_2)} - 1}{x_1 + \beta}\right] [x_1(1 - x_1) - u x_1] \\ + \alpha e^{-\alpha(T-x_2)} \ln(x_1 + \beta), \end{aligned} \tag{217}$$

and, with $W_0 = x_0 + W(\mathbf{x})$

$$\begin{aligned} \dot{W}_0(\mathbf{x}, u) = -u x_1 + \left[\frac{e^{-\alpha(T-x_2)} - 1}{x_1 + \beta}\right] [x_1(1 - x_1) - u x_1] \\ + \alpha e^{-\alpha(T-x_2)} \ln(x_1 + \beta). \end{aligned} \tag{218}$$

The switching function is

$$\sigma = -x_1 \left[1 + \frac{\partial W}{\partial x_1}\right]$$

$$= -x_1 \left[1 + \frac{e^{-\alpha(T-x_2)} - 1}{x_1 + \beta}\right], \tag{219}$$

with

$$\frac{\partial \sigma}{\partial x_1} = \frac{\beta - 2\beta x_1 - \beta^2 - x_1^2 - \beta e^{-\alpha(T-x_2)}}{(x_1+\beta)^2} \tag{220}$$

$$\frac{\partial \sigma}{\partial x_2} = -\frac{\alpha x_1 e^{-\alpha(T-x_2)}}{x_1 + \beta}, \tag{221}$$

and

$$\dot{\sigma} = \frac{\partial \sigma}{\partial \mathbf{x}} \dot{\mathbf{x}}$$

$$= \left[\frac{\beta - 2\beta x_1 - \beta^2 - x_1^2 - \beta e^{-\alpha(T-x_2)}}{(x_1+\beta)^2}\right] [x_1 (1 - x_1) - u x_1] \tag{222}$$
$$- \left[\frac{\alpha x_1 e^{-\alpha(T-x_2)}}{x_1 + \beta}\right].$$

Singular control is specified by requiring that $\sigma = \dot{\sigma} \equiv 0$ for a nonzero time interval. Setting (219) to zero yields the singular manifold S

$$S = \left\{(x_1, x_2) \ : 1 + \frac{e^{-\alpha(T-x_2)} - 1}{x_1 + \beta} = 0\right\}. \tag{223}$$

Setting (222) equal to zero yields the control u that will maintain a trajectory on $\mathcal{S}$

$$u_s = 1 - x_1 + \frac{\alpha\left(\beta + x_1\right) e^{-\alpha(T-x_2)}}{\beta - 2\beta x_1 - \beta^2 - x_1^2 - \beta e^{-\alpha(T-x_2)}}. \tag{224}$$

The reasons for choosing $W\left(\mathbf{x}\right)$ as in (214) are as follows. The parameters α and β provide the analyst control over the qualitative shape of the singular manifold. The parameter α controls the time at which S intersects the $x_1 = 0$ axis. The parameter β dictates the long-term population value the singular manifold approaches. We have from (223)

$$x_1 = 1 - e^{-\alpha(T-x_2)} - \beta \tag{225}$$

which implies that

$$\lim_{(T-x_2)\to\infty} (x_1) = 1 - \beta. \tag{226}$$

Equations (208) and (209) are satisfied by (219) and (222) respectively.

With $W\left(\mathbf{x}\right)$ specified we may state the control law by minimizing (218). Forming the Lagrangian function and finding its gradient with respect to u we have

$$L = \dot{W}_0 - \gamma_1 h_1 - \gamma_2 h_2 \tag{227}$$

$$\frac{\partial L}{\partial u} = \sigma - \gamma_1 + \gamma_2. \tag{228}$$

If $\sigma < 0$, $\partial L/\partial u = 0$ requires $u = u_{\max}$. If $\sigma > 0$, $\partial L/\partial u = 0$ requires $u = u_{\min}$, therefore

$$u = \begin{cases} u_{\max} & \text{if} \quad \sigma < 0 \\ u_s & \text{if} \quad \sigma = 0 \text{ and } u_{\min} \leq u_{\mathcal{S}} \leq u_{\max} \\ u_{\min} & \text{if} \quad u_{\min} \text{ if } \sigma > 0. \end{cases} \tag{229}$$

Figure 5 displays the state space trajectories for the LOSC optimal trajectories generated by (229) with $u_{\max} = 1$. For the general case, singular control may not be part of the solution, even if it is allowed by Pontryagin's Minimum Principle. Figure 6 illustrates this fact; the control bounds have been changed to $0 = u_{\min} \leq u \leq u_{\max} = 0.15$. All trajectories in Fig 6 were generated with $u = u_{\max} = 0.15$. The parameter values $\alpha = 1.75$ and $\beta = 0.53$ for Figs. 5 and 6 were determined by minimizing (202) over a typical trajectory, specifically the trajectory $x_1(0) = 1$ and $x_2(0) = T - 10$. These sub-optimal results mimic the actual optimal control results [1, pp. 404-409] to a high degree but without having to solve two-point boundary-value problems or having to integrate the adjoint equations.

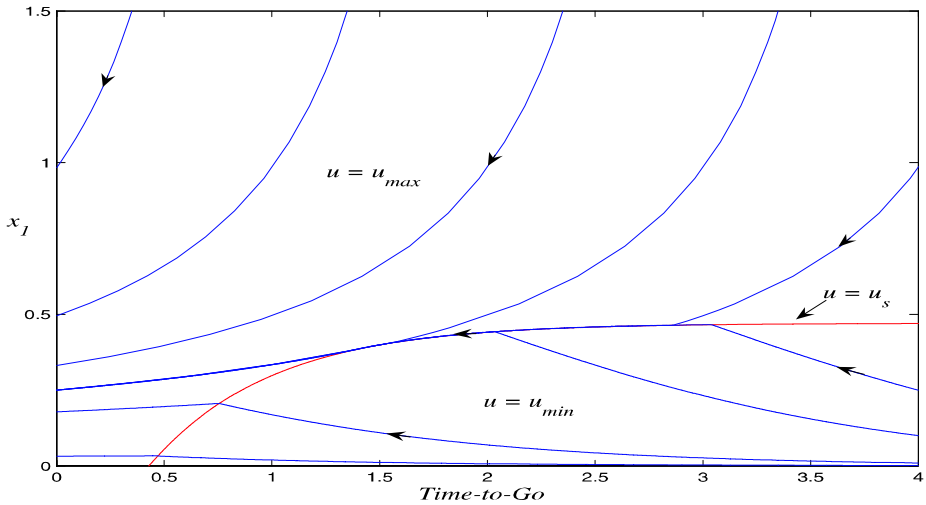

Figure 5: LOSC Optimal Trajectories for Example 4, $\alpha = 1.75$, $\beta = 0.53$.

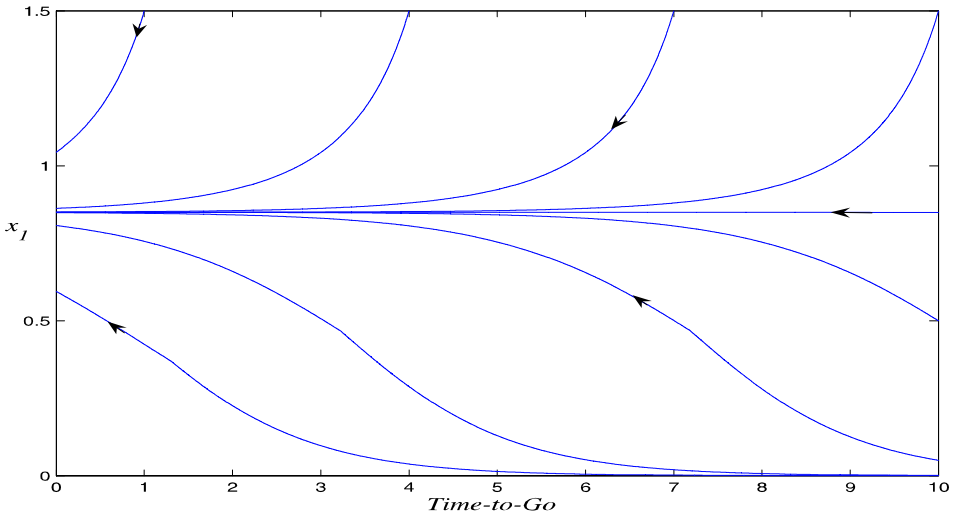

Figure 6: LOSC Optimal Trajectories for Example 4, $\alpha = 1.75$, $\beta = 0.53$, $u_{\max} = 0.15$.

CHAPTER IV

TRAJECTORY FOLLOWING RESEARCH

In this section, the LOSC method is combined with trajectory-following optimization. Of particular interest is the presence of disparate time scales; an augmented system of differential equations may exist on two time scales due to large system gains, or due to a perturbation parameter on a state equation. Therefore, we briefly survey existing singular perturbation methodologies before presenting our research.

4.1 State of the Art in Singular Perturbation Methods

A great deal of research has been devoted to the analysis of time scales present in systems of differential equations. A major reason for this activity is due to the many theoretical and numerical issues that arise due to these time scales. Identification then separation of slow and fast modes are nontrivial; these tasks have been the subject of many publications. In [27] a three-dimensional aircraft point-mass approximation is considered and a new fast variable is found. In [28] the computational singular perturbation method is discussed. This numerical method was originally developed to study complex chemical reactions; it provides information regarding system behavior and time scale analysis during the course of the solution. The asymptotic accuracy of this method in a chemical kinetic setting is studied in [29].

Once the primarily slow and fast modes are identified, complications may arise as the analyst attempts to design control laws that capture slow and fast system phenomena. In [30], a feedback control law is designed for three-dimensional minimum-time interception

by explicitly treating slow and fast variables. In [31, p. 531] and [32] development of H^∞ optimal controls for singularly perturbed systems are considered. It is noted that specification of such a control differs greatly from the singularly perturbed regulator problem. Near-optimum regulators for singularly perturbed systems are developed in [2]. In

4.2 Research

Feedback solutions of linear and nonlinear optimal control problems are of great utility; widely applicable throughout the sciences and engineering. However, the process by which the analyst may obtain such solutions is nontrivial. Modern optimal control theory provides necessary conditions for the determination of such strategies and in certain cases a means to specify these strategies. Unfortunately, analytical solutions may not exist and numerical solution methods can be difficult to implement in an efficient, practical manner. We address the design and implementation of robust, sub-optimal control strategies that provide an attractive alternative when optimal solutions cannot be found at a reasonable cost.

First, differential-equation-based sub-optimal control strategies are derived that are applicable to linear and nonlinear problems. This derivation will rely heavily upon trajectory-following optimization (TF) and Lyapunov optimizing control (LOC) techniques. Theoretical concerns associated with the use of this methodology will be addressed during the design process. The design will explicitly consider the issue of multiple time scales and stiff systems of differential equations along with relevant convergence and singularity issues. What results is a family of sub-optimal differential equation based control strategies which are practical and easy to implement in real time.

Secondly, the advantages of these strategies are demonstrated through a numerical study. Example problems will illustrate the ease of implementation and robustness of the strategies when faced with time scales, switching surfaces, and other difficulties. These characteristics

allow the control strategy to be developed on-line; the control and state differential equations will form an augmented set of state equations. This allows the control strategy to be integrated along with the state, producing a control that adapts in real time to the state and does not require any user input or calculation during the process. Use of the TF method makes the solution of (possibly) nonlinear optimization problems at each point along the state trajectory unnecessary. Such trajectory-following strategies are efficient, if we can reduce or eliminate numerical stiffness.

4.2.1 Linear Systems – Minimum-Time Optimal Control

Consider the minimum-time optimal control problem of Section 3.1, with a bounded scalar control u. A new algorithm is developed by combining the LOSC control method with trajectory-following optimization. Several key issues are of particular concern throughout the derivation of a differential equation update $\dot{u}$. Such an update must be able to satisfy (91); two classes of algorithms are developed to accomplish this. The first, derived from the optimal control necessary conditions, may be considered a variable structure trajectory-following control. The differential equation for $\dot{u}$ is discontinuous across a switching surface S with saturation at the upper and lower bounds of u. The second class of algorithms that we develop yield an update $\dot{u}$ that saturates at the upper and lower bounds u, but is continuous across the switching surface. This class is especially appealing; the control contains similarities to traditional PID control. Implementation of a control u via a differential equation for $\dot{u}$ eliminates numerical chatter; however, finite time interval switching control [1, p. 294] may be observed. Strategies are developed that address this issue. We wish to specify $\dot{u}$ such that the resulting augmented set of (state plus control) differential equations are not stiff. This task is not trivial; high gains on $\dot{u}$ may be introduced to enforce an operating condition but the penalty for this is a stiff set of differential equations. Slow and fast modes

of the augmented set of differential equations for state space systems that exist on a single time scale and for state space systems that are singularly perturbed will be investigated. Derivation of appropriate trajectory-following implementations of the LOSC algorithm follows from the requirements that $u = u_{\max}$ or $u = u_{\min}$ off S and that $\sigma = \dot{\sigma} = \ddot{\sigma} = 0$ on S. Practical considerations dictate how much we deviate from satisfaction of the conditions; such considerations will be noted as we proceed.

4.2.1.1 Updates via Necessary Conditions

Consider update strategies derived directly from the optimal control necessary conditions which produced (91) for the unperturbed state space-system. Recall from (101) that

$$\begin{aligned} \dot{\sigma}(\mathbf{x}, u) &= \mathbf{b}^{\intercal} \frac{\partial^2 \Psi}{\partial \mathbf{x}^2} [\mathbf{A}\mathbf{x} + \mathbf{b}u] \\ &= \frac{\partial \sigma}{\partial \mathbf{x}} [\mathbf{A}\mathbf{x} + \mathbf{b}u] \end{aligned} \tag{230}$$

with time derivative

$$\begin{aligned} \ddot{\sigma}(\mathbf{x}, u) &= \frac{d\dot{\sigma}}{dt} \\ &= \frac{\partial \dot{\sigma}}{\partial \mathbf{x}} \dot{\mathbf{x}} + \frac{\partial \dot{\sigma}}{\partial u} \dot{u} \\ &= \frac{\partial \sigma}{\partial \mathbf{x}} \mathbf{A} (\mathbf{A}\mathbf{x} + \mathbf{b}u) + \frac{\partial \sigma}{\partial \mathbf{x}} \mathbf{b}\dot{u}. \end{aligned} \tag{231}$$

For intermediate control $\sigma = \dot{\sigma} = \ddot{\sigma} = 0$; this suggests, from (231), that

$$\dot{u}_s = -\frac{(\partial\sigma/\partial\mathbf{x})\,\mathbf{A}\,(\mathbf{A}\mathbf{x} + \mathbf{b}u)}{(\partial\sigma/\partial\mathbf{x})\,\mathbf{b}}. \tag{232}$$

In addition to satisfying necessary conditions on S, the control must converge to upper and lower bounds as appropriate. To this end, consider the following variable structure trajectory-following control where again ϵ is a small, positive, constant

$$\dot{u} = \begin{cases} -\dfrac{1}{\epsilon}\,(u - u_{\max}) & \text{if} \quad \sigma\,(\mathbf{x}) < 0 \\ \dot{u}_s & \text{if} \quad \sigma\,(\mathbf{x}) = 0 \\ -\dfrac{1}{\epsilon}\,(u - u_{\min}) & \text{if} \quad \sigma\,(\mathbf{x}) > 0 \end{cases} \tag{233}$$

Note that $\dot{u}$ may switch discontinuously but u will be continuous under the control law (233). Now, consider the application of (233) to Example 1 but to better illustrate finite time interval switching control we have chosen $\sigma\,(\mathbf{x}) = x_1 + 5x_2$. For clarity, consider one typical trajectory. Let $x_1\,(0) = 0$ and $x_2\,(0) = 0.25$; since $\sigma > 0$ for these initial conditions, let $u\,(0) = -1$. Integration of the system state and control differential equations produces Fig. 7. In a highly expanded view near the origin, Fig. 8 illustrates the presence of finite time interval switching control, which corresponds to the numerical integration step size. A fourth-order Runge-Kutta integration routine was used, with fixed step size $\Delta t = 0.0002$.

Specification of $\dot{u}$ by setting $\ddot{\sigma} = 0$ does have particular drawbacks. In the following section, a new control strategy for the minimum-time problem of Section 3.1 is developed. Several factors encourage the development of this control law. Consider the control law (233) derived from the optimal control necessary conditions. In a trajectory-following setting, such a law may not be practical. The minimum or maximum control may not be obtained

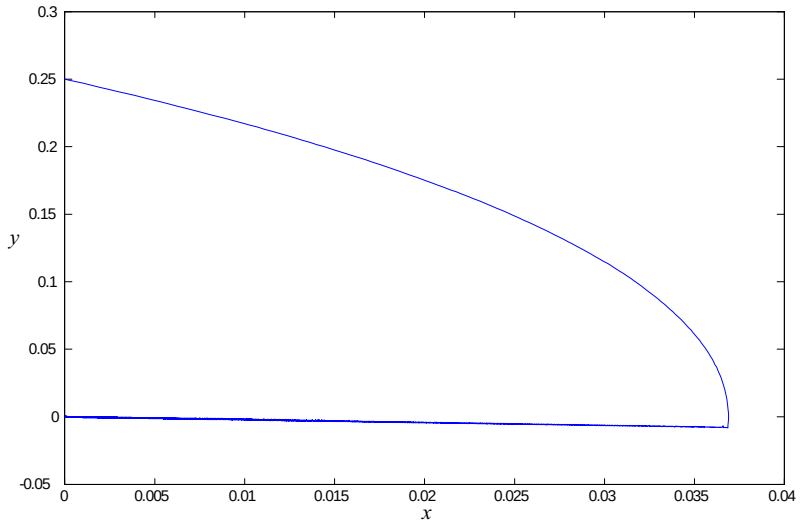

Figure 7: Typical trajectory for Example 1 under control law (233).

exactly. Furthermore, unless the numerical integration finds S exactly, intermediate control $\dot{u}_s$ will never be realized. Suppose we implement $\dot{u}_s$ in some neighborhood of S with $\sigma \neq 0$. The update will attempt to keep $\dot{\sigma}$ and $\ddot{\sigma}$ zero; therefore trajectories may asymptotically approach a point that is not the origin. This is especially important when trajectory-following optimization techniques are employed. When some trajectory, under control law (233) reaches S the "initial condition" for $\dot{u}_s$ will either be $u_s(0) = 1$ or $u_s(0) = -1$; this initial condition is not likely to be equal to the value of u found by setting $\dot{\sigma} = 0$. Therefore, the trajectory will not stay exactly on S; $\dot{u}_s$ will again force asymptotic convergence to a point other than the origin. We desire a strategy that addresses this issue; additionally, explicit consideration is given to time scales and finite-time-interval switching control. Several characteristics of the resulting strategy are similar to those of traditional PID control. The result is a control strategy $\dot{u}$ that can produce the control law (91).

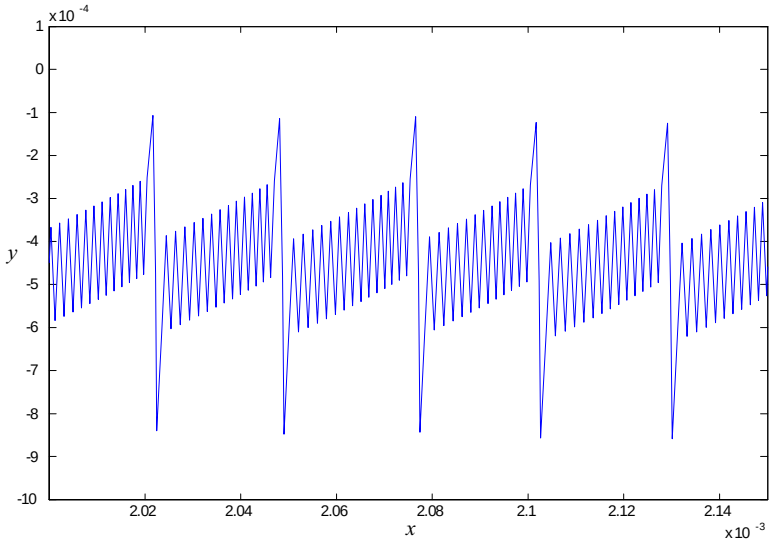

Figure 8: Finite time period switching control for Example 1 under control law (233).

4.2.1.2 PID Control

Toward satisfaction of (91) let

$$\epsilon \dot{u}_I = -\sigma(\mathbf{x}) \tag{234}$$

as in [22]. With $\epsilon > 0$ arbitrarily small, (234) will force the control to saturate at the appropriate upper or lower bounds on u. With

$$e = \sigma|_S - \sigma(\mathbf{x}) = -\sigma(\mathbf{x}) \tag{235}$$

as an error measure, we may think of (234) as implementing integral control. Consider the strategy (234), applied to Example 1. With $\sigma = x_1 + x_2 > 0$, $x_1(0) = 0.25$, and $x_2(0) = 0.25$ we let $u(0) = -1$. The singular perturbation parameter is taken to be $\epsilon = 0.001$

This control cannot stand alone; in Fig. 9 we see that the trajectory, influenced by the singular perturbation ϵ (or gain $1/\epsilon$), oscillates about the target. The presence of finite-time-interval switching control is evident; we need additional control action that damps

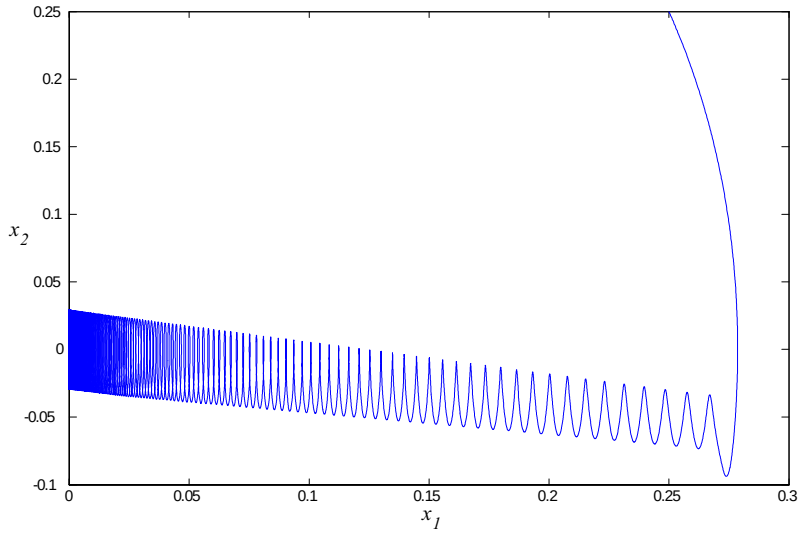

Figure 9: Integral trajectory following control applied to Example 1.

oscillation and promotes convergence to the target. To introduce damping into the system consider derivative control update of the form

$$\epsilon \dot{u}_D = \ddot{e} = -\ddot{\sigma}. \tag{236}$$

From (231) we have

$$\epsilon \dot{u}_D = -\frac{\partial \sigma}{\partial \mathbf{x}} \mathbf{A} \left(\mathbf{A}\mathbf{x} + \mathbf{b}u \right) - \frac{\partial \sigma}{\partial \mathbf{x}} \mathbf{b} \dot{u}_D \tag{237}$$

which results in

$$\left(\epsilon + \frac{\partial \sigma}{\partial \mathbf{x}} \right) \dot{u}_D = -\frac{\partial \sigma}{\partial \mathbf{x}} \mathbf{A} \left(\mathbf{A}\mathbf{x} + \mathbf{b}u \right) \tag{238}$$

or

$$\dot{u}_D = -\frac{\left(\partial \sigma / \partial \mathbf{x} \right) \mathbf{A} \left(\mathbf{A}\mathbf{x} + \mathbf{b}u \right)}{\epsilon + \partial \sigma / \partial \mathbf{x}}. \tag{239}$$

This update strategy is appealing. Comparison of the limit

$$\lim_{\epsilon \to 0} \frac{(\partial \sigma / \partial \mathbf{x})\, \mathbf{A}\, (\mathbf{A}\mathbf{x} + \mathbf{b}u)}{\epsilon + \partial \sigma / \partial \mathbf{x}} = \frac{(\partial \sigma / \partial \mathbf{x})\, \mathbf{A}\, (\mathbf{A}\mathbf{x} + \mathbf{b}u)}{\partial \sigma / \partial \mathbf{x}} \tag{240}$$

with (232) shows that (239) converges to the control dictated by the interior control necessary conditions, as the gain $1/\epsilon$ is increased. Again, note that placement of $\partial \sigma / \partial \mathbf{x}$ has a much greater effect on system time scales than does a gain corresponding to a singular perturbation ϵ.

Each strategy (234) and (239) has distinct advantages and disadvantages. Taken together, they produce an excellent combined integral and derivative strategy

$$\begin{aligned} \dot{u} &= \dot{u}_I + \dot{u}_D \\ \\ \dot{u} &= -\frac{1}{\epsilon}\sigma - \frac{(\partial \sigma / \partial \mathbf{x})\, \mathbf{A}\, (\mathbf{A}\mathbf{x} + \mathbf{b}u)}{\epsilon + \partial \sigma / \partial \mathbf{x}}. \end{aligned} \tag{241}$$

As $\epsilon \to 0$ the $\dot{u}_I$ term in (241) is sufficiently large so that the control is forced to saturate at its maximum or minimum value when the trajectory is not on S. When the trajectory is on the switching surface S, the $\dot{u}_D$ term introduces damping while providing the control needed to satisfy the necessary conditions for singular control. Consider the strategy (241), applied to Example 1 with $\sigma = x_1 + x_2$. Several typical trajectories are shown in Fig. 10; the initial condition on the control was $u = u^* = -\operatorname{sgn}(\sigma)$. Due to the nonstiff nature of the LOSC algorithm, all trajectories in Fig. 10 were generated using a fixed-step-size fourth-order Runge-Kutta integration scheme with $\Delta t = 0.0002$.

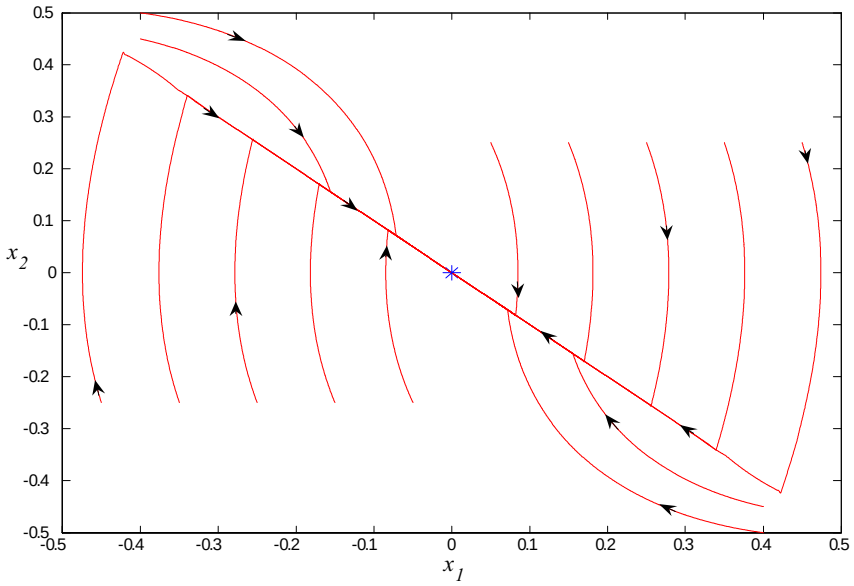

Figure 10: Typical LOSC trajectories for Example 1 using trajectory following PI control.

4.2.2 Nonlinear Systems

4.2.2.1 State-Augmented Control Descent Strategy Development

Solution of the minimization problem (47)–(51) may not yield analytical results; note that in this section, we allow (47)–(51) to be a general, possibly nonlinear, function of the state and control variables. Numerical optimization techniques must then be used; this may be difficult to do in an on-line manner. We will derive a family of player strategy updates that approximately minimize (47) and do not require the solution of the minimization problem, *even at the initial point of the trajectory.* This analysis will yield what we term the State-Augmented Control Descent algorithm (SACD). As in the LOSC method we will specify sub-optimal control updates by choosing a descent function $W(\mathbf{x})$, corresponding to an approximate optimal return function $W_0 = x_0 + W(\mathbf{x})$, and then minimizing the function $\dot{W}_0$ with respect to $\mathbf{u}$. Once again, the descent function for the general optimal control

problem is denoted by $W(\mathbf{x})$. Consider $\min_{\mathbf{u}} \dot{W}_0$ for which a necessary condition is

$$\left[\frac{\partial \dot{W}_0}{\partial \mathbf{u}}\right]^{\mathsf{T}} = \mathbf{0} \tag{242}$$

at each point along the state trajectory, if $\mathbf{u}$ is interior to $\mathcal{U}$. Any $\mathbf{u}$-equilibrium resulting from trajectory-following control updates should satisfy (242). The control strategy, and therefore $\dot{W}_0$, must contain a term such that the state is driven to the target set; this requires that we drive some measure of the distance to the target to zero, i.e.

$$W(\mathbf{x}) \to 0 \text{ as } t \to \infty. \tag{243}$$

In addition $\dot{W}_0$ now will contain a possibly nonlinear cost term f_0.

Implementation of Newton's Method In view of (242) and (243), we wish to drive the function

$$\boldsymbol{\sigma} = \left[\frac{\partial \dot{W}_0}{\partial \mathbf{u}}\right]^{\mathsf{T}} \tag{244}$$

to zero as $t \to \infty$. We will derive a player strategy update $\dot{\mathbf{u}}$ by applying Newton's method to (244) and by modifying certain matrices to ensure nonsingularity, yielding the SACD algorithm.

Newton's method requires that we set

$$\dot{\boldsymbol{\sigma}} = -\boldsymbol{\sigma} \tag{245}$$

yielding

$$\boldsymbol{\sigma}(t) = \boldsymbol{\sigma}(0)\, e^{-t}. \tag{246}$$

We have

$$\dot{\boldsymbol{\sigma}} = \frac{\partial \boldsymbol{\sigma}}{\partial \mathbf{x}} \dot{\mathbf{x}} + \frac{\partial \boldsymbol{\sigma}}{\partial \mathbf{u}} \dot{\mathbf{u}} \tag{247}$$

where we let

$$\frac{\partial \boldsymbol{\sigma}}{\partial \mathbf{x}} = \frac{\partial^2 \dot{W}_0}{\partial \mathbf{x} \partial \mathbf{u}} \tag{248}$$

$$\mathbf{G}_{\mathbf{u}} = \frac{\partial \boldsymbol{\sigma}}{\partial \mathbf{u}} = \frac{\partial^2 \dot{W}_0}{\partial \mathbf{u}^2}. \tag{249}$$

Setting $\dot{\boldsymbol{\sigma}} = -\boldsymbol{\sigma}$ and isolating $\dot{\mathbf{u}}$ yields

$$\dot{\mathbf{u}} = -\mathbf{G}_{\mathbf{u}}^{-1} \left[\boldsymbol{\sigma} + \dot{\boldsymbol{\sigma}} \right]. \tag{250}$$

If $\mathbf{G}_{\mathbf{u}}(\mathbf{x},\mathbf{u})$ is nonsingular along the state trajectory the only equilibrium will occur when our necessary condition (244) is satisfied, i.e. when $\boldsymbol{\sigma} \equiv \mathbf{0}$.

Nonsingularity of System Matrices We employ an adaptation of the Gradient Enhanced Newton (GEN) optimization method of [7]. The GEN method provides global asymptotic stability to the minimum point for nonlinear functions that have a single proper minimum and satisfy a Lyapunov growth condition. With

$$\bar{\mathbf{F}}(\mathbf{x}) = \left[\gamma \left\| \bar{\mathbf{g}} \right\| \mathbf{I} + \bar{\mathbf{G}} \right]^{-1}$$

the form of the GEN method is

$$\dot{\mathbf{x}} = -\bar{\mathbf{F}}(\mathbf{x}) \, \bar{\mathbf{g}} = - \left[\gamma \left\| \bar{\mathbf{g}} \right\| \mathbf{I} + \bar{\mathbf{G}} \right]^{-1} \bar{\mathbf{g}}, \tag{251}$$

where $\bar{\mathbf{g}}$ is the gradient of the cost function, $\bar{\mathbf{G}}$ is the Hessian of the cost function, and γ is a positive constant. It is shown in [7] that for sufficiently large γ the matrix $\bar{\mathbf{F}}$ remains positive definite for all $\mathbf{x}$; this ensures that the only equilibrium of (251) occurs when $\bar{\mathbf{g}} = \mathbf{0}$. We will adapt this algorithm for use in (250), ensuring that the matrix $\mathbf{G}_{\mathbf{u}}^{-1}$ remains positive definite for all $\mathbf{x}$ and $\mathbf{u}$. As shown in [7] the GEN optimization method is generally nonstiff; we will exploit this quality to produce a control differential equation that exists primarily on the same time scale as the state.

SACD Specification The State-Augmented Control Descent algorithm takes the form

$$\dot{\mathbf{u}} = -\left[\gamma\left(\|\boldsymbol{\sigma}\| + \|\dot{\boldsymbol{\sigma}}\|\right)\mathbf{I} + \mathbf{G}_{\mathbf{u}}\right]^{-1}\left[\boldsymbol{\sigma} + \dot{\boldsymbol{\sigma}}\right], \tag{252}$$

with γ a positive constant. Let

$$\hat{\mathbf{F}} = \gamma\left(\|\boldsymbol{\sigma}\| + \|\dot{\boldsymbol{\sigma}}\|\right)\mathbf{I} + \mathbf{G}_{\mathbf{u}}, \tag{253}$$

with μ_i, $i = 1, \ldots, m$, the eigenvalues of $\mathbf{G}_{\mathbf{u}}$. The eigenvalues of $\hat{\mathbf{F}}$ are then $\hat{\mu}_i = \mu_i + \gamma\left(\|\boldsymbol{\sigma}\| + \|\dot{\boldsymbol{\sigma}}\|\right)$, $i = 1, \ldots, m$. For some $\mathbf{x} = \tilde{\mathbf{x}}$, a sufficient condition for asymptotic stability of the point $\mathbf{u}^* \in R^m$ with $\boldsymbol{\sigma} = 0$ is that the matrix $\hat{\mathbf{F}}\left(\tilde{\mathbf{x}},\mathbf{u}\right)$ be positive definite for all $\mathbf{u}$.

Theorem 17 *If the minimization problem* $\min_{\mathbf{u}} \dot{W}_0$ *is solved at any point of the state trajectory, yielding* $\mathbf{u}\left(\bar{t}\right) = \mathbf{u}^*\left(\bar{t}\right) \in int[\mathcal{U}]$*, then the subsequent state trajectory generated by the SACD algorithm is equivalent to that found by carrying out the minimization at each point along the state trajectory for* $t > \bar{t}$*.*

Proof. Beginning at some point $\mathbf{x}^*\left(\bar{t}\right), \mathbf{u}^*\left(\bar{t}\right)$, where $\mathbf{u}$ has been found through the exact LOSC minimization $\min_{\mathbf{u}} \dot{W}_0$ we need to show that the SACD control differential equation

reduces to the LOSC-optimal differential equation, for the particular choice of $W(\mathbf{x})$, found by the minimization *(??)*. For a LOSC-optimal trajectory, with $\mathbf{u} \in \text{int}[\mathcal{U}]$ we have

$$\left[\frac{\partial \dot{W}_0}{\partial \mathbf{u}}\right]^{\intercal} = \mathbf{0} \; \forall \; t > \bar{t}. \tag{254}$$

This requires that

$$\frac{d}{dt}\left[\frac{\partial \dot{W}_0}{\partial \mathbf{u}}\right]^{\intercal} = \frac{\partial}{\partial \mathbf{u}}\left[\frac{\partial \dot{W}_0}{\partial \mathbf{u}}\right]^{\intercal} \dot{\mathbf{u}} + \frac{\partial}{\partial \mathbf{x}}\left[\frac{\partial \dot{W}_0}{\partial \mathbf{u}}\right]^{\intercal} \dot{\mathbf{x}} = \mathbf{0}, \tag{255}$$

which implies that

$$\dot{\mathbf{u}}|_{t \geq \bar{t}} = -\left[\frac{\partial^2 \dot{W}_0}{\partial \mathbf{u}^2}\right]^{-1} \frac{\partial^2 \dot{W}_0}{\partial \mathbf{x} \partial \mathbf{u}} \dot{\mathbf{x}}. \tag{256}$$

Consider the SACD algorithm (252) at $\mathbf{x}^*(\bar{t}), \mathbf{u}^*(\bar{t})$ with

$$\left[\frac{\partial \dot{W}_0(\mathbf{x}^*, \mathbf{u}^*)}{\partial \mathbf{u}}\right]^{\intercal} = \boldsymbol{\sigma} = \mathbf{0}. \tag{257}$$

We now have

$$\dot{\mathbf{u}}|_{t \geq \bar{t}} = -\left[\gamma\left(\|\dot{\boldsymbol{\sigma}}\|\right)\mathbf{I} + \mathbf{G}_{\mathbf{u}}\right]^{-1} \dot{\boldsymbol{\sigma}} \tag{258}$$

and if $\gamma = 0$ the SACD algorithm reduces to

$$\dot{\mathbf{u}}|_{t \geq \bar{t}} = -\mathbf{G}_{\mathbf{u}}^{-1} \dot{\boldsymbol{\sigma}} = -\left(\frac{\partial^2 \dot{W}_0}{\partial \mathbf{u}^2}\right)^{-1} \left(\frac{\partial^2 \dot{W}_0}{\partial \mathbf{x} \partial \mathbf{u}} \dot{\mathbf{x}}\right), \tag{259}$$

which is identical to (255) and completes the proof. ■

Qualitative Behavior of SACD We are concerned with the overall efficiency of any algorithm that is developed. The SACD algorithm (252) was designed with this in mind;

the player strategy differential equation is on the same time scale as the state. Therefore the augmented state has not introduced any additional stiffness to the problem. This augmented state is easy to implement and generates the player strategy on-line.

Special Cases of the SACD Family of Algorithms

1) For a given point $\mathbf{x}$ in state space, it may be possible for the sum $\boldsymbol{\sigma}(\mathbf{x},\mathbf{u}) + \dot{\boldsymbol{\sigma}}(\mathbf{x},\mathbf{u})$ to pass through zero at a point where $\mathbf{G_u}$ is singular in (250). To keep the integration from breaking down numerically, $\hat{\mathbf{F}}$ is specified as in (252), rather than

$$\hat{\mathbf{F}} = \gamma \|\boldsymbol{\sigma} + \dot{\boldsymbol{\sigma}}\| \mathbf{I} + \mathbf{G_u} \text{ or } \hat{\mathbf{F}} = \gamma \|\boldsymbol{\sigma}\| \mathbf{I} + \mathbf{G_u}.$$

2) For a particular choice of $W(\mathbf{x})$, the result of Theorem 17 allows us to follow the LOSC-optimal trajectory if $\mathbf{x}^*$ and $\mathbf{u}^*$ have been found at some time t.

3) For small $\gamma \|\boldsymbol{\sigma} + \dot{\boldsymbol{\sigma}}\|$, the SACD algorithm behaves like Newton's method on (242).

4) For small $\dot{\boldsymbol{\sigma}}$, or where $\mathbf{x}$ is constant, SACD behaves like the Gradient Enhanced Newton method of [7, pp. 143-145].

5) Near $\partial \dot{W}_0 / \partial \mathbf{u} = \mathbf{0}^\intercal$, $\|\dot{\boldsymbol{\sigma}}\|$ dominates, ensuring that effort is focused upon moving the state toward the target set rather than chattering about the switching surface itself.

Numerical Study The effectiveness of the SACD algorithm is demonstrated by considering the following nonlinear examples.

Example 5 *Consider a linearized inverted pendulum* [1, pp. 530-532]*, where the state*

$$\dot{\mathbf{x}} = \mathbf{f}(\mathbf{x}, u) = \mathbf{A}\mathbf{x} + \mathbf{B}u = \begin{bmatrix} 0 & 1 \\ 0 & 0 \end{bmatrix} \begin{bmatrix} x_1 \\ x_2 \end{bmatrix} + \begin{bmatrix} 0 \\ 1 \end{bmatrix} u \tag{260}$$

evolves under the control of an input vector $u \in R^1$*, with* $\mathbf{x} \in R^2$*. The analyst chooses* u *and desires to minimize*

$$J[\mathbf{u}(\cdot)] = \frac{1}{2}\int_0^{t_f} \left(x_1^2 + x_2^2 + u^2\right) dt. \tag{261}$$

The minimum cost descent algorithm is found by first assembling an appropriate descent function. Let the descent function to the target be taken as

$$W(\mathbf{x}) = \frac{1}{2}\mathbf{x}^{\intercal} \begin{bmatrix} 1 & \frac{1}{2} \\ \frac{1}{2} & 1 \end{bmatrix} \mathbf{x} = \frac{1}{2}\left(x_1^2 + x_1 x_2 + x_2^2\right), \tag{262}$$

where we then have

$$\begin{aligned} \dot{W}_0 &= \dot{x}_0 + \frac{\partial W(\mathbf{x})}{\partial \mathbf{x}} \mathbf{f}(\mathbf{x},\mathbf{u}) \\ &= \frac{1}{2}\left(x_1^2 + x_2^2 + u^2\right) + u\left(\frac{1}{2}x_1 + x_2\right) + x_2\left(x_1 + \frac{1}{2}x_2\right). \end{aligned} \tag{263}$$

The state variable x_1 *is the angular displacement of the pendulum from the vertical; the control* u *is the torque. The target is given by equality constraints on the state, which for*

this example are

$$\begin{aligned} x_1 &= 0 \\ x_2 &= 0. \end{aligned} \tag{264}$$

To implement the SACD control strategy calculate

$$\sigma = \left[\frac{\partial \dot{W}_0}{\partial u}\right]^{\intercal} = \frac{1}{2}x_1 + x_2 + u$$

$$\begin{aligned} \dot{\sigma} &= \frac{\partial \boldsymbol{\sigma}}{\partial \mathbf{x}}\dot{\mathbf{x}} + \frac{\partial \sigma}{\partial u}\dot{u} = \begin{bmatrix} \frac{1}{2} & 1 \end{bmatrix} \begin{bmatrix} x_2 \\ u \end{bmatrix} + \dot{u} \\ &= \frac{1}{2}x_2 + u + \dot{u} \end{aligned}$$

and

$$\mathbf{G}_u^{-1} = \left[\frac{\partial \sigma}{\partial u}\right]^{-1} = 1$$

The resulting SACD control strategy, with $\gamma = 0$, is

$$\begin{aligned} \dot{\mathbf{u}} &= -\mathbf{G}_{\mathbf{u}}^{-1}\left[\boldsymbol{\sigma} + \dot{\boldsymbol{\sigma}}\right] \\ &= -\left[\frac{1}{2}x_1 + \frac{3}{2}x_2 + 2u + \dot{u}\right] \end{aligned}$$

which yields

$$\dot{u} = -\left(\frac{1}{4}x_1 + \frac{3}{4}x_2 + u\right). \tag{265}$$

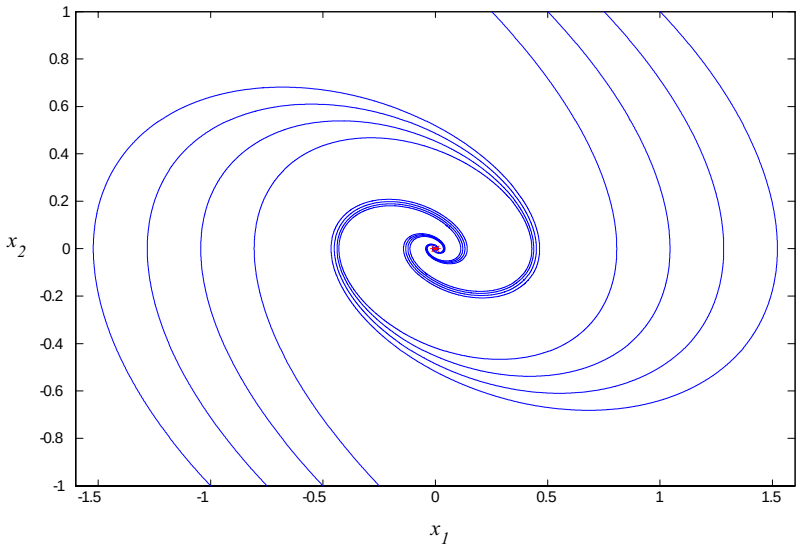

Figure 11: *State Trajectories for Example 5.*

We now have the augmented dynamical system

$$\begin{bmatrix} \dot{x}_1 \\ \dot{x}_2 \\ \dot{u} \end{bmatrix} = \begin{bmatrix} 0 & 1 & 0 \\ 0 & 0 & 1 \\ -\frac{1}{4} & -\frac{3}{4} & -1 \end{bmatrix} \begin{bmatrix} x_1 \\ x_2 \\ u \end{bmatrix} \tag{266}$$

with eigenvalues $\mu_1 = -1/2$, $\mu_2 = -1/4 - i\sqrt{7}/4$, *and* $\mu_3 = -1/4 + i\sqrt{7}/4$. *We note that this is a nonstiff system of differential equations and the origin is globally asymptotically stable. Figure 11 illustrates state trajectories generated by the augmented state* (266). *Note that initial conditions for* u *were picked arbitrarily, that is we did not solve the minimization problem* $\min_{\mathbf{u}} \dot{W}_0$ *at any point of the state trajectory.*

Example 6 *Consider Zermelo's problem* [22] *where a swimmer attempts to reach some point in a river in minimum time. The swimmer navigates the river at a velocity 1, swimming against a current of velocity 2. The swimmer controls their direction, given by the*

angle u. The dynamical system is

$$\begin{aligned} \dot{x}_1 &= \cos u - 2 \\ \dot{x}_2 &= \sin u \end{aligned} \tag{267}$$

and the objective is to reach a circular buoy centered at the origin while minimizing the accumulated time, given by

$$J\left[u\left(\cdot\right)\right] = \int_0^{t_f} dt. \tag{268}$$

We choose a descent function

$$W\left(\mathbf{x}\right) = x_1^2 + x_2^2, \tag{269}$$

which yields an augmented cost-descent function W_0, with rate of change

$$\dot{W}_0\left(\mathbf{x}, u\right) = 1 + 2x_1\left(\cos u - 2\right) + 2x_2\left(\sin u\right). \tag{270}$$

With $\dot{W}_0$ given by (270) *we calculate*

$$\sigma = \frac{\partial \dot{W}_0}{\partial u} = 2x_2 \cos u - 2x_1 \sin u \tag{271}$$

$$G_u = \frac{\partial^2 \dot{W}_0}{\partial u^2} = -2x_1 \cos u - 2x_2 \sin u \tag{272}$$

$$\frac{\partial \sigma}{\partial \mathbf{x}} = \frac{\partial^2 \dot{W}_0}{\partial \mathbf{x} \partial u} = \begin{bmatrix} -2\sin u & 2\cos u \end{bmatrix}$$

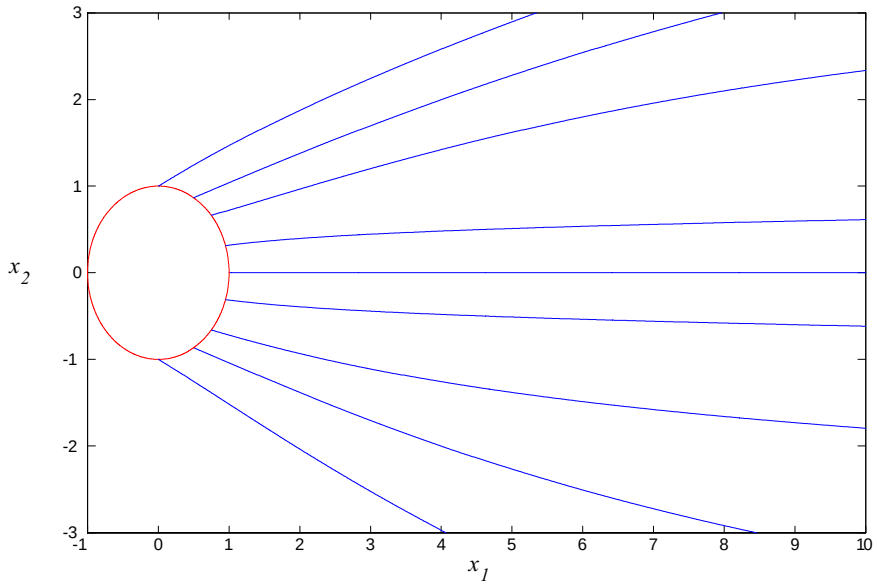

Figure 12: *State Trajectories for Zermelo's problem, Example 6.*

$$\begin{aligned}\dot{\sigma} &= \frac{\partial \sigma}{\partial \mathbf{x}}\dot{\mathbf{x}} + \frac{\partial \sigma}{\partial u}\dot{u} \\ &= -2\sin u\,(\cos u - 2) + 2\cos u \sin u - (2x_2 \sin u + 2x_1 \cos u)\,\dot{u} \qquad (273)\end{aligned}$$

Substitution of the quantities in (270) *into* (252) *yields the SACD control strategy update differential equation* $\dot{u}$*. Figure 12 shows the state trajectories for a variety of initial conditions* $\mathbf{x}(0) = [x_1(0) \quad x_2(0)]^{\mathsf{T}}$*, where we let* $\gamma = 0$*. The minimization problem* $\min_{\mathbf{u}} \dot{W}_0$ *was not solved at any point along the state trajectory. The differential equation for* $\dot{u}$ *is*

$$\dot{\mathbf{u}} = -\mathbf{G}_{\mathbf{u}}^{-1}\left[\boldsymbol{\sigma} + \dot{\boldsymbol{\sigma}}\right] \qquad (274)$$

where (271)–(273) *and* $\gamma = 0$ *complete the specification of* (273)*.*

4.2.2.2 Design Step Summary and Conclusion

Optimal control solutions of a given problem require the analyst to confront a two-point boundary-value problem associated with the adjoint vector along with (possibly) nonlinear optimization problems at each point along the state trajectory. We have used Lyapunov optimizing control techniques to eliminate the two-point boundary-value problem and trajectory-following optimization methods to avoid solving the optimization problem at each point along the state trajectory. This results in sub-optimal controls that are easy to implement in an on-line manner. For linear, minimum-time optimal control problems, we have adapted the LOSC algorithm. For the general optimal control problems, we have used an adaptation of the Gradient Enhanced Newton optimization method to design an algorithm that is generally nonstiff and produces an equilibrium only when an appropriate necessary condition is satisfied.

CHAPTER V

EXTENSION TO DIFFERENTIAL GAMES

A natural extension of this research is to min-max differential games. This section presents some practical results that should be considered by the analyst during implementation of a trajectory-following control algorithm in a min-max differential game setting. We are particularly interested in the stiff systems of differential equations that arise due to algorithmic gains.

Once again, let ϵ denote a small, positive, singular perturbation parameter. It may occur that such a perturbation ϵ, or a gain $1/\epsilon$, creates a more robust strategy update $\dot{\mathbf{u}}$. That is, we have the following augmented system of differential equations

$$\begin{aligned} \dot{\mathbf{x}} &= \mathbf{f}(\mathbf{x},\mathbf{u},\mathbf{v}) \\ \epsilon\dot{\mathbf{u}} &= \hat{\mathbf{f}}(\mathbf{x},\mathbf{u},\mathbf{v}), \end{aligned} \tag{275}$$

where $\mathbf{x} \in R^n, \mathbf{u} \in \mathcal{U} \in R^m, \mathbf{v} \in \mathcal{V} \in R^p$ The system (275) possesses a two-time-scale property with n slow modes and m fast modes [2, p. 531]. Equations (275) represent a stiff system of differential equations, which can make numerical integration difficult. Singular perturbation solution methodology will be used to relieve the numerical stiffness and produce a fast, efficient trajectory-following algorithm. Stiff differential equation solvers can handle (275), but we will address this issue up front and give the analyst low-level control over the process.

Singular perturbation theory provides a means by which the system (275) may be converted into slow and fast subsystems [2, p. 531]. Each subsystem may be examined on a single time scale to determine information about the original system. In this dissertation we will extract such information from the slow and fast subsystems to develop a trajectory-following update $\dot{\mathbf{u}}$ that can be efficiently handled with a nonstiff numerical integrator for differential equations. Prior to the derivation of a generally nonstiff algorithm we consider the following linear-quadratic differential game.

Example 7 *Consider a two-player linear-quadratic differential game where the state, governed by*

$$\dot{\mathbf{x}} = \mathbf{f}(\mathbf{x}, u, v) = \mathbf{A}\mathbf{x} + \mathbf{B}u + \mathbf{E}v$$

$$= \begin{bmatrix} 0 & 1 \\ 0 & 0 \end{bmatrix} \begin{bmatrix} x_1 \\ x_2 \end{bmatrix} + \begin{bmatrix} 0 \\ 1 \end{bmatrix} u + \begin{bmatrix} 0 \\ 1 \end{bmatrix} v, \tag{276}$$

evolves under the control of two inputs $u \in R^1$ and $v \in R^1$, with $\mathbf{x} \in R^2$. The u and v players seek to minimize and maximize, respectively, a quadratic cost functional

$$J[u(\cdot), v(\cdot)] = \frac{1}{2} \int_0^{t_f} \left(\mathbf{x}^\intercal \mathbf{Q} \mathbf{x} + \mathbf{u}^\intercal \mathbf{R} \mathbf{u} - \rho^2 \mathbf{v}^\intercal \mathbf{v} \right) dt$$

$$= \frac{1}{2} \int_0^{t_f} \left(x_1^2 + x_2^2 + u^2 - \rho^2 v^2 \right) dt, \tag{277}$$

subject to $|u| \leq u_{\max} = 2$ and $|v| \leq v_{\max} = 1$. We consider v as a worst-case disturbance input. Let the descent function to the target (the origin; more precisely, a small radius of

the origin) be given by

$$W(\mathbf{x}) = \frac{1}{2}\mathbf{x}^{\mathsf{T}} \begin{bmatrix} 1 & \frac{1}{2} \\ \frac{1}{2} & 1 \end{bmatrix} \mathbf{x} = \frac{1}{2}\left(x_1^2 + x_1 x_2 + x_2^2\right), \tag{278}$$

and we now have

$$\dot{W}_0 = \frac{1}{2}\left(x_1^2 + x_2^2 + u^2 - \rho^2 v^2\right) + \frac{\partial W(\mathbf{x})}{\partial \mathbf{x}} \mathbf{f}(\mathbf{x},u,v). \tag{279}$$

We let the parameter $\rho^2 = 1.1$ *and refer the reader to* [1, pp. 530–531] *for further information. This system corresponds to a linearized inverted pendulum, where a gravitational term has been replaced by the uncertain input* v [36, p. 531]*. The state variable* x_1 *is the angular displacement of the pendulum from the vertical,* x_2 *is the angular velocity, and the control* u *is the applied nongravitational torque. Player* 1*, controlling* u*, desires to minimize* (277) *while driving the system to the target. The target is given by equality constraints on the state, which for this example are*

$$g(\mathbf{x}) = x_1^2 + x_2^2 - r^2 = 0, \tag{280}$$

where r *is a specified small radius from the origin (we take* $r = 10^{-4}$*). Player* 2*, controlling the uncertain input* v*, desires to maximize* (277) *while driving the system away from the target* (280)*.*

5.1 Minimum Cost Descent Algorithm

We define the Minimum Cost Descent (MCD) trajectory-following algorithm by setting the $\dot{\mathbf{u}}$ strategy update for player 1 equal to the negative of the gradient of $\dot{W}_0$ with respect to

u. That is,

$$\dot{\mathbf{u}} = -\left[\frac{\partial \dot{W}_0}{\partial \mathbf{u}}\right]^{\intercal}. \tag{281}$$

For Example 7 this yields

$$\dot{u} = -\frac{\partial \dot{W}_0}{\partial u} = -\left(\frac{1}{2}x_1 + x_2 + u\right), \tag{282}$$

which is desirable since $\dot{u} \to 0$ only as $\partial \dot{W}_0/\partial u \to 0$. We use a "saturation" version of (281); if u is at its upper- or lower-bound and $\dot{u}$ from (281) would cause u to exceed its bounds then instead we set $\dot{u} = 0$.

Assuming that the minimizing strategy variable u has not saturated and ignoring the uncertain input v for the moment, we may examine the eigenvalues of the augmented linear system (276). We have

$$\begin{bmatrix} \dot{x}_1 \\ \dot{x}_2 \\ \dot{u} \end{bmatrix} = \begin{bmatrix} 0 & 1 & 0 \\ 0 & 0 & 1 \\ -\frac{1}{2} & -1 & -1 \end{bmatrix} \begin{bmatrix} x_1 \\ x_2 \\ u \end{bmatrix} \tag{283}$$

with eigenvalues $\mu_1 = -0.1761 + i0.8607$, $\mu_2 = -0.1761 - i0.\,8607$, and $\mu_3 = -0.6478$. The MCD algorithm is not stiff.

5.2 Total Descent Algorithm

Consider a trajectory-following update for the minimizing strategy variable by minimizing $\dot{W}_0$ with respect to **u**. From the necessary conditions for an interior minimum we have $\mathbf{0}^{\intercal} = \partial \dot{W}_0/\partial \mathbf{u}$. One technique would be to set the time derivative of this condition to zero.

This suggests that we update $\mathbf{u}$ according to

$$\mathbf{0} = \frac{\partial}{\partial \mathbf{u}} \left[\frac{\partial \dot{W}_0}{\partial \mathbf{u}} \right]^{\mathsf{T}} \dot{\mathbf{u}} + \frac{\partial}{\partial \mathbf{x}} \left[\frac{\partial \dot{W}_0}{\partial \mathbf{u}} \right]^{\mathsf{T}} \dot{\mathbf{x}}. \tag{284}$$

That is, we set

$$\dot{\mathbf{u}} = - \left[\frac{\partial^2 \dot{W}_0}{\partial \mathbf{u}^2} \right]^{-1} \frac{\partial^2 \dot{W}_0}{\partial \mathbf{x} \partial \mathbf{u}} \dot{\mathbf{x}}, \tag{285}$$

resulting in the Total Descent (TD) algorithm. Implementing this strategy for Example 7, with $v \equiv 0$, results in

$$\dot{u} = - \left(\frac{1}{2} x_2 + u \right) \tag{286}$$

and once again, we use a saturation version of (286). Assuming that the minimizing strategy variable u has not saturated and ignoring the uncertain input v, we may examine the eigenvalues of the augmented linear system (276). We have

$$\begin{bmatrix} \dot{x}_1 \\ \dot{x}_2 \\ \dot{u} \end{bmatrix} = \begin{bmatrix} 0 & 1 & 0 \\ 0 & 0 & 1 \\ 0 & -\frac{1}{2} & -1 \end{bmatrix} \begin{bmatrix} x_1 \\ x_2 \\ u \end{bmatrix} \tag{287}$$

with eigenvalues $\mu_1 = -\frac{1}{2} + i\frac{1}{2}$, $\mu_2 = -\frac{1}{2} - i\frac{1}{2}$, and $\mu_3 = 0$. Thus the TD algorithm is not stiff.

Let the initial conditions for Example 7 be given by $x_1(0) = 1$, $x_2(0) = 1$, $u(0) = -1.5$ and for the moment let $v = 0$. Trajectories evolving from these initial conditions for the MCD and TD trajectory-following algorithms are shown in Fig. 13. The terminal costs (277) for the MCD and TD algorithms were 5.37 and 3.31, respectively, and each algorithm drove the state to the target. The TD algorithm has driven the state to the target and done

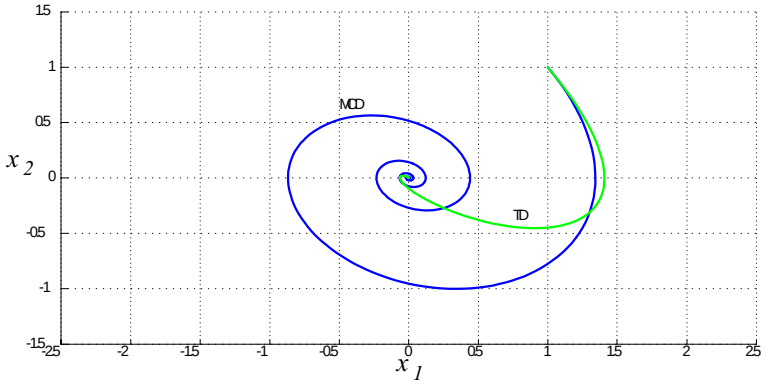

Figure 13: TD and MCD state trajectories for Example 7 $[u(0) = -1.5]$

so at a lower cost than the MCD algorithm.

Now let the initial conditions be given by $x_1(0) = 1$, $x_2(0) = 1$, and $u(0) = -2$ where again we let $v(t) \equiv 0$. Trajectories evolving from these initial conditions for the MCD and TD trajectory-following algorithms are shown in Fig. 14. The MCD algorithm drove the system to the target with a terminal cost of 6.62; the TD algorithm failed to drive the system to the target. We expected this latter result as one eigenvalue of (287) is zero; previous convergence to the target was a product of the choice of initial conditions. Given $x_1(0) = 1$ and $x_2(0) = 1$, $\min\left[\dot{W}_0(1, 1, u)\right] \Rightarrow u^*(0) = -1.5$.

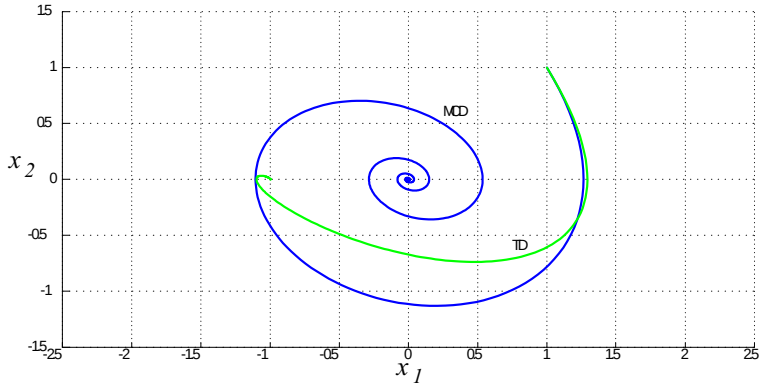

Figure 14: TD and MCD state trajectories for Example 7 $[u(0) = -2]$

The results of Example 7, along with Figs. 13 and 14, illustrate the behavior of the MCD and TD algorithms. In particular we note that the TD algorithm could only drive the system to the target for very specific initial conditions, *even in the absence of the disturbance*!

We now turn to the v-reachable set [1, p. 504] to provide a qualitative means by which we may compare the effectiveness of any player 1 strategy $u(\mathbf{x})$ in the presence of the disturbance v.

Definition 1 *A given point in state space is v-**reachable** from the origin if there exists an admissible control law for $\mathbf{v}$ such that, under a given admissible control law for $\mathbf{u}(\mathbf{x})$, the system can be driven from the origin to the point in finite time.*

Definition 2 *The v-**reachable set** is the set of all v-reachable points under the specified control law $\mathbf{u}(\mathbf{x})$.*

The v-reachable set provides a qualitative measure of the capabilities of the disturbance to drive the system to points other than the origin (target) that is particularly well suited for two-dimensional problems. Under a specified control law $\mathbf{u}(\mathbf{x})$, the v-reachable set is determined by finding the reachable set [1, p. 315] from the origin for the v player. That is, this process reduces to an "abnormal optimal control" problem for the v player. Necessary conditions for trajectories lying in the boundary of the v-reachable set are given as the reachability maximum principle [1, p. 342]. The v-reachable set is found by integrating the system state equations forward in time, starting near the origin, subject to the input v obtained from the reachability maximum principle [1, p. 507]. For Example 7, this input is $v = v_{\max}\,\mathrm{sgn}(x_2)$.

The v-reachable set for the MCD algorithm, which is not shown, is unbounded. The

"unknown" disturbance is able to drive the system from the origin to any point in state space. Modification of (282) is needed to counter the effect of the disturbance, resulting in a bounded v-reachable set. We did not include the TD algorithm in this analysis, since the "state variable" u has a state constraint $|u| \leq 2$. This would make the determination of the boundary of the v-reachable set very difficult [37]. In point of fact, setting $v = v_{\max} \operatorname{sgn}(x_2)$ and integrating (287) forward in time results in a trajectory that approaches infinity as time approaches infinity. So the v-reachable set for the TD algorithm is also unbounded.

5.3 Singular Perturbation Minimum Cost Descent Algorithm

A singular perturbation will be incorporated into the MCD algorithm to counter the effect of the disturbance input. We then have the Singular Perturbation Minimum Cost Descent algorithm (SPMCD)

$$\epsilon \dot{u} = -\frac{\partial \dot{W}_0}{\partial u} = -\left(\frac{1}{2}x_1 + x_2 + u\right), \tag{288}$$

with saturation. Assuming that the minimizing strategy variable has not saturated and ignoring the uncertain input, we may examine the eigenvalues of the augmented linear system,

$$\begin{bmatrix} \dot{x}_1 \\ \dot{x}_2 \\ \epsilon \dot{u} \end{bmatrix} = \begin{bmatrix} 0 & 1 & 0 \\ 0 & 0 & 1 \\ -\frac{1}{2} & -1 & -1 \end{bmatrix} \begin{bmatrix} x_1 \\ x_2 \\ u \end{bmatrix}. \tag{289}$$

The SPMCD algorithm is stiff, with eigenvalues $\mu_1 = -0.5 + i0.5$, $\mu_2 = -0.5 - i0.5$, and $\mu_3 = -9999$ for $\epsilon = 0.0001$.

Let the initial conditions for Example 7 be given by $x_1(0) = 1$, $x_2(0) = 1$, $u(0) = -2.0$, with $v = 0$. Figure 15 displays the state trajectories for all three trajectory-following algorithms we have considered to this point. As before, the MCD algorithm drove the state

to the target while the TD algorithm did not. The SPMCD algorithm drove the state to the target with a terminal cost of 3.311.

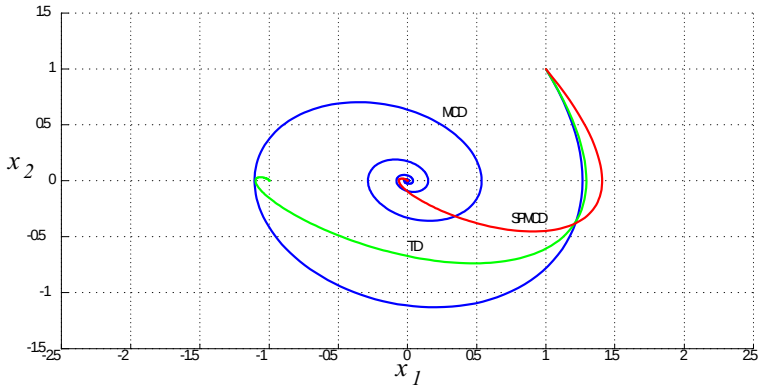

Figure 15: State trajectories for Example 7 $[u(0) = -2]$

We examine the v-reachable set for SPMCD; Fig. 16 displays the resulting limit cycle boundary of the v-reachable set. The SPMCD algorithm yields a bounded v-reachable set; the algorithm is much more robust in regards to the unknown disturbance than the MCD or TD algorithms.

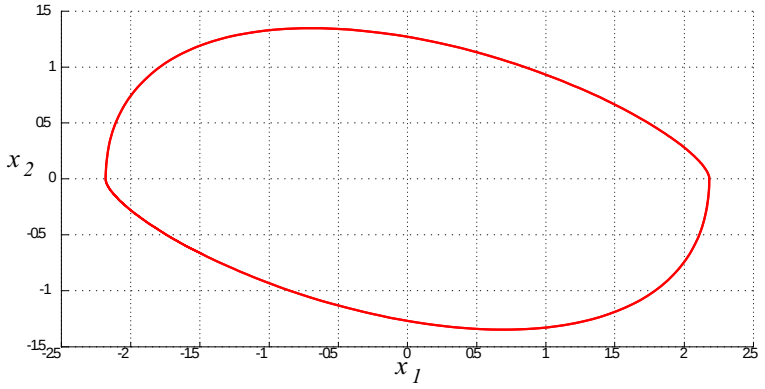

Figure 16: The v-reachable set for the SPMCD algorithm, Example 7

The results of Example 7 illustrate the strengths and weaknesses of each of the three algorithms MCD, TD, and SPMCD. The MCD algorithm drove the system to the target

but only in the absence of the input disturbance. The TD algorithm only drove the system to the target for very specific initial conditions; when it did work its terminal cost was quite low. Both the MCD and TD algorithms operated on a single time scale (nonstiff) as shown by their eigenvalues. In the absence of a disturbance the SPMCD converged to the target and its terminal cost was the smallest. The eigenvalues of (289) clearly show that the SPMCD algorithm yields a stiff system of differential equations.

In the presence of a bounded disturbance v, the v-reachable set for Example 7 is all of R^2 for the MCD algorithm, and is at least unbounded for the TD algorithm, but is a bounded set for the SPMCD algorithm. We now appeal to singular perturbation analysis techniques to derive a trajectory-following algorithm for player 1 of the differential game that drives the system to the target in the absence of the disturbance input. This algorithm should be generally nonstiff and therefore easily implemented numerically. Finally, we desire that the v-reachable set be no larger than that of the SPMCD algorithm.

In Example 7, in the absence of a disturbance v, the SPMCD algorithm drove the system to the target and the terminal cost was lower than that of the MCD and TD algorithms. With a disturbance the v-reachable set was unbounded for the MCD and TD algorithms, but was bounded for the SPMCD algorithm, suggesting that the primary shortcoming of the SPMCD method is stiffness, which makes numerical calculations difficult. The Efficient Cost Descent algorithm that we develop later is derived from the time scale decomposition of the SPMCD algorithm. Singular perturbation theory [2, p. 531] tells us that the fast modes of a given system of differential equations are important only during a short initial period; at the conclusion of this period the slow modes determine the behavior of the system. This suggests that the effect of the perturbation ϵ in (289) need only be felt during a short initial time interval. Limiting the use of the perturbation would immediately relieve the

stiffness of the system of differential equations. Neglecting ϵ completely degrades the overall performance of the algorithm, as seen by comparing the terminal costs and v-reachable sets of MCD and SPMCD in Example 7.

5.3.1 Slow Subsystem

We derive the primarily slow subsystem of (289) by assuming the fast modes are infinitely fast. That is, we let $\epsilon = 0$. We have

$$\begin{bmatrix} \dot{x}_{1\mathrm{s}} \\ \dot{x}_{2\mathrm{s}} \\ 0 \end{bmatrix} = \begin{bmatrix} 0 & 1 & 0 \\ 0 & 0 & 1 \\ -\frac{1}{2} & -1 & -1 \end{bmatrix} \begin{bmatrix} x_{1\mathrm{s}} \\ x_{2\mathrm{s}} \\ u_{\mathrm{s}} \end{bmatrix}, \tag{290}$$

where a subscript "s" represents a slow variable. In (289) we have set $\epsilon\dot{u} = -\partial\dot{W}_0/\partial u$; as a product of that choice we see that the slow system contains the original dynamics and the necessary condition for $\min_u \dot{W}_0$ for this problem. This suggests that the bulk of the information needed to drive this system along the SPMCD trajectory is contained in the slow system, on a single time scale.

5.3.2 Fast Subsystem

During the derivation of the primarily fast subsystem, we assume that the slow variables are constant. In the case of Example 7 we then have $\dot{x}_{1\mathrm{s}} = \dot{x}_{2\mathrm{s}} = \dot{u}_{\mathrm{s}} = 0$. With x_1 and x_2 given as slow variables, the third equation in (289) may be rewritten as $\epsilon\dot{u} = -\frac{1}{2}x_{1\mathrm{s}} - x_{2\mathrm{s}} - u$. We may substitute u_{s} from (289) into (290) and noting that $\dot{u}_{\mathrm{s}} = 0$ we have, $\epsilon\left(\dot{u} - \dot{u}_{\mathrm{s}}\right) = u_{\mathrm{s}} - u$. If we let $u_{\mathrm{f}} = u - u_{\mathrm{s}}$ we have $\epsilon\dot{u}_{\mathrm{f}} = -u_{\mathrm{f}}$, which has a solution $u_{\mathrm{f}} = u_{\mathrm{f}}\left(0\right)e^{-t/\epsilon}$. We observe that in a trajectory-following setting, where we have introduced a singular perturbation on the player strategy, the fast system for Example 7 depends only upon the strategy variable

itself. For this particular type of example, where the strategy differential equation is linear in u, the fast system variable u_{f} is given by a rapidly decaying exponential function. This suggests that the SPMCD algorithm (289) may be modified with an exponential function to reduce the effect of ϵ yet still produce the desired results.

5.4 Efficient Cost Descent Algorithm

The ECD algorithm is based upon singular perturbation techniques applied to the SPMCD algorithm. It consists of three components taken from the full system, the slow subsystem, and the fast subsystem. Taken together, these components create a state trajectory that approximates that of the SPMCD algorithm, but is generally nonstiff and therefore much more efficient.

5.4.1 Slow Subsystem Component

Consider general, possibly nonlinear, algebraic equations found by setting $\epsilon = 0$ in an augmented system of differential equations. Ignoring $\mathbf{v}$ for the moment, the resulting equations are of the form $\hat{\mathbf{g}}(\mathbf{x}, \mathbf{u}) = \mathbf{0}$ [$\hat{g}(\mathbf{x}, u) = \partial \dot{W}_0 / \partial u = -\hat{f}(\mathbf{x}, u)$ for SPMCD in Example 7], which is on the same time scale as the state variables. An update strategy for $\mathbf{u}$ may be found by differentiating the constraint $\hat{\mathbf{g}}(\mathbf{x}, \mathbf{u})$ with respect to time [3, p. 47],

$$\mathbf{0} = \frac{\partial \hat{\mathbf{g}}(\mathbf{x}, \mathbf{u})}{\partial \mathbf{u}} \dot{\mathbf{u}} + \frac{\partial \hat{\mathbf{g}}(\mathbf{x}, \mathbf{u})}{\partial \mathbf{x}} \dot{\mathbf{x}}, \tag{291}$$

yielding

$$\dot{\mathbf{u}} = -\left[\frac{\partial \hat{\mathbf{g}}(\mathbf{x}, \mathbf{u})}{\partial \mathbf{u}} \right]^{-1} \frac{\partial \hat{\mathbf{g}}(\mathbf{x}, \mathbf{u})}{\partial \mathbf{x}} \dot{\mathbf{x}}. \tag{292}$$

This update (292) cannot stand alone; if $\partial\hat{\mathbf{g}}(\mathbf{x},\mathbf{u})/\partial\mathbf{u}$ is singular the $\dot{\mathbf{u}}$ algorithm, from (291), could cause convergence to an equilibrium point that is not contained in the target set, which is undesirable. The SPMCD strategy update algorithm is stiff in Example 7, but it only produces an equilibrium point when $\hat{\mathbf{g}}(\mathbf{x},\mathbf{u}) = \mathbf{0}$.

5.4.2 Fast Subsystem Component

The solution to a possibly nonlinear system of differential equations $\epsilon\dot{\mathbf{u}}_{\mathrm{f}} = -\hat{\mathbf{g}}(\mathbf{u}_{\mathrm{f}})$ will not in general reduce to a simple exponential function. However singular perturbation theory states that the fast subsystem is only important during a short initial period. For this reason we will design the ECD algorithm to contain a term of the form

$$\dot{\mathbf{u}} = -\frac{1}{\epsilon}e^{-\alpha t}\hat{\mathbf{g}}, \tag{293}$$

which is not on the same time scale as the state variables. This second time scale quickly decays with the exponential term.

5.4.3 Full Subsystem Component

If $\partial\hat{\mathbf{g}}(\mathbf{x},\mathbf{u})/\partial\mathbf{u}$ is not singular along a trajectory generated by the augmented state equations, the components (292) and (293) attempt to drive the system to the target with only a very short initial period of stiffness. If $\partial\hat{\mathbf{g}}(\mathbf{x},\mathbf{u})/\partial\mathbf{u}$ is singular along that trajectory we need a third component to our algorithm to ensure that progress toward the target is made. To this end we let the ECD algorithm contain the following term

$$\dot{\mathbf{u}} = -\beta\,\|\hat{\mathbf{g}}\|\,\hat{\mathbf{g}}. \tag{294}$$

The initial form of the ECD algorithm is defined by its three components (292)–(294)

yielding

$$\dot{\mathbf{u}} = -\left[\frac{1}{\epsilon}e^{-\alpha t} + \beta \left\|\hat{\mathbf{g}}\right\|\right]\hat{\mathbf{g}} - \left[\frac{\partial \hat{\mathbf{g}}}{\partial \mathbf{u}}\right]^{-1}\frac{\partial \hat{\mathbf{g}}}{\partial \mathbf{x}}\dot{\mathbf{x}}, \tag{295}$$

with saturation. The ECD algorithm is generally nonstiff and therefore efficient. This behavior is inherited from the slow subsystem decomposition of SPMCD representing the far right term in (295). At locations where $\|\hat{\mathbf{g}}\|$ is small, the algorithm behaves like the TD algorithm. The ECD algorithm does not require the solution of a (possibly) nonlinear optimization problem, even at the initial point of the trajectory. The fast subsystem information contained in the exponential term of (295) drives the state near a point where the necessary conditions $\partial \dot{W}_0/\partial \mathbf{u} = \mathbf{0}^\intercal$ are satisfied despite a poor choice for $\mathbf{u}(0)$. The nonnegative constants α and β may be chosen to further control the speed of the algorithm and to avoid points where $\partial \hat{\mathbf{g}}(\mathbf{x}, \mathbf{u})/\partial \mathbf{u}$ is singular. For Example 7 we note that $\partial \hat{\mathbf{g}}(\mathbf{x}, \mathbf{u})/\partial \mathbf{u} = \partial^2 \dot{W}_0/\partial \mathbf{u}^2 \equiv 1$ is nonsingular.

5.4.4 Performance Comparison – ECD and SPMCD

Figure 17 illustrates the trajectory generated by the ECD algorithm for Example 7; the SPMCD trajectory was not included as it quickly converged to the ECD trajectory. The initial conditions for each strategy, with $\epsilon = 10^{-4}$, were $x_1(0) = 1$, $x_2(0) = 1$, $u(0) = -2.0$, $v = 0$. We have chosen $\alpha = 100$ and $\beta = 0$. The terminal costs for the SPMCD and ECD algorithms were both 3.311. The v-reachable set for the ECD algorithm, found by introducing the uncertain input, is shown in Fig. 18. The ECD algorithm produces a v-reachable set identical to that of the SPMCD algorithm but in a nonstiff (efficient) manner.

The CPU time to carry out the integration was found using Matlab's built in stopwatch timer commands tic, toc for the ECD and SPMCD algorithms. We terminated this integration when the distance to the target (origin) fell below $r = 10^{-4}$. With $\epsilon = 10^{-4}$, initial

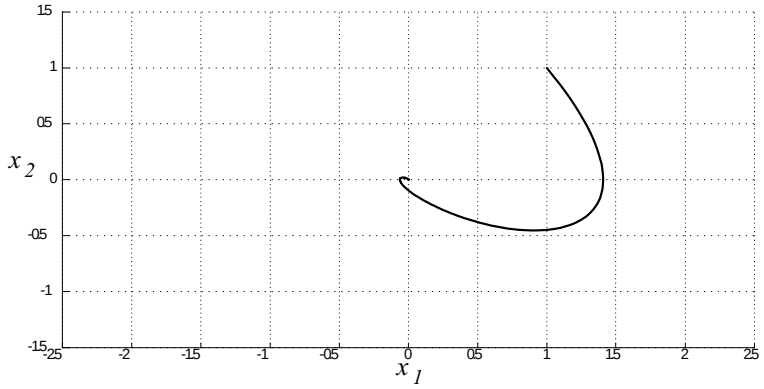

Figure 17: State trajectory for the ECD algorithm, Example 7 [$u(0) = -2$]

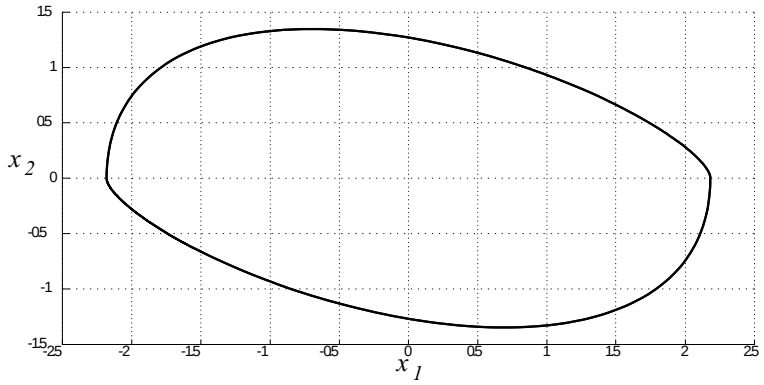

Figure 18: The v-reachable set for the ECD algorithm in Example 7

conditions $x_1(0) = 1$, $x_2(0) = 1$, $u(0) = -2.0$, $v = 0$, and using Matlab's ode45 integrator we found the CPU time for the ECD and SPMCD algorithms to be 0.047 seconds and 209.23 seconds, respectively. The ECD method was approximately 4450 times as fast as SPMCD. The efficiency of the ECD algorithm can be related to its generally nonstiff behavior. We can study the stiffness of the ECD algorithm by examining its Lyapunov exponent time histories [1, pp. 205–207]. In Fig. 19 we see widely separated Lyapunov exponents for a short initial period, followed by closely grouped exponents for the vast majority of the integration. This behavior is in stark contrast to that of the SPMCD algorithm with widely separated eigenvalues.

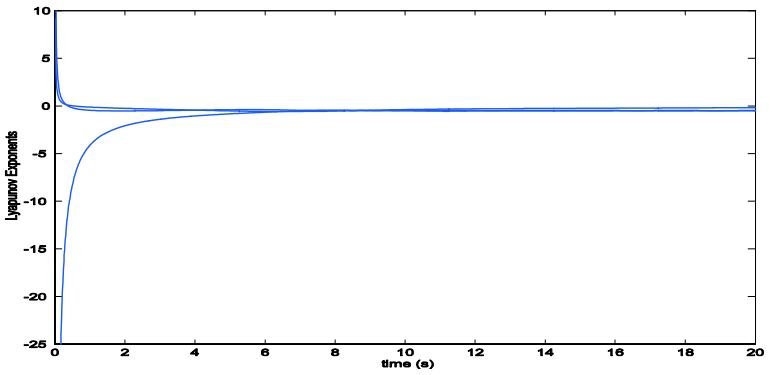

Figure 19: Lyapunov exponents for the ECD algorithm applied to Example 7

5.4.4.1 Performance Comparison – ECD and Min-Max

The ECD algorithm generates on-line, closed-loop, minimizing-player strategies. These strategies are derived from $\dot{W}_0$, a function that exhibits the optimal structure of the Hamilton-Jacobi-Bellman equation [38, p. 222]

$$0 = \min_{u} \left[f_0 \left(\mathbf{x}, \mathbf{u}, \mathbf{v} \right) + \frac{\partial V}{\partial \mathbf{x}} \mathbf{f} \left(\mathbf{x}, \mathbf{u}, \mathbf{v} \right) \right], \tag{296}$$

where $V(\mathbf{x})$ is the so-called value function. If we select $W(\mathbf{x}) = V(\mathbf{x})$, we can recover the optimal solution for the particular problem; this task may be quite difficult as we must solve a partial differential equation to obtain $V(\mathbf{x})$. Instead, we have selected a descent function to the target and made trajectories decrease this function over time. Aside from solving (296), the selection of an appropriate descent function is qualitative in nature; some quantitative guidelines for determining such a function are presented in Chapter III. However, for a given descent function we can show that this method produces results comparable to a game-theoretic controller. We will accomplish this task by modifying the ECD algorithm and comparing the before and after v-reachable sets with those that result from the use of

a min-max control algorithm [1, pp. 530–531].

5.4.5 ECD Modification

Having specified an approximation to the value function, the ECD algorithm was developed by essentially neglecting the disturbance $\mathbf{v}$. We can improve performance by adding a term to the ECD algorithm that counters the effect of that disturbance.

Once $W_0 = x_0 + W(\mathbf{x})$ is specified, we have

$$\dot{W}_0 = f_0(\mathbf{x}, \mathbf{u}, \mathbf{v}) + \frac{\partial W(\mathbf{x})}{\partial \mathbf{x}} \mathbf{f}(\mathbf{x}, \mathbf{u}, \mathbf{v})$$

$$= \tfrac{1}{2}\left(\mathbf{x}^\intercal \mathbf{Q}\mathbf{x} + \mathbf{u}^\intercal \mathbf{R}\mathbf{u} - \rho^2 \mathbf{v}^\intercal \mathbf{v}\right) + \frac{\partial W(\mathbf{x})}{\partial \mathbf{x}} (\mathbf{A}\mathbf{x} + \mathbf{B}u + \mathbf{E}v). \tag{297}$$

Player 1, controlling $\mathbf{u}$, expects Player 2, controlling $\mathbf{v}$, to maximize (297). The necessary conditions for unconstrained maximization of $\dot{W}_0$ with respect to $\mathbf{v} \in R^p$ are given by

$$\frac{\partial \dot{W}_0}{\partial \mathbf{v}} = -\rho^2 \mathbf{v}^\intercal + \frac{\partial W(\mathbf{x})}{\partial \mathbf{x}} \mathbf{E} = \mathbf{0}^\intercal, \tag{298}$$

which yields

$$\mathbf{v} = \frac{1}{\rho^2}\left[\frac{\partial W(\mathbf{x})}{\partial \mathbf{x}} \mathbf{E}\right]^\intercal. \tag{299}$$

Consider the time rate of change of $W(\mathbf{x})$ in Example 7,

$$\dot{W}(\mathbf{x}) = \frac{\partial W(\mathbf{x})}{\partial \mathbf{x}} \dot{\mathbf{x}}$$

$$= x_2\left(x_1 + \tfrac{1}{2}x_2\right) + u\left(x_2 + \tfrac{1}{2}x_1\right) + v\left(x_2 + \tfrac{1}{2}x_1\right). \tag{300}$$

From (299), with $\rho^2 = 1.1$, we have

$$v = \frac{1}{1.1}\left(\tfrac{1}{2}x_1 + x_2\right). \tag{301}$$

Player 1 may counter the increase in $\dot{W}$ caused by the disturbance through the addition of the term

$$u_v = \frac{-1}{1.1}\left(\frac{1}{2}x_1 + x_2\right)$$

or

$$\dot{u}_v = \frac{-1}{1.1}\left(\tfrac{1}{2}\dot{x}_1 + \dot{x}_2\right). \tag{302}$$

The final form of the ECD algorithm is now

$$\dot{\mathbf{u}} = -\left[\frac{1}{\epsilon}e^{-\alpha t} + \beta\left\|\hat{\mathbf{g}}\right\|\right]\hat{\mathbf{g}} - \left[\frac{\partial\hat{\mathbf{g}}}{\partial\mathbf{u}}\right]^{-1}\frac{\partial\hat{\mathbf{g}}}{\partial\mathbf{x}}\dot{\mathbf{x}} + \dot{\mathbf{u}}_v. \tag{303}$$

Figure 20 illustrates the initial "a" and final "b" v-reachable sets for the ECD algorithm, based upon equations (295) and (303) respectively, along with the "c" v-reachable set of the min-max controller of [1, p. 531]. The addition of the term $\dot{\mathbf{u}}_v$ has greatly reduced the size of the v-reachable set for the ECD algorithm. We observe that the final form of the ECD algorithm produces a v-reachable set that is larger than that given by the min-max algorithm; clearly then ECD is not optimal. However, we have specified a closed-loop, on-line controller that does not require us to solve partial differential equations or two-point boundary-value problems.

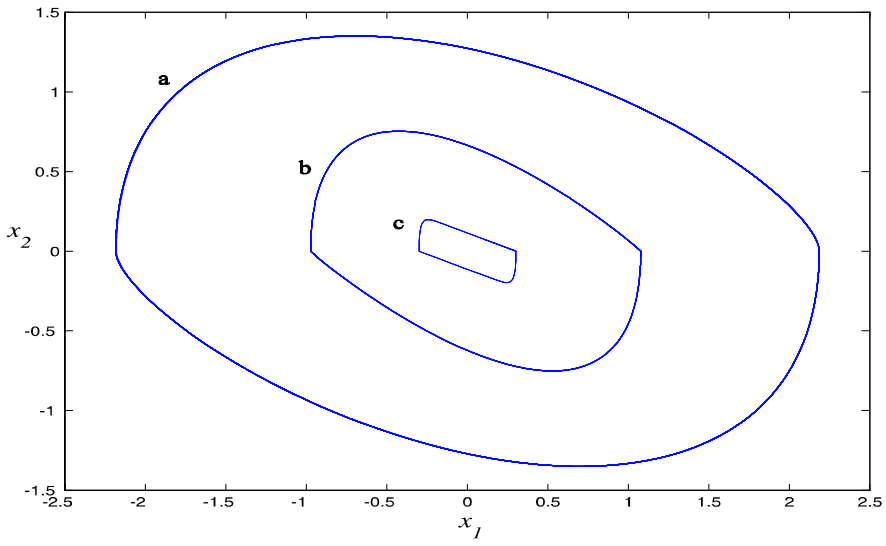

Figure 20: The v-reachable sets for: a) initial ECD, b) final ECD, and c) Min-Max.

5.5 Design Summary and Conclusion

In this chapter we have specified minimizing player strategies for min-max games through trajectory-following methods. These differential equation strategies were derived from a function that represents a trade-off between the current rate of cost accumulation and the penetration rate for the minimizing player's descent function, and eliminates the need to solve min-max problems and two-point boundary-value problems at each state. Minimum Cost Descent (MCD) and Total Descent (TD) trajectory-following algorithms were applied to a linear quadratic differential game. We observed that a more robust strategy with respect to the uncertain, or maximizing player's, input could be obtained by introducing a singular perturbation onto the minimizing player's strategy. This yielded the Singular Perturbation Minimum Cost Descent (SPMCD) algorithm, which we found to be very stiff. Analysis of the SPMCD algorithm using well-known singular perturbation techniques led to the Efficient Cost Descent (ECD) algorithm. ECD was generally nonstiff and provided the same desirable performance characteristics as the SPMCD algorithm. The ECD algorithm

is sub-optimal, but the performance is comparable with game theoretic controllers, even with the unknown disturbance v implementing a game theoretic strategy, as seen in Fig. 20.

CHAPTER VI

CONCLUSIONS

6.1 Lyapunov Optimizing Control

For the minimum-time optimal control problem, linear in the state and the scalar control, a sub-optimal feedback control algorithm was derived that explicitly considered periods of intermediate, or singular, control. Development of this algorithm, termed Lyapunov Optimizing Switching Control (LOSC), was carried out by assuming a positive definite approximation to the optimal return function. To aid in this development, several types of system behavior were considered. Conditions were established that guarantee that trajectories do not converge to nonzero equilibrium points or manifolds. The presence of chatter about the switching surface S was thoroughly investigated; two theorems clearly illuminate situations where the LOSC control methodology induces chatter. Finally, the presence of time scales within the state space equations was considered. It was proven that a singular perturbation parameter multiplying the highest time derivative did not effect stiffness on the singular manifold S; the particular form of $\Psi(\mathbf{x})$ does. For the more general optimal control problem, a qualitative approach was suggested that produced excellent results. This approach relied heavily upon satisfaction of the optimal control necessary conditions on the singular and terminal manifolds along with numerical tuning along typical reference trajectories.

6.2 Trajectory Following Optimization

Derivation of a trajectory-following algorithm applicable to linear, minimum-time systems has been developed. This controller takes on an appealing PID structure and results in a continuous control **u**. Again, practical issues provided inspiration for much of the design. The PID structure was developed to ensure progress to the switching manifold and the target, the presence of finite-time-interval switching control was discussed as well. These factors were considered against the backdrop of time scales that permeated the analysis. The end result of the analysis is a continuous-time control that is especially appealing in an on-line setting. For the more general nonlinear optimal control problem, a State-Augmented Control Descent algorithm was developed. The SACD algorithm was inspired by the Gradient Enhanced Newton optimization algorithm of [7]. Adaptation of GEN into the Lyapunov optimizing control setting allows the analyst to employ an efficient trajectory-following strategy to nonlinear problems that avoids nonzero equilibrium points and manifolds. In addition, the SACD algorithm is robust in that it does not require that an optimization problem be solved for **u** at any point along the state trajectory. SACD also benefits from the generally nonstiff characteristics of GEN.

6.3 Differential Games

An algorithm, termed Efficient Cost Descent, was developed for application in min-max differential games. A fundamental outcome of that development is the characterization of implementation issues that arise when implementing Lyapunov optimizing control and trajectory-following optimization in such an application. Future work will focus upon application of the LOSC methodology in a game setting to help improve the choice of a player descent function.

REFERENCES

[1] Vincent, T. L. and Grantham, W. J., *Nonlinear and Optimal Control Systems*, Wiley, New York, 1997.

[2] Chow, J. H. and Kokotovic, P. V., "A Decomposition of Near Optimum Regulators for Systems with Slow and Fast Modes," *I.E.E.E. Trans. on Automatic Control*, Vol. 21, No. 5, 1976, pp. 701–705.

[3] O'Malley, R. E., *Introduction to Singular Perturbations*, Academic Press, New York, 1974.

[4] Lagerstrom, P. A., *Matched Asymptotic Expansions*, Springer-Verlag, New York, 1988.

[5] O'Malley, R. E., *Singular Perturbation Methods for Ordinary Differential Equations*, Springer-Verlag, New York, 1991.

[6] Chang, K. W. and Howes, F. A., *Nonlinear Singular Perturbation Phenomena: Theory and Application*, Springer-Verlag, New York, 1984.

[7] Grantham, W. J. "Trajectory Following Optimization by Gradient Transformation Differential Equations," *Proc. 42nd I.E.E.E. Conf. on Decision and Control,* Maui, HI, December 2003, pp. 5496–5501.

[8] Grantham, W. J. and Lee, B. S., "A Chaotic Limit Cycle Paradox," Dynamics and Control, Vol. 3, No. 2, April 1993, pp. 159–173.

[9] Utkin, V., I., "Variable Structure Systems with Sliding Modes," IEEE Transactions on Automatic Control, Vol. AC-22, No. 2, April 1977, pp. 212–222.

[10] Xiong, Y., Liu, J., Shin, K., and Zhao, W., "On the Modeling and Optimization of Discontinuous Network Congestion Control Systems," *Proc. 23rd Conference of the I.E.E.E. Communications Society*, Hong Kong, March 7–11 2004, Vol. 4, pp. 2821–2832.

[11] Zlateva, P. "Variable Structure Control Design for a Class of Nonlinear Uncertain Processes," *1996 I.E.E.E. Workshop on Variable Structure Systems*, Tokyo, December 5–6 1996, pp. 61–66.

[12] Kwatny, H. G., Teolis, C., and Mattice, M., "Variable Structure Control of Systems with Nonlinear Friction," *Proc. 38th I.E.E.E. Conf. on Decision and Control,* Phoenix, Arizona, December, 1999, vol. 5, pp. 5164–5169.

[13] Bartolini, G., Ferrara, A., and Usai, E., "Chattering Avoidance by Second-Order Sliding Mode Control," *IEEE Transactions on Automatic Control*, Vol. 43, No. 2, February 1998, pp. 241–246.

[14] Flugge-Lotz, Irmgard, *Discontinuous and Optimal Control*, McGraw-Hill, New York, 1968.

[15] Scokaert, P. O. M. and Mayne, D., Q., "Min-Max Feedback Model Predictive Control for Constrained Linear Systems," *IEEE Transactions on Automatic Control*, Vol. 43, No. 8, August 1998, pp. 1136–1142.

[16] Scokaert, P. O. M., Mayne, D., Q., and Rawlings, J. B., "Suboptimal Model Predictive Control (Feasibility Implies Stability)," *IEEE Transactions on Automatic Control*, Vol. 44, No. 3, March 1999, pp. 648–654.

[17] Grantham, W. J. and Vincent, T. L., *Modern Control Systems Design and Analysis*, Wiley, New York, 1993.

[18] Watkins, D. S., *Fundamentals of Matrix Computations*, Wiley, New York, 1991.

[19] Brown, A. A. and Bartholomew-Biggs, M. C., "Some Effective Methods for Unconstrained Optimization Based on the Solution of Systems of Ordinary Equations," *Journal of Optimization Theory and Applications*, Vol. 62, No. 2, pp. 211–224.

[20] Gomulka, J., "Remarks on Branin's Method for Solving Nonlinear Equations," in *Towards Global Optimization*, Dixon, L. C. W. and Szego, G. P., eds., North-Holland, Amsterdam, 1972, pp. 96–106.

[21] Gomulka, J., "Two Implementations of Branin's Method: Numerical Experience," in *Towards Global Optimization 2*, Dixon, L. C. W. and Szego, G. P., eds., North-Holland, Amsterdam, 1978, pp. 151–164.

[22] Vincent, T. L. and Grantham, W.J., "Trajectory Following Methods in Control System Design," *J. of Global Optimization*, Vol. 23, 2002, pp. 267–282.

[23] Grantham, W. J., "Gradient Transformation Trajectory Following Algorithms for Determining Stationary Min-Max Saddle Points," *Proc. of the 11th Int'l Symposium on Dynamic Games and Applications*, Tucson, AZ, December 2004, pp. 320–338.

[24] Vincent, T. L., Goh, B. S., and Teo, K. L., "Trajectory Following Algorithms for Min-Max Optimization Problems," *J. of Optimization Theory and Applications*, Vol. 75, No. 3, 1992, pp. 501–519.

[25] Goh, B. S., "Algorithms for Unconstrained Optimization via Control Theory," *J. of Optimization Theory and Applications*, Vol. 92, No. 3, 1997, pp. 581–604.

[26] Gradshteyn, I. S. and Ryzhik, I. M. "Routh-Hurwitz Theorem." §15.715 in Tables of Integrals, Series, and Products, 6th ed., San Diego, CA: Academic Press, p. 1076, 2000.

[27] Ardema, M. A. and Rajan, N., "Slow and Fast State Variables for Three-Dimensional Flight Dynamics," *J. of Guidance, Control, and Dynamics*, Vol. 8, No. 4, 1985, pp. 532–535.

[28] Ardema, M. A., "Computational Singular Perturbation Method for Dynamic Systems," *J. of Guidance, Control, and Dynamics*, Vol. 14, No. 3, 1991, pp. 661–665.

[29] Zagaris, A., Kaper, H. G., and Kaper, T. J., "Analysis of the Computational Singular Perturbation Reduction Method for Chemical Kinetics," *J. of Nonlinear Science*, Vol. 14, 2004, pp. 59–91.

[30] Sheu, D., Vinh, N. X., and Howe, R. M., "Application of Singular Perturbation Methods for Three-Dimensional Minimum-Time Interception," *J. of Guidance, Control, and Dynamics*, Vol. 14, No. 2, 1991, pp. 360–367.

[31] Pan, Z. and Basar, T., "H-infinity Optimal Control for Singularly Perturbed Systems. Part I: Perfect State Measurements," *Automatica*, Vol. 29, No. 2, March 1993, pp. 401–423.

[32] Pan, Z. and Basar, T., "H-infinity Optimal Control for Singularly Perturbed Systems. Part II: Imperfect State Measurements," *I.E.E.E. Trans. on Automatic Control*, Vol. 39, No. 2, 1994, pp. 280–298.

[33] Saberi, A. and Khalil, H., "Quadratic-Type Lyapunov Functions for Singularly Perturbed Systems," *I.E.E.E. Transactions on Automatic Control*, Vol. AC-29, No. 6, pp. 542–550.

[34] Vincent, T. L. and Grantham, W. J., *Optimality in Parametric Systems*, Wiley, New York, 1981.

[35] Luenberger, D. G., *An Introduction to Dynamic Systems*, Wiley, New York, 1979.

[36] Vincent, T. L. and Lin, Y. C., "Some Performance Measures Useful in the Design of Controllers for Two-Dimensional Dynamical Systems Subject to Uncertain Inputs," *Dynamics and Control*, Vol. 5, 1995, pp. 69–98.

[37] Grantham, W. J., *A Controllability Minimum Principle*, Ph.D. dissertation, Aerospace and Mechanical Engineering, University of Arizona, Tucson, AZ, 1973.

[38] Basar, T. and Olsder, G. J., *Dynamic Noncooperative Game Theory*, Academic Press, London, 1982.